ACCSCIENCE PUBLISHING

# Brain & Heart

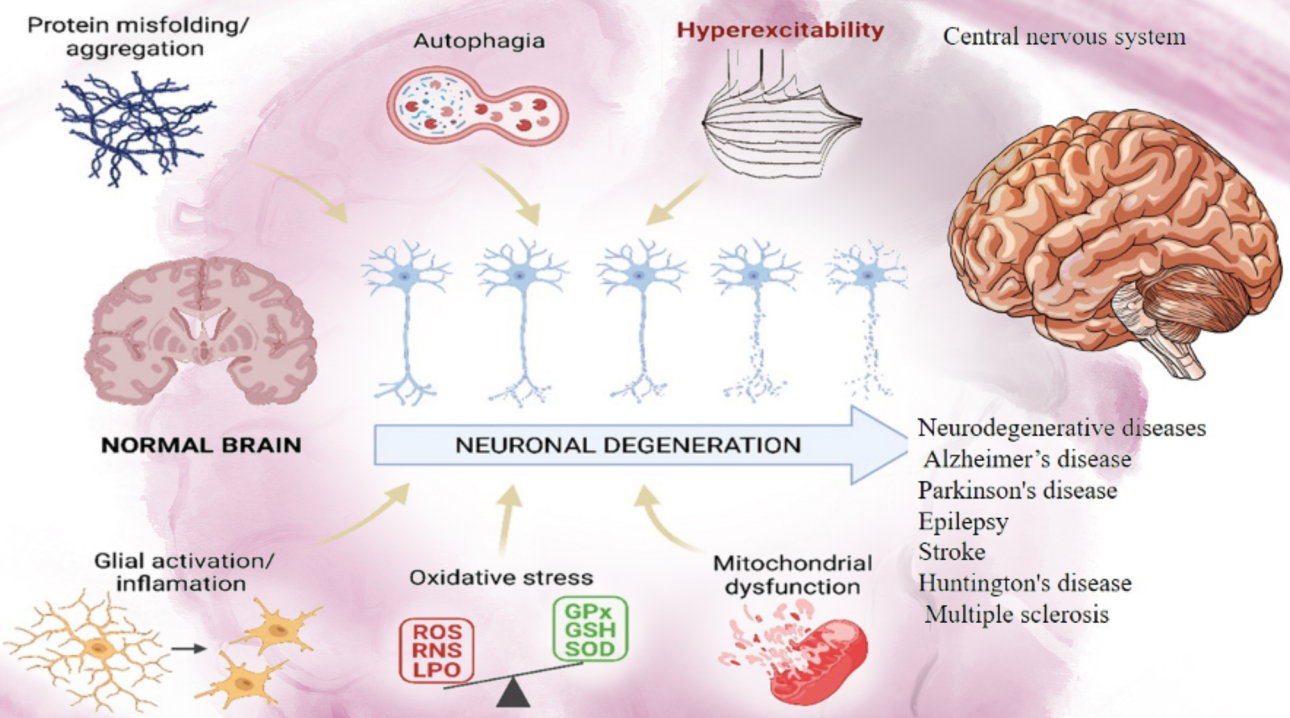


## Oxidative stress and neurological disorders: Therapeutic strategies and pharmacological intervention

ACCSCIENCE PUBLISHING
Volume 2 · Issue 2
May 2024
ISSN: 2972-4139 (Online)

Online ISSN: 2972-4139

# Brain & Heart

***Brain & Heart*** focuses on neurocardiology, a neurology and cardiology-based interdisciplinary subject that studies the circulatory mechanism of the human body, as well as the mechanisms of the interplay between the cardiovascular system and the nervous system.

The article types accepted by *Brain & Heart* include the following: original research article, review article, perspective article, case report, letter, editorial, and special feature article.

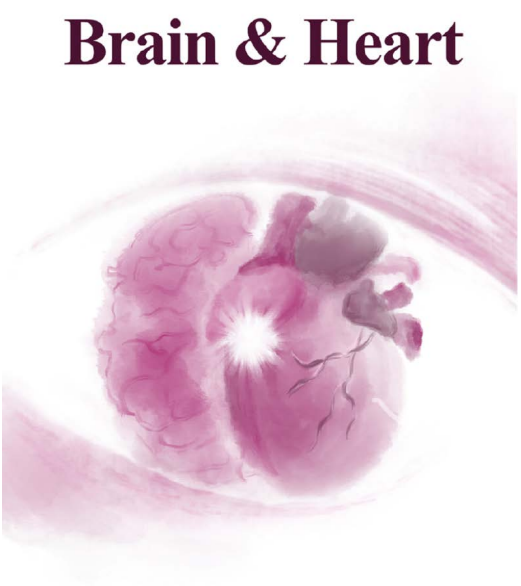


## About the Publisher

**AccScience Publishing** is a publishing company based in Singapore. We publish a range of high-quality, open-access, peer-reviewed journals and books from a broad spectrum of disciplines.

Contact Us

**Managing Editor**
bh.office@accscience.sg

**AccScience Publishing**
8 Burn Road, #15-03 Trivex, Singapore 369977.

Volume 2 • Issue 2 • May 2024
ISSN 2972-4139 (online)

# BRAIN & HEART



ACCSCIENCE PUBLISHING

Access Science Without Barriers

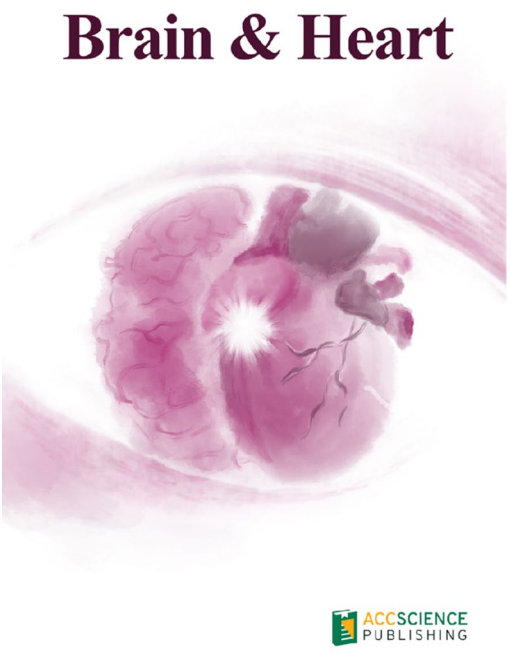


***BRAIN & HEART***

ISSN: 2972-4139 (online)

**Editorial and Production Credits**

Publisher: AccScience Publishing
Managing Editor: Naomi Li
Production Editor: Sharmila Velapasamy
Article Layout and Typeset: Sinjore Technologies (India)

For all advertising queries, contact bh.office@accscience.sg.

**Supplementary file**

Supplementary files of articles can be obtained at https://accscience.com/journal/BH/2/2.

Brain & Heart

Editorial Board

## Editors-in-Chief



## Associate Editor



## Editorial Board Members*



*Editorial Board Members as of March 19, 2024

ACCSCIENCE PUBLISHING

Volume 2 | Issue 2 | May 2024 |

**Brain & Heart**

https://accscience.com/journal/BH

# CONTENTS

ACCSCIENCE PUBLISHING

Brain & Heart

REVIEW ARTICLE

# Oxidative stress and neurological disorders: Therapeutic strategies and pharmacological intervention

**Nikhila Khola†, Kareena Moar†, and Pawan K. Maurya***

Department of Biochemistry, School of Interdisciplinary and Applied Sciences, Central University of Haryana, Mahendergarh, Haryana, India

## Abstract

Oxidative stress plays a significant role in cerebral biochemical dysfunction, contributing to the increased sensitivity of the central nervous system to reactive oxygen species (ROS)-mediated injury. It is characterized by an imbalance between the production of ROS and the antioxidant capacity of the cell, which results in a variety of pathological disorders and diseases, including neurological conditions such as Parkinson's disease, Alzheimer's disease, schizophrenia, bipolar disorder, and anxiety. In this review, we delve into the role of oxidative stress in neurodegenerative disorders. We conducted a comprehensive search across various databases, including Google Scholar, ScienceDirect, and PubMed, with a focus on literature published within the past decade. Our search utilized terms such as "oxidative stress and neurological disorders," "pharmacological interventions for neurological disorders," "oxidative stress, free radicals, and neurological disorders," and "free radicals and neurological disorders. Our aim was to elucidate the relationship between oxidative stress and neurological disorders, as well as to summarize available therapies and pharmacological interventions for these conditions.

***Keywords:*** Oxidative stress; Neurological disorder; Reactive oxygen species; Pharmacological interventions; Therapy

*†These authors contributed equally to the work*

***Corresponding author:**
Pawan Kumar Maurya
(pkmaurya@cuh.ac.in)

**Citation:** Khola N, Moar K, Maurya PK. Oxidative stress and neurological disorders: Therapeutic strategies and pharmacological intervention. *Brain & Heart.* 2024;2(2):2704.
doi: 10.36922/bh.2704

**Received:** January 10, 2024

**Accepted:** March 20, 2024

**Published Online:** May 14, 2024



## 1. Introduction

Oxidative stress arises from an imbalance between the production and accumulation of reactive oxygen species (ROS) in cells and tissues, where pro-oxidants outnumber antioxidants. Initially, it was believed that ROS, comprising reactive molecules and free radicals originating from molecular oxygen, were released solely from mitochondrial metabolism. However, further research has revealed that cellular enzymes, such as nicotinamide adenine dinucleotide phosphate oxidases, also contribute to ROS production in humans.[1]

When ROS levels rise, they can cause irreparable damage to biological molecules, resulting in cell dysfunction and, in severe cases, cell death.[2] Oxidative stress is implicated in numerous age-related disorders, such as diabetes, cancer, cardiovascular, and neurological disorders.[3] Oxidative stress is mainly the disturbance of homeostasis inside the environment of the cell. Neurological disorders are particularly notable due

to the irreversible changes in neurons that they induce.[4] For the normal functioning of eukaryotic cells, oxygen is crucial. The demand for oxygen varies depending on the type of cells and tissues. For example, in the brain, astrocytes and neurons primarily require a high supply of oxygen and glucose.

Despite of essentiality of oxygen, hyperoxia can lead to toxicity, including neurotoxicity. Although the complete pathways affected and the mechanisms underlying this situation are not completely understood, many mechanisms are directly or indirectly affected by oxidative stress, ultimately resulting in neuronal death. These mechanisms include mitochondrial dysfunction, altered proteosis, and deregulation of antioxidant pathways. Several studies on animal models and postmortem human brain specimens have reported that increased levels of ROS and reactive nitrogen species (RNS) lead to damage of proteins, lipids, and nucleic acids.[5]

Oxidative stress serves as a common denominator in neuronal loss, responsible for all types of neurological disorders. The role of oxidative stress is evident in the oxidative damage of many proteins reported in postmortem studies of Alzheimer's disease and Parkinson's disease. When low concentrations of ROS are maintained, they serve as signaling molecules and play a positive role in defense mechanisms.[6] Astrocytes and glial cells are responsible for maintaining homeostasis in the brain under normal physiological conditions. However, in high levels of oxidative stress, the appropriate functioning of these glial cells is disturbed, leading to a weakened blood-brain barrier.[7]

In neurodegeneration, Alzheimer's disease and Parkinson's disease account for a significant portion of cases, with oxidative stress playing an important role in both conditions. This oxidative stress can lead to the oxidation of mitochondrial DNA, a phenomenon closely associated with aging. Studies indicate that age-related declines in mitochondrial function contribute to impairments in the expression and processing of amyloid precursor protein (APP).[8] The expression of APP is responsible for the production of ROS in the brain, which leads to neurotoxicity and the accumulation of amyloid β, a hallmark of Alzheimer's disease.[9] Furthermore, oxidative stress and mitochondrial dysfunction are implicated in a cascade of events culminating in the loss of dopaminergic neurons, a defining feature of Parkinson's disease. The primary pathology in Parkinson's disease is the degeneration of dopaminergic neurons in the substantia nigra, a region crucial for regulating motor function. Elevated levels of oxidative biomarkers, such as 8-hydroxy-guanosine, have been observed in the brains of Parkinson's disease patients.[10]

It is well understood that oxidative stress initiates a series of cellular events that collectively contribute to neuronal demise.[11] Consequently, targeting oxidative stress represents a potential strategy for interrupting this detrimental cascade. Therefore, many researchers are now emphasizing therapeutic interventions aimed at modulating key components involved in regulating oxidative stress.

## 2. Effects of oxidative stress on the central nervous system

Due to the high metabolic rate in the central nervous system (CNS), adenosine triphosphate production is notably elevated through the electron transport chain and oxidative phosphorylation. Consequently, neurons and glial cells generate substantial amounts of ROS and RNS. Neurons and other CNS cells are particularly susceptible to oxidative stress due to their unique biochemical pathways and intrinsic properties.[10] The influence of oxidative stress on tissue and cellular levels varies depending on the internal structure of impacted brain regions, notably the hippocampus, prefrontal cortex, amygdala, and cerebral cortex, which are among the most vulnerable regions to oxidative stress.[5] According to the free radical theory of aging proposed by Harman,[12] the CNS is highly susceptible to oxidative stress due to its substantial oxygen requirement, which accounts for 20% of the total body oxygen utilized for metabolic activities.[4] Neurons exhibit heightened sensitivity to oxidative stress due to their non-dividing, terminally differentiated nature, rendering them unable to be replaced even in the face of damage or mitochondrial dysfunction during their late lifespan.[13] Aging of the brain further exacerbates its vulnerability to oxidative stress, leading to increased levels of oxidative biomarkers such as DNA damage, metal toxicity, and deficits in protein metabolism. In addition, brain aging promotes the upregulation of genes that compensate for age-associated deficits, including those involved in protein folding (e.g., heat shock protein 70 and alpha-crystallin) and metal-ion homeostasis. Neuronal membranes primarily consist of polyunsaturated fatty acids such as docosahexaenoic acid (DHA), rendering them more susceptible to lipid peroxidation.[14] Neurotransmitters, the chemical messengers facilitating signal transmission between neurons and target cells, including dopamine and epinephrine, are prone to auto-oxidizable. Excessive oxygen species react with dopamine, serotonin, and norepinephrine, initiating their oxidation and leading to the synthesis of more ROS and quinones in various brain regions.[15] Ultimately, oxidative stress sets off a cascade of metabolic phenomena culminating in neurotoxicity. ROS toxicity contributes to protein mis-folding, glial cell

activation, mitochondrial dysfunction, and subsequent cellular apoptosis.

### 2.1. Role of antioxidants

Oxidative stress is a pivotal factor in most chronic neurological disorders, making antioxidants a promising therapeutic approach by reducing oxidative stress through the quenching/scavenging of free radical intermediates.[16] Antioxidants effectively interrupt the cascade of oxidative stress reactions. Within biological systems, inherent endogenous antioxidants maintain homeostasis. These antioxidants include enzymatic entities such as superoxide dismutase (SOD), glutathione peroxidase, and catalase, as well as non-enzymatic compounds such as glutathione, α-lipoic acid, uric acid, and coenzyme Q10.[17] Another category comprises exogenous or synthetic antioxidants, which are synthesized from modifications of natural antioxidant or their conjugation with other effective molecules. Synthetic antioxidants exhibit superior capacities for scavenging free radicals, metabolic stability, and bioavailability compared to natural ones.[18] Examples of synthetic antioxidants include propyl gallate, butylated hydroxytoluene, and polyphenols such as curcumin, resveratrol, and anthocyanin.[19] Recent research on synthetic antioxidants has yielded favorable results against oxidative stress and multiple targets in neurodegenerative diseases.[20] Treatment with various types of antioxidants such as α-lipoic acid[21] Vitamin C,[16] α-tocopherol,[22] crocin,[23] resveratrol,[24] and epicatechin[25] has demonstrated significant reductions in brain edema, infarct brain volume, oxidative damage, and apoptosis. In addition, antioxidant treatment preserves the integrity of the blood-brain barrier, ameliorates ischemic injury, and upregulates the expression of brain-derived neurotrophic factor and nerve growth factor mRN.[26] Since neurological disorders are multifactorial disorders and oxidative is a common pathophysiological process affecting multiple targets, effective antioxidant therapy or combination therapy could have broad therapeutic applicability in clinical trials.[27] However, certain challenges hinder translation to clinical practice, such as low bioavailability, inadequate dosing, limited transportation to CNS, and transient retention. Nanoparticle-based drug delivery could address some of these issues.

## 3. Cellular pathways affected during oxidative stress in the central nervous system

Researchers have shifted their focus toward the cellular or metabolic pathways implicated in oxidative stress. Stress induces apoptotic injury characterized by early membrane fragility loss and genomic DNA destruction.[28] Affected cellular pathways include activation of glycogen synthase kinase-3β activation, the Akt pathway, loss of mitochondrial permeability, alterations in glutamate metabolism, dysregulation of cytokine, and inflammation involving microglial.[29] Ultimately, these events culminate in neuronal loss or irreparable nerve injury. Understanding these cellular pathways holds promise for identifying potential novel therapies for acute and chronic neuronal and vascular injuries. Studies have reported that deficiency in the PINK1 gene, responsible for maintaining mitochondrial calcium homeostasis, leads to impaired respiration and increased production of ROS due to inhibition of complex 1 in the mitochondrial electron transport chain.[30] Antioxidant response enzymes (AREs) are activated upon binding with the transcription factor nuclear factor erythroid 2-related factor 2 (Nrf2).[31] The ARE-Nrf2 complex serves as a neuroprotectant. However, oxidative stress can disrupt this binding, leading to the loss of Nrf function[32] (Figure 1).

## 4. Role of sigma receptors in neurological disorders

Sigma receptors represent a unique class of intracellular receptors, distinct from G-coupled receptors and ionotropic receptors, and play a significant role in modulating a collection of cellular processes in neurodegeneration.[33] These receptors consist of two subtypes: sigma-1 and sigma-2, both present in CNS. Each subtype is distinguished by its unique pharmacological properties and structural composition.[34] In recent years, sigma receptors have gained interest for their involvement in altering pathways related to cell survival and functions, offering potential therapeutic targets in neurodegenerative conditions. Sigma-1 receptors are multifunctional transmembrane proteins distributed on the mitochondrial and endoplasmic reticulum membrane,[35] participating in both cellular and intracellular activities. In the CNS, sigma-1 receptors are found on neurons, oligodendrocytes, microglial cells, and astrocytes, contributing to various physiological activities such as synaptic plasticity and the secretion of neurotransmitters such as glutamic acid, serotonin, adrenaline, dopamine, and neurosteroids.[36] On the other hand, sigma-2 receptors are still under investigation. Current knowledge suggests that they are transmembrane proteins with four domains, with N- and C-terminals extending into the cytoplasm,[35] and weigh approximately 18 – 21 kDa. No endogenous receptors for sigma-2 receptors have been identified thus far. These receptors are implicated in cholesterol homeostasis, sterol transport, and the regulation of intracellular calcium ion concentrations.[37] However, a comprehensive understanding of their chemical structure, physiological

role, and distribution throughout the body remains incomplete. Given the limited information available about sigma-2 receptors, further studies and research are warranted to elucidate their role in cellular processes and potential therapeutic implications in neurodegenerative disorders[38] (Figure 2).

## 5. Factors affecting oxidative stress

### 5.1. Aging

Aging represents a progressive physiological change in organisms, leading to a decline in biological activities. According to free radical theory, aging cells exhibit

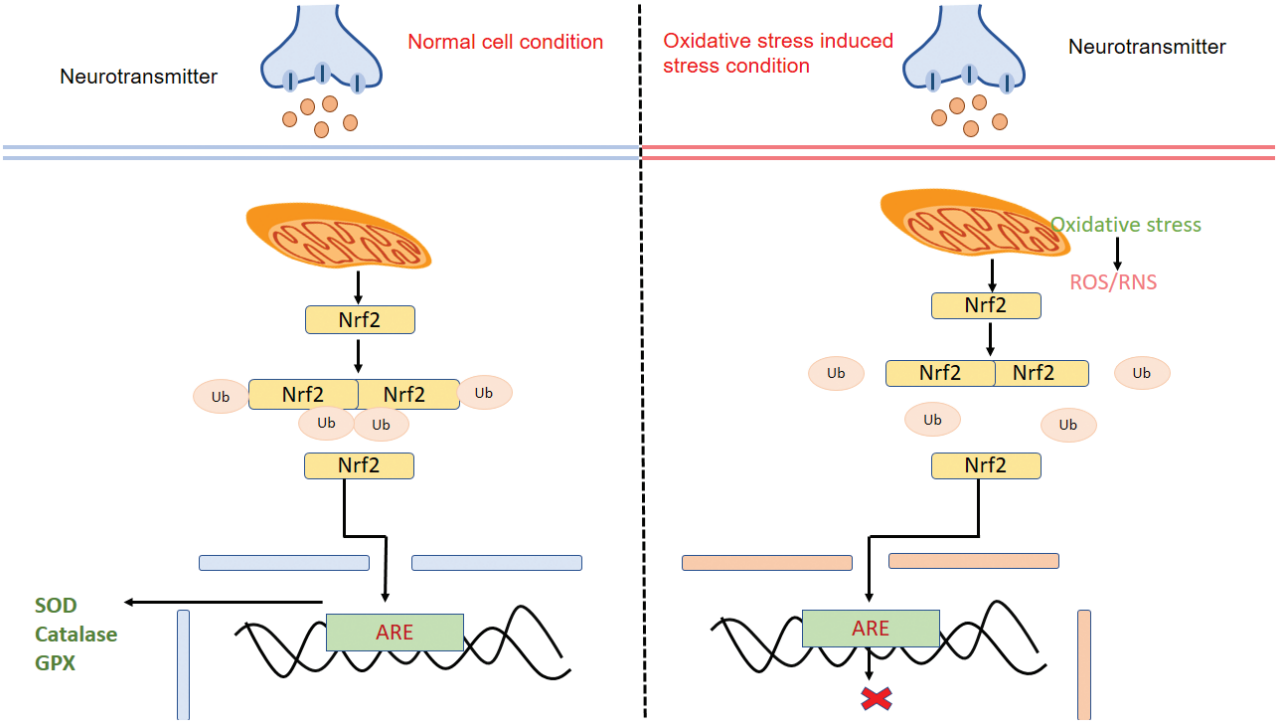


**Figure 1.** The alteration in metabolic pathways induced by oxidative stress across synapses.
Abbreviations: ARE: Antioxidant response enzymes; GPX: Glutathione peroxidase; Nrf2: Nuclear factor erythroid 2-related factor 2; SOD: Superoxide dismutase; Ub: Ubiquitin.

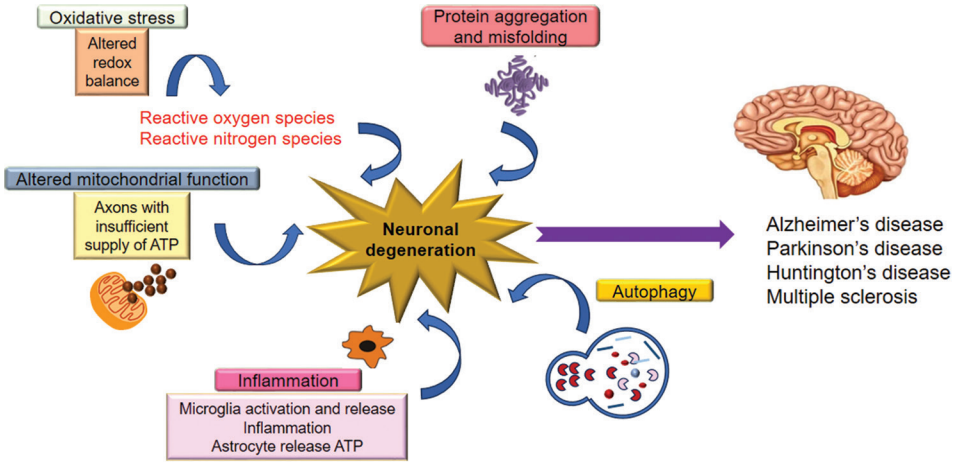


**Figure 2.** Various factors responsible for neurodegeneration.
Abbreviations: GPX: Glutathione peroxidase; GSH: Glutathione; LPO: Lipid peroxidation; RNS: Reactive nitrogen species; ROS: Reactive oxygen species; SOD: Superoxide dismutase.

increased production of free radicals, which are responsible for age-associated functional damage to macromolecules.[39] This heightened production of ROS during aging induces various physiological changes, such as the inhibition of cell proliferation and the production of interleukins, chemokines, and other proinflammatory components, ultimately leading to cell senescence.[40] Cellular senescence contributes to the onset of several acute and chronic disorders, as aging disrupts cellular homeostasis, particularly through oxidative damage. Oxidative stress-induced aging triggers mitochondrial dysfunction, further exacerbating cellular aging. As a result, the lifespan of cells is reduced due to the functional inefficiency of enzymes, proteins, and other biomolecules.[9] In addition, oxidative stress accelerates peroxidative damage to membrane lipids, degrades membrane proteins, and reduces the concentration of fatty lipids. ROS also play a role in premature aging by causing errors in DNA replication, accumulation of DNA modifications, insufficient organelle turnover, and impaired proteosis.[41]

### 5.2. Obesity

Obesity, characterized by excessive body fat, exerts multifactorial effects on health, increasing the risk of various health problems. It typically arises from a surplus intake of calories not offset by physical exercise and daily activities.[42] Obesity has been associated with systemic oxidative stress, which stems from increased production of adipokines and the development of metabolic syndrome.[43] Oxbiosis-induced oxidative stress is attributed to increased adipocyte numbers that lead to elevated levels of proinflammatory cytokines such as interleukin-6 and indicative of chronic inflammation within the body.[44] Moreover, the increased mechanical load and myocardial demand associated with obesity escalate oxygen consumption, resulting in the overproduction of free radicals. Jia *et al.*[45] suggest that if obesity persists for a prolonged duration, antioxidants such as catalase and SOD also become depleted. As adipocytes increase, cellular metabolism is affected, leading to an overproduction of ROS. Weight loss, along with antioxidant supplements such as Vitamin E, can help reduce the pathologies related to oxidative stress.[45] Even at the hepatic level, obesity induces lipid peroxidation, oxidative stress, and autophagy. ROS are involved in the signal transduction and differentiation of adipocytes from stem cells.[46] However, complete information about this process still needs to be elucidated, as it involves many transcription factors, cell cycle proteins, small molecules, and hormones.[47] Elevated ROS levels may result in modified differentiation of adipocytes and their function, and also alter the browning process in obesity. Accumulation of fatty acids and lipids is accompanied by alterations in insulin signaling pathways. High glucose levels elevate the production of ROS, which transforms mitochondrial enzymes, consumption, and deposition of nutrients, ultimately resulting in metabolic disorders.[48] In obese individuals, mitochondrial dysfunctioning leads to decreased fatty acid oxidation and energy generation. ROS alter the metabolism of lipids and fats and elevates the rate of apoptosis.[49]

### 5.3. Inflammation

Inflammation represents a biological response to external stimuli, constituting a complex immune protective mechanism of the body against external injury, allergy, or chemical irritants.[50] Chronic inflammation can precipitate diseases related to a hyperresponsive immune system, such as rheumatoid arthritis, chronic asthma, and other neurological disorders. Tissues injured by trauma undergo cellular death or injury,[51] releasing ROS, superoxide anion, hydrogen peroxide, nitric oxide, and cytokines. Chronic inflammation is a major contributor to free radical production, thereby playing a pivotal role in the onset of numerous diseases. In CNS, inflammatory lesions produced as an immune response consist of CD4+ and CD8+ T-cells.[52] The higher accumulation of immune cells correlates with an elevated expression of inflammatory cytokines. NRLP3 serves as an intracellular sensor detecting environmental stimuli and endogenous danger signals. Chronic inflammation activates NRLP3, leading to the formation of inflammasomes, which, in turn, induces mitochondrial dysfunction, resulting in increased production of mitochondrial ROS. The NF-κB pathway is intricately interconnected with various cellular pathways and inflammation.[5] This transcription factor plays an important role in maintaining cellular homeostasis and is markedly upregulated during aging, contributing to chronic inflammation. Activation of the NF-$\kappa$B pathway amplifies inflammatory responses through positive feedback, leading to an increase in ROS/RNS within cells, thereby fostering stressful conditions within the cellular environment.[53]

### 5.4. Mitochondrial dysfunction

After the nucleus, only the mitochondria is the cell organelle having its own DNA. Due to the activity of electron chain transport, ROS are a major byproduct within the mitochondria.[54] Oxidative stress-related disarrangements within the mitochondria and proinflammatory signaling are indicators of neurodegeneration. Mitochondria form an interconnected network with other organelles such as lysosomes, endoplasmic reticulum, actin cytoskeleton, and the Golgi apparatus. Neuroinflammation is linked to many neurological disorders,[4] in which mitochondrial-derived vesicles are a common factor in disease progression.

Mitochondrial-derived vesicles are also associated with the activation of hyper-fragmented mitochondria and giant mitochondria nucleoids, which can trigger the immune response.[55] Altered mitochondrial metabolism, increased membrane permeability, decreased membrane potential, and excess production of ROS and energy deficits are associated with neurological disorders and their progression.[56]

## 6. Neurological disorder

Neurological disorders are defined medically as conditions that affect biochemical, structural, or electrical abnormalities in the brain, spinal cord, or other nerves, often resulting in a range of symptoms such as paralysis, muscle weakness, poor coordination, loss of sensation, seizures, and altered levels of consciousness.[57] Broadly, neurological disorders are classified into three categories: (i) neuropsychiatric disorders, such as schizophrenia, bipolar disorder, anxiety, and seizures; (ii) neurodegenerative disorders, such as Parkinson's disease, Huntington's disease, and Alzheimer's disease; and (iii) neurocognitive disorders, such as dementia, autism, and delirium. Neuropsychiatric disorders represent a spectrum of syndromes where an individual's cognitive, behavioral, and emotional abilities are affected.[58] Common examples include schizophrenia, major depressive disorder (MDD), attention deficit hyperactivity disorder (ADHD), and bipolar disorder. Despite their high prevalence, these disorders can have profoundly debilitating effects. In addition, anxiety stands out as a major neuropsychiatric problem, particularly prevalent during adolescence (Table 1).

## 7. Oxidative stress in neuropsychiatric disorders

### 7.1. Schizophrenia

Schizophrenia is a severe mental disorder that affects approximately 0.4% of the global population, imposing significant emotional and financial burdens on both patients and their families. Characterized by a diverse range of symptoms, schizophrenia manifests as a heterogeneous disorder, encompassing both positive and negative symptoms. Positive symptoms include thought disorders, hallucinations, and delusions, whereas negative symptoms include social withdrawal and poverty of thought. Notably, 50–90% of schizophrenia patients exhibit negative symptoms during their first episode of illness.[66]

Patients diagnosed with schizophrenia experience auditory verbal hallucinations (AVHs), which are prevalent in around 70% of cases. AVHs involve patients hearing voices that are unreal, without any external sound stimuli. In general, these voices consist of insulting comments or negative remarks directed toward the patients, potentially prompting self-harm, suicidal tendencies, or extreme violence.[67]

Psychiatrists managing schizophrenia often emphasize the adage, "Time is cognition." Emerging but limited evidence suggests that early intervention before the onset of psychosis is crucial for preserving patients' functional ability and cognition. Therapy, social support, and psychoeducation are all very important and significant aspects of the treatment of different stages of schizophrenia. Antipsychotics serve as the primary pharmacological

**Table 1. Changes in the activity of synaptic protein in neurological disorders**

| Synaptic proteins | Functions of protein Name of proteins | Change in activity of protein | Location in brain | References |
|---|---|---|---|---|
| α-synuclein | Presynaptic chaperone | Decreased | Cultured neurons and brain homogenates | 59 |
| VAMP2 | VAMP2 in the synaptic vesicles | Decreased | Primary motor, somatosensory, and parietal areas of the cerebral cortex, synaptosomes | 60 |
| PSD-95 | Postsynaptic density protein | Increased | Cortical layers I, II/III, and V | 61 |
| Synaptophysin | Synaptic vesicle membrane protein involved in endocytosis | Decreased | Rostral cortex | 62 |
| Complexin-1 | Exocytosis of synaptic vesicles | Decreased | Hippocampus | 63 |
| Syntaxin-1A | SNARE complex | Decreased | Hippocampus | 64 |
| MAP1A | Microtubule cross-linking protein | Decreased | Hippocampus | 65 |
| Homer-1 | Protein in the post-synaptic density of excitatory synapses | Decreased | Primary motor, somatosensory, and parietal areas of the cerebral cortex | 66 |
| SNAP25 | t-SNARE | Decreased | Synaptosomes | 67 |
| MAP1B | Microtubule cross-linking protein | Decreased | Hippocampus | 68 |

Abbreviations: MAP1A: Microtubule-associated protein 1A; MAP1B: Microtubule-associated protein 1B; PSD-95: Postsynaptic density protein 95; SNAP25: Synaptosomal-associated protein, 25kDa; VAMP2: Vesicles-associated membrane protein-2.

treatment for schizophrenia.[68] Despite being one of the most commonly prescribed treatments, 5–25% of patients may continue to experience symptoms and encounter unwanted side effects. Talking therapies are frequently used alongside medications.[69] The following outlines different treatment options for schizophrenia:

#### *7.1.1. Supportive therapy*

In supportive therapy, patients receive general support. After consulting with a health professional, time is allocated for listening to people's concerns, providing encouragement, and even assisting them with their day-to-day activities. Support from family and friends also falls within the realm of supportive therapy. Certain interventions in supportive psychotherapy require a trained therapist, while others, like "befriending," do not require specific training.[70]

#### *7.1.2. Avatar therapy*

Certain symptoms of schizophrenia, such as AVHs, may resist conventional treatment methods. Avatar therapy, utilizing virtual reality, has emerged as a potential intervention for these treatment-resistant symptoms. Recently integrated into schizophrenia treatment options,[71] this therapy utilized virtual reality to create a controlled environment. A computer program generates an avatar, human or non-human, resembling the entity the patient believes interacts with them through voices. Designed to encourage and control dialogue between the patient and the avatar, the therapy employs a virtual reality environment and voice morphing program for avatar creation. Finally, the therapist uses the avatar to engage in dialog with patients and subsequently administer treatment.[72]

#### *7.1.3. Cognitive behavior therapy*

Cognitive behavior therapy (CBT) is a psychosocial treatment aimed at assisting patients in re-evaluating their experiences to alleviate distress and modify problematic behavior. The National Institute of Health and Care Excellence (NICE) recommends CBT as an adjunctive treatment for schizophrenic patients.[73] Developed by Aaron T. Beck, CBT applies general principles such as case formulation based on a cognitive model, goal setting, and homework assignments to address negative symptoms.[74] Current evidence suggests that CBT may be beneficial for patients with chronic schizophrenia. However, its use during acute phases should be considered based on patient cooperation and feasibility issues.[75]

### 7.2. Major depressive disorder

Major depressive disorder, also known as unipolar depressive disorder or clinical depressive disorder, ranks among the most common psychiatric conditions globally, affecting over 264 million individuals.[76] It stands as the leading cause of disability, according to the World Health Organization. Characterized by its deleterious effects, high prevalence, and early onset, MDD imposes significant disability, mortality, and financial burden on affected individuals and their families. Moreover, its negative effects are further exacerbated by family turmoil, social upheaval, and divorces.[77] Symptoms of MDD include impaired cognitive and vegetative functions, mood swings, and loss of interest and pleasure in activities.[78] The treatment of MDD encompasses the following therapeutic modalities:

#### *7.2.1. Hormonal therapies*

Some patients generally fail to respond satisfactorily to chemical antidepressants. Consequently, there is a pressing need for more effective methods targeting depression treatment. Alterations in hormonal concentrations and endocrine functions play a significant role in the pathophysiology of depression.[79] Cortisol, estrogen, and thyroid hormones, in particular, are important in addressing behavioral disorders. Extensive clinical and preclinical studies have laid the foundation for a deeper understanding of the clinical application of hormonal therapy in depression treatment in the forthcoming years.[80]

#### *7.2.2. Cognitive behavioral therapy*

Many patients with chronic depressive symptoms become resistant to conventional antidepressant treatments. Typically, those suffering from depressive symptoms for 2 years or more do not respond to chemical treatments. Therefore, patients with severe to moderate symptoms require a novel strategy that combines both pharmacological and psychological treatments.[77] CBT represents one such approach. It is a goal-oriented, well-structured talk therapy aimed at alleviating symptoms associated with various mental health conditions, particularly depression and anxiety. CBT is widely regarded as the most effective treatment for substance abuse and co-occurring mental disorders.[81] Through this therapy, patients acquire skills to adopt healthier thinking patterns and habits, enabling them to overcome negative thoughts and behaviors. CBT can be used alone or in conjunction with other therapies and medications. Sessions typically involve a question-and-answer format, facilitating the development of improved coping mechanisms for stress, pain, and difficult situations.[82] CBT is suitable for individuals of all age groups, including children. Grounded in theory- and expertise-based conversations, CBT provides a factual treatment approach within a safe, supportive, non-judgmental, and positive environment, fostering open communication between patients and mental health professionals.[83]

#### *7.2.3. Electroconvulsive therapy*

Treating and managing MDD represents a major public health challenge nowadays. MDD is considered a substantial psychological and social disruption. The American Psychiatric Association acknowledges electroconvulsive therapy as a treatment generally reserved for patients with severe MDD unresponsive to other treatments. It involves brief electrical stimulation of the brain under general anesthesia, resulting in changes in brain chemistry and homeostasis.[84] This procedure is generally considered safe and low-risk. Often employed as a "quick fix," electroconvulsive therapy serves as an alternative to prolonged medication regimens and hospitalization. Several studies have proven the efficacy of electroconvulsive therapy, particularly in patients with treatment-resistant depression.[85]

### 7.3. Bipolar disorder

Individuals afflicted with bipolar disorder experience episodes of mania and depression, punctuated by periods of euthymia characterized by normal mood, behavior, and energy levels.[86] Manic episodes entail racing thoughts, reduced need for sleep, elevated mood, and impulsive behavior, whereas depressive episodes are marked by sadness, feelings of guilt, and disinterest in daily activities. Globally, the prevalence rate of bipolar disorder ranges from approximately 2–5%.[87] The DSM-IV further classifies bipolar disorder into two types: bipolar I disorder, characterized by clear episodes of mania, and bipolar II disorder, which features milder forms of mania.[88] The average age of onset for bipolar I disorder is 18 years, while for bipolar II disorder, it is 22 years. Both sexes are equally affected by bipolar I disorder, while women are more susceptible to bipolar II disorder.[89]

Treatment guidelines for bipolar disorder are continuously revised and modified to incorporate advancements in pharmacological and psychological interventions. The latest and most elaborated treatment strategies involve chemical interventions, with mood stabilizers such as lithium and valproic acid being common options. These medications demonstrate efficacy as monotherapy or in combination with antipsychotic drugs. Recent additions to the treatment repertoire include lurasidone and cariprazine.

### 7.4. Attention deficit hyperactivity disorder

Attention deficit hyperactivity disorder (ADHD) is characterized by patterns of inattention, impulsivity, hyperactivity, and restlessness. It typically manifests in childhood and involves neurological and neurodevelopmental issues. The etiology of ADHD is multifactorial, representing a heterogenous disorder influenced by various factors such as heritability, severe brain injuries, premature birth, and consanguineous marriage.[90] Prevalence estimates indicate that ADHD affects approximately 5% of children and nearly 4% of adults worldwide.[91] ADHD impacts academic performance, family dynamics, and social relationships, leading to emotional and financial burdens for both the patient and their family.[92]

### 7.5. Anxiety

Anxiety is a neuropsychiatric disorder characterized by feelings of fearfulness, worry, and nervousness, often accompanied by a sense of helplessness and distress. Individuals with anxiety tend to avoid stimuli perceived as dangerous. Various types of anxiety disorders exist, including generalized anxiety disorder (GAD), social anxiety disorder (SAD), separation anxiety disorder, and panic disorder.[93] GAD entails excessive worry about a broad array of day-to-day circumstances of life.[94] SAD involves a persistent fear of being insulted and humiliated by others, leading individuals to avoid social interactions such as speaking with strangers, participating in group conversations, or engaging in telephonic conversations.[95] Separation anxiety disorder manifests as anxiety related to being separated from home or from attachment figures.[96] Panic disorder is characterized by unexpected and recurrent panic attacks, marked by sudden onset anxiety symptoms including rapid heartbeat, chest pain, trembling, and sweating.[97]

## 8. Oxidative stress in neurodegenerative disorders

Oxidative stress initiates a cascade of metabolic events through mitochondrial dysfunction, neuroinflammation, apoptosis, and tissue loss in the CNS. This disruption of homeostasis is a prominent cause of several neurodegenerative disorders, such as Alzheimer's disease, amyotrophic lateral sclerosis, Parkinson's disease, and Huntington's disease. Common features among these neurodegenerative diseases include mitochondrial dysfunction, Abnormal protein aggregation, and oxidative damage.[6] Excessive oxidative stress can impair the proteosome-ubiquitin system,[5,98] leading to the accumulation of abnormally aggregated proteins. In addition, it contributes to excitotoxicity, changes in iron metabolism, and inflammation.[99] Oxidative damage is evidenced by increased levels of lipid peroxidation end products, DNA base oxidation products, and oxidative protein damage. Abnormal protein aggregates frequently contain nitrated proteins, carbonyl residues, and advanced glycation end products. These events initiate

a cascade of metabolic processes, ultimately resulting in neuronal loss.[7]

### 8.1. Parkinson's disease

The hallmark of Parkinson's disease is the progressive loss of dopaminergic neurons, particularly in the substantia nigra region. Physiological changes associated with the disease include resting tremors, slowing of voluntary movements (bradykinesia), muscle rigidity, mask-like facial expression, and postural instability.[100] Parkinson's disease presents as a syndrome characterized by a range of symptoms, including posture instability, depression, impaired body equilibrium, and various other mental health issues. Pathologically, the disease is marked by the presence of Lewy bodies and the accumulation of various proteins such as α-synuclein, ubiquitin, and neurofilaments. Recent research suggests that an imbalance between oxidative stress and the antioxidant defense mechanism may contribute to the etiology of Parkinson's disease.[101] Studies have demonstrated the presence of oxidative markers in the cerebrospinal fluid (CSF) and blood of Parkinson's disease patients. In addition, deficiencies in the mitochondrial complex system have been observed in these patients.[102] This deficiency leads to an excessive production of ROS in the frontal cortex, fibroblasts, and platelets. Dopamine, an unstable molecule, undergoes auto-oxidation, thereby converting into dopamine quinones and free radicals. Under normal conditions, the concentration of dopamine is regulated by the enzymatic activities of monoamine oxidase (MAO)-A and MAO-B. However, in Parkinson's disease and aging, MAO concentration decreases in glial cells, contributing to dopamine autoxidation.[103] While the exact mechanism underlying oxidative stress and Parkinson's disease pathology remains unknown, oxidative stress is recognized as a common mechanism that leads to cellular dysfunction and, eventually, cell apoptosis. Treatment approaches primarily aim to provide symptomatic relief and include cell therapy, surgery, and medication.

### 8.2. Treatment of Parkinson's disease

#### *8.2.1. Pharmacological intervention*

Over the past 50 years, dopamine precursors in the form of syndopa, levodopa, or carbidopa have been used as symptomatic therapies for Parkinson's disease. These supplements, such as l-dihydroxyphenylalanine (L-DOPA), serve as precursors of dopamine, which are absorbed into nerve cells in the brain and subsequently converted into dopamine.[104] However, due to the progressive nature of Parkinson's disease, long-term use of these medications may result in fluctuations in patient outcomes. In addition, prolonged use of these drugs may lead to side effects such as hallucinations, constipation, mood swings, uncontrolled and involuntary movements, delusions, joint rigidity, and increased frequency of tremors. Another class of drugs used in Parkinson's therapy includes MAO inhibitors, which target enzymes involved in the metabolism of auto-oxidation of dopamine. Examples of these inhibitors include rasagiline, selegiline, and safinamide, which can be used either as an alternative to syndopa or levodopa or in combination with them. However, these drugs carry side effects such as nausea, vomiting, dizziness, fever, headaches, and vivid dreams.[105] In addition to these medications, other drugs may be employed in therapy to alleviate the side effects of levodopa. These drugs include clozapine and amitriptyline for addressing mental health issues, as well as rivastigmine and donepezil for managing dementia.

#### *8.2.2. Surgical therapy*

This procedure is effective in addressing various symptoms of Parkinson's disease, such as bradykinesia, tremors, instability in body postures, and rigidity in voluntary movements. It entails a neurosurgical intervention primarily intended for patients with movement disorders.[105] These movement disorders mainly arise from disorganized signals within the areas of the CNS responsible for controlling movements.[106] Conceptually, this procedure operates similarly to a pacemaker for the heart. Continuous pulses emitted from the neurostimulator are transmitted through leads to the brain. This treatment has been found beneficial for Parkinson's disease patients, often leading to improvements in symptoms such as tremors, stiffness, and bradykinesia. In addition, reports indicate that a deep brain stimulation (DBS) procedure can reduce the need for medication and improve symptom management in patients.[107] However, it is important to note that Parkinson's disease is a progressive disorder, and while these treatments can alleviate symptoms, a complete cure is not currently attainable.

#### *8.2.3. Cell replacement therapy (CRT)*

Patients treated with levodopa and DBS may develop problematic side effects such as speech problems, hallucinations, and neuropsychiatric effects. Therefore, targeted therapies such as CRT are urgently needed.[108] CRT is used for long-term treatment of motor movements by slowing down disease progression. It involves the use of cells such as neural stem cells, mesenchymal stem cells, and induced neural cells. While stem cells show promise in treatment, their use as a mainline treatment for Parkinson's disease presents several challenges.[109] Any type of graft or

stem cell requires a neurosurgical procedure along with a series of immunosuppression sessions. Allografts also carry the risk of infection and malignancy.[110]

### 8.3. Alzheimer's disease

Alzheimer's disease stands as the leading cause of neurodegeneration, affecting 4% of individuals above 65 years of age. It is a progressive neurodegenerative disorder with deadly consequences.[111] The pathological hallmarks of Alzheimer's disease include amyloid plaques (abnormal clumps), neurofibrillary or tau tangles (tangled bundles of fibers), and loss of neuronal connections.[112] These abnormal physiological and morphological changes in the brain result in memory loss, impaired reasoning or judgment, and issues in vision or spatial perception.[113]

#### *8.3.1. Oxidative stress in Alzheimer's disease*

Increased oxidative stress in Alzheimer's disease patients results in various clinical manifestations, including impairment in brain transition metal homeostasis, activation and overexpression of oxidases such as MAO, and mitochondrial dysfunctioning.[114] Numerous *in vitro* and *in vivo* studies have reported that amyloid β accumulation promotes ROS production and induces oxidative stress.[115-118] Mitochondrial dysfunctioning is considered the primary cause of Alzheimer's disease pathogenesis,[119] leading to a cascade of metabolic events such as altered expression and functioning of APP,[120] decreased mitochondrial transmembrane potential,[121] reduced activity of the sodium-potassium pump, and disruption of calcium and glutamate transportation.[122] As human life expectancy increases, the pathology of Alzheimer's disease becomes more complex. Consequently, there is an urgent need for solutions to address this emerging problem. Given that Alzheimer's disease involves a number of intricate metabolic pathways, oxidative stress and its effects on neurons are considered the central mechanism underlying its physiological manifestations.[123]

#### *8.3.2. Treatment of Alzheimer's disease*

The current treatment strategies primarily focus on inhibiting disease progression, as radical cures or disease-modifying treatments for Alzheimer's disease are still undergoing extensive research by researchers.[124] Treatment approaches for Alzheimer's disease involve

**Table 2. Clinical trials investigating polyphenols as a medication for neurological disorders**

| Trial ID | Phase | Condition | Intervention | Results | References |
|---|---|---|---|---|---|
| NCT01982578 | Phase II | 32 prodromal Alzheimer's patients (amyloid-positive cognitive impairment) | Oral supplementation of 120 mg of genistein for 12 months | Genistein may have a therapeutic role in delaying the onset of Alzheimer's disease with mild cognitive impairment | 131 |
| NCT00599508 | Preliminary clinical trial | 21 patients with age-related cognitive impairment | A daily dose of 148 g of blueberry powder for 16 weeks. | An increase in activation in the left lobe of the pre-central and pre-frontal gyrus during working memory load conditions, but there is no clear enhancement of working memory | 132 |
| NCT04685590 | Phase 2 | Five patients with early-onset Alzheimer's disease. | Daily dosage of 100 mg of dasatinib and 1000 mg of quercetin for 12 consecutive weeks | The central nervous system drug penetrance in Alzheimer's patients remains unknown | 133 |
| NCT01669317 | NA | 10 patients with chronic insomnia | Daily dosage of 240 ml of tart cherry juice for 14 weeks | The tart cherry juice is effective in the treatment of insomnia. It is an active ingredient in the reduction of plasma kynurenine and tryptophan enhancement | 134 |
| NCT03419039 | Phase 2 | 206 patients with mild cognitive impairment | 80 mg tablets of anthocyanins twice a day for 24 weeks | There was no significant difference in dementia in the treated group | 135 |
| NCT00799890 | Phase 2 | 31 patients with multiple sclerosis | Daily dosage of 1200 mg of oral EGCG for 36 months | Orally applied EGCG decreased the T-cell proliferation, suppression of NF-κB and inhibited the neuronal cell death | 136 |
| NCT02660112 | Phase 2 | 10 patients with Friedreich's ataxia | A daily dosage of 150 mg per day of epicatechin provided orally for 24 weeks | Improvement in neuronal functioning was measured using Friedreich's Ataxia Rating Scale, as epicatechin helps in mitochondrial biogenesis | 137 |

Abbreviation: NA: Not available; EGCG: Epigallocatechin gallate.

both pharmacological and non-pharmacological therapies due to the multifaceted nature of symptoms and the irreversible damage occurring at multiple levels, such as molecular, cellular, intercellular, and synaptic interactions. Early diagnosis and understanding of the disease's etiology can help alleviate symptoms, and numerous clinical trials and preclinical are underway. Medications approved by the United States Food and Drug Administration (US FDA) to reduce symptoms and alleviate disability include acetylcholine inhibitors such as donepezil, galantamine, rivastigmine, and N-methyl-d-aspartate antagonists. These medications are often combined with other drugs, such as benzodiazepines for anxiety and acetaminophen for sleep issues and pain relief. Risperidone is sometimes prescribed for severe agitation and psychosis. In later stages, Alzheimer's disease may manifest significant neuropsychiatric symptoms and behavioral issues, including language difficulties, disorientation, and changes in sleep cycle and mood swings.

#### *8.3.3. Antibody-based immunotherapies*

The primary pathological cause of Alzheimer's disease reported to date is the abnormal accumulation of amyloid plaques. US FDA has approved two monoclonal antibodies for use as drugs: aducanumab and lecanemab.[125] Numerous clinical trials and *in vitro* studies have reported that these are anti-amyloid antibodies capable of slowing down the deposition of amyloid and reducing cognitive decline.[126] These anti-amyloid β monoclonal antibodies are administrated intravenously to provide passive immunization. Several other monoclonal antibodies are still undergoing phase III clinical trials.[127] All these antibodies aim to counteract amyloid accumulation and halt the cascade of neurodegeneration. These interventions should decelerate the process of neurodegeneration and functional and cognitive decline.[128] Recently, four FDA-approved monoclonal antibodies targeting amyloid β are in late-phase clinical development, including lecanemab, aducanumab, gantenerumab, and donanemab. All of these are monoclonal IgG antibodies synthesized to act against amyloid aggregates.[129] Clinical trials investigating these four antibodies provide evidence of the intermediate effect of the drug on biomarkers and amyloid removal. However, the field of Alzheimer's disease trials is still progressing, and more additional favorable treatments for Alzheimer's disease are likely to be developed in the future[130] (Table 2).

## 9. Conclusion and future perspectives

Numerous studies have demonstrated the existence of several chronic pathologies induced by oxidative stress. However, the precise mechanism of cellular physiology remains undefined. It is well-established that oxidative stress triggers a cascade of events leading to neuronal damage. Given the multifaceted nature of these diseases, their underlying mechanisms remain elusive. Further, comprehensive studies are required to elucidate the signals induced by oxidative stress that contributes to physiological alternations in organs or neurons. Biomarkers of oxidative stress hold promise as diagnostic tools and therapeutic targets for early detection. Antioxidant therapy, along with a diet rich in antioxidants such as flavonoids, polyphenolic acids, lipoic acid, and vitamins, can serve as effective therapies. One significant consequence of ROS production is the overactivation of glutamate receptors. Therapeutic agents targeting these approaches show promise. Administering antioxidant therapy early, before neuronal loss, could prove beneficial. Several intriguing therapies, such as monoclonal antibodies against protein accumulation, modulation of calcium homeostasis, and anti-inflammatory agents, could complement antioxidant therapy in combination treatments. Natural products are being investigated and modified to focus on more biochemical pathways and enzymatic processing, which may aid in controlling and curing diseases with minimal side effects.

## Acknowledgments

None.

## Funding

Nihila Khola is a recipient of a fellowship from the Central University of Haryana. Kareena Moar is a recipient of a junior research fellowship from the Haryana State Council for Science, Innovation and Technology (HSCIT-3946). This agency had no role in the interpretation or writing the manuscript. The Indian Council of Medical Research (ICMR), Government of India, is gratefully acknowledged by Pawan Kumar Maurya for giving financial assistance (5/10/FR/03/2021-RBMCH).

## Conflict of interest

The authors declare no conflicts of interest.

## Author contributions

*Conceptualization:* Nikhila Khola, Kareena Moar
*Writing-original draft:* Kareena Moar
*Writing-review & editing:* Pawan Kumar Maurya

## Ethics approval and consent to participate

Not applicable.

## Consent for publication

Not applicable.

## Availability of data

Not applicable.

## References

1. Bardaweel SK, Gul M, Alzweiri M, Ishaqat A, ALSalamat HA, Bashatwah RM. Reactive oxygen species: The dual role in physiological and pathological conditions of the human body. *Eurasian J Med*. 2018;50(3):193-201.

   doi: 10.5152/eurasianjmed.2018

2. Jomova K, Raptova R, Alomar SY, *et al*. Reactive oxygen species, toxicity, oxidative stress, and antioxidants: Chronic diseases and aging. *Arch Toxicol*. 2023;97(10):2499-2574.

   doi: 10.1007/s00204-023-03562-9

3. Sun YY, Zhu HJ, Zhao RY, *et al*. Remote ischemic conditioning attenuates oxidative stress and inflammation via the Nrf2/HO-1 pathway in MCAO mice. *Redox Biol*. 2023;66:102852.

   doi: 10.1016/j.redox.2023.102852

4. Islam MT. Oxidative stress and mitochondrial dysfunction-linked neurodegenerative disorders. *Neurol Res*. 2017;39(1):73-82.

   doi: 10.1080/01616412.2016.1251711

5. Teleanu DM, Niculescu AG, Lungu II, *et al*. An overview of oxidative stress, neuroinflammation, and neurodegenerative diseases. *Int J Mol Sci*. 2022;23(11):5938.

   doi: 10.3390/ijms23115938

6. Singh A, Kukreti R, Saso L, Kukreti S. Oxidative stress: A key modulator in neurodegenerative diseases. *Molecules*. 2019;24(8):1583.

   doi: 10.3390/molecules24081583

7. Fischer R, Maier O. Interrelation of oxidative stress and inflammation in neurodegenerative disease: Role of TNF. *Oxid Med Cell Longev*. 2015;2015:610813.

   doi: 10.1155/2015/610813

8. Elfawy HA, Das B. Crosstalk between mitochondrial dysfunction, oxidative stress, and age-related neurodegenerative disease: Etiologies and therapeutic strategies. *Life Sci*. 2019;218:165-184.

   doi: 10.1016/j.lfs.2018.12.029

9. Hajam YA, Rani R, Ganie SY, *et al*. Oxidative stress in human pathology and aging: Molecular mechanisms and perspectives. *Cells*. 2022;11(3):552.

   doi: 10.3390/cells11030552

10. Olufunmilayo EO, Gerke-Duncan MB, Holsinger RMD. Oxidative stress and antioxidants in neurodegenerative disorders. *Antioxidants* (*Basel*). 2023;12(2):517.

    doi: 10.3390/antiox12020517

11. Simpson DSA, Oliver PL. ROS generation in microglia: Understanding oxidative stress and inflammation in neurodegenerative disease. *Antioxidants* (*Basel*). 2020;9(8):743.

    doi: 10.3390/antiox9080743

12. Harman D. Free radical theory of aging. *Mutat Res*. 1992;275:257-266.

    doi: 10.1016/0921-8734(92)90030-s

13. Ionescu-Tucker A, Cotman CW. Emerging roles of oxidative stress in brain aging and Alzheimer's disease. *Neurobiol Aging*. 2021;107:86-95.

    doi: 10.1016/j.neurobiolaging.2021.07.014

14. Banks WA, Reed MJ, Logsdon AF, Rhea EM, Erickson MA. Healthy aging and the blood-brain barrier. *Nat Aging*. 2021;1(3):243-254.

    doi: 10.1038/s43587-021-00043-5

15. Halliwell B. Oxidative stress and neurodegeneration: Where are we now. *J Neurochem*. 2006;97(6):1634-1658.

    doi: 10.1111/j.1471-4159.2006.03907.x

16. Moritz B, Schmitz AE, Rodrigues ALS, Dafre AL, Cunha MP. The role of vitamin C in stress-related disorders. *J Nutr Biochem*. 2020;85:108459.

    doi: 10.1016/j.jnutbio.2020.108459

17. Ullah A, Munir S, Badshah SL, *et al*. Important flavonoids and their role as a therapeutic agent. *Molecules*. 2020;25(22):5243.

    doi: 10.3390/molecules25225243

18. Calderaro A, Patanè GT, Tellone E, *et al*. The neuroprotective potentiality of flavonoids on Alzheimer's disease. *Int J Mol Sci*. 2022;23(23):14835.

    doi: 10.3390/ijms232314835

19. Singh SK, Srivastav S, Castellani RJ, Plascencia-Villa G, Perry G. Neuroprotective and antioxidant effect of *Ginkgo biloba* extract against AD and other neurological disorders. *Neurotherapeutics*. 2019;16(3):666-674.

    doi: 10.1007/s13311-019-00767-8

20. Carvalho AN, Firuzi O, Gama MJ, Horssen JV, Saso L. Oxidative stress and antioxidants in neurological diseases: Is there still hope? *Curr Drug Targets*. 2017;18(6):705-718.

    doi: 10.2174/1389450117666160401120514

21. Khan H, Singh TG, Dahiya RS, Abdel-Daim MM. α-Lipoic acid, an organosulfur biomolecule a novel therapeutic agent for neurodegenerative disorders: An mechanistic

perspective. *Neurochem Res*. 2022;47(7):1853-1864.

doi: 10.1007/s11064-022-03598-w

22. Singh S, Chauhan K. Pharmacological approach using doxycycline and tocopherol in rotenone induced oxidative stress, neuroinflammation and Parkinson's like symptoms. *Int J Neurosci*. 2022;132:1-6.

doi: 10.1080/00207454.2022.2154670

23. Ahmed S, Hasan MM, Heydari M, *et al*. Therapeutic potentials of crocin in medication of neurological disorders. *Food Chem Toxicol*. 2020;145:111739.

doi: 10.1016/j.fct.2020.111739

24. Zhou DD, Luo M, Huang SY, *et al*. Effects and mechanisms of resveratrol on aging and age-related diseases. *Oxid Med Cell Longev*. 2021;2021:9932218.

doi: 10.1155/2021/9932218

25. Sebastiani G, Almeida-Toledano L, Serra-Delgado M, *et al*. Therapeutic effects of catechins in less common neurological and neurodegenerative disorders. *Nutrients*. 2021;13(7):2232.

doi: 10.3390/nu13072232

26. Rahman MH, Akter R, Kamal MA. Prospective function of different antioxidant containing natural products in the treatment of neurodegenerative diseases. *CNS Neurol Disord Drug Targets*. 2021;20(8):694-703.

doi: 10.2174/1871527319666200722153611

27. Rauchová H. Coenzyme Q10 effects in neurological diseases. *Physiol Res*. 2021;70(Suppl 4):S683-S714.

doi: 10.33549/physiolres.934712

28. Mor A, Tankiewicz-Kwedlo A, Krupa A, Pawlak D. Role of Kynurenine pathway in oxidative stress during neurodegenerative disorders. *Cells*. 2021;10(7):1603.

doi: 10.3390/cells10071603

29. Eskandari MR, Eftekhari P, Abbaszadeh S, Noubarani M, Shafaghi B, Pourahmad J. Inhibition of different pain pathways attenuates oxidative stress in glial cells: A mechanistic view on neuroprotective effects of different types of analgesics. *Iran J Pharm Res*. 2021;20(3):204-215.

doi: 10.22037/ijpr.2021.114476.14871

30. Moraes CA, Zaverucha-do-Valle C, Fleurance R, Sharshar T, Bozza FA, d'Avila JC. Neuroinflammation in sepsis: Molecular pathways of microglia activation. *Pharmaceuticals* (*Basel*). 2021;14(5):416.

doi: 10.3390/ph14050416

31. Sharma V, Kaur A, Singh TG. Counteracting role of nuclear factor erythroid 2-related factor 2 pathway in Alzheimer's disease. *Biomed Pharmacother*. 2020;129:110373.

doi: 10.1016/j.biopha.2020.110373

32. Johnson JA, Johnson DA, Kraft AD, *et al*. The Nrf2-ARE pathway: An indicator and modulator of oxidative stress in neurodegeneration. *Ann N Y Acad Sci*. 2008;1147:61-69.

doi: 10.1196/annals.1427.036

33. Nguyen L, Lucke-Wold BP, Mookerjee SA, *et al*. Role of sigma-1 receptors in neurodegenerative diseases. *J Pharmacol Sci*. 2015;127(1):17-29.

doi: 10.1016/j.jphs.2014.12.005

34. Piechal A, Jakimiuk A, Mirowska-Guzel D. Sigma receptors and neurological disorders. *Pharmacol Rep*. 2021;73(6):1582-1594.

doi: 10.1007/s43440-021-00310-7

35. Ren P, Wang J, Li N, *et al*. Sigma-1 receptors in depression: Mechanism and therapeutic development. *Front Pharmacol*. 2022;13:925879.

doi: 10.3389/fphar.2022.925879

36. Jia J, Cheng J, Wang C, Zhen X. Sigma-1 receptor-modulated neuroinflammation in neurological diseases. *Front Cell Neurosci*. 2018;12:314.

doi: 10.3389/fncel.2018.00314

37. Smith SB. Introduction to sigma receptors: Their role in disease and as therapeutic targets. *Adv Exp Med Biol*. 2017;964:1-4.

doi: 10.1007/978-3-319-50174-1_1

38. Zhang G, Li Q, Tao W, *et al*. Sigma-1 receptor-regulated efferocytosis by infiltrating circulating macrophages/microglial cells protects against neuronal impairments and promotes functional recovery in cerebral ischemic stroke. *Theranostics*. 2023;13(2):543-559.

doi: 10.7150/thno.77088

39. Liguori I, Russo G, Curcio F, *et al*. Oxidative stress, aging, and diseases. *Clin Interv Aging*. 2018;13:757-772.

doi: 10.2147/CIA.S158513

40. López-Otín C, Blasco MA, Partridge L, Serrano M, Kroemer G. Hallmarks of aging: An expanding universe. *Cell*. 2023;186(2):243-278.

doi: 10.1016/j.cell.2022.11.001

41. Zhang H, Davies KJA, Forman HJ. Oxidative stress response and Nrf2 signaling in aging. *Free Radic Biol Med*. 2015;88(Pt B):314-336.

doi: 10.1016/j.freeradbiomed.2015.05.036

42. Pérez-Torres I, Castrejón-Téllez V, Soto ME, Rubio-Ruiz ME, Manzano-Pech L, Guarner-Lans V. Oxidative stress, plant natural antioxidants, and obesity. *Int J Mol Sci*. 2021;22(4):1786.

doi: 10.3390/ijms22041786

43. Sun Y, Ge X, Li X, *et al*. High-fat diet promotes renal injury by inducing oxidative stress and mitochondrial dysfunction. *Cell Death Dis*. 2020;11(10):914.

doi: 10.1038/s41419-020-03122-4

44. Pestel J, Blangero F, Watson J, Pirola L, Eljaafari A. Adipokines in obesity and metabolic-related-diseases. *Biochimie*. 2023;212:48-59.

doi: 10.1016/j.biochi.2023.04.008

45. Jia G, Aroor AR, Jia C, Sowers JR. Endothelial cell senescence in aging-related vascular dysfunction. *Biochim Biophys Acta Mol Basis Dis*. 2019;1865(7):1802-1809.

doi: 10.1016/j.bbadis.2018.08.008

46. Miller AA, Spencer SJ. Obesity and neuroinflammation: A pathway to cognitive impairment. *Brain Behav Immun*. 2014;42:10-21.

doi: 10.1016/j.bbi.2014.04.001

47. Han YP, Tang X, Han M, *et al.* Relationship between obesity and structural brain abnormality: Accumulated evidence from observational studies. *Ageing Res Rev*. 2021;71:101445.

doi: 10.1016/j.arr.2021.101445

48. Tan BL, Norhaizan ME, Liew WP. Nutrients and oxidative stress: Friend or foe? *Oxid Med Cell Longev*. 2018;2018:9719584.

doi: 10.1155/2018/9719584

49. Dikalov S, Itani H, Richmond B, *et al*. Tobacco smoking induces cardiovascular mitochondrial oxidative stress, promotes endothelial dysfunction, and enhances hypertension [published correction appears in *Am J Physiol Heart Circ Physiol*. 2019;316(4):H939]. *Am J Physiol Heart Circ Physiol*. 2019;316(3):H639-H646.

doi: 10.1152/ajpheart.00595.2018

50. Caliri AW, Tommasi S, Besaratinia A. Relationships among smoking, oxidative stress, inflammation, macromolecular damage, and cancer. *Mutat Res Rev Mutat Res*. 2021;787:108365.

doi: 10.1016/j.mrrev.2021.108365

51. Durazzo TC, Mattsson N, Weiner MW, Alzheimer's Disease Neuroimaging Initiative. Smoking and increased Alzheimer's disease risk: A review of potential mechanisms. *Alzheimers Dement*. 2014;10(3 Suppl):S122-S145.

doi: 10.1016/j.jalz.2014.04.009

52. Hahad O, Lelieveld J, Birklein F, Lieb K, Daiber A, Münzel T. Ambient air pollution increases the risk of cerebrovascular and neuropsychiatric disorders through induction of inflammation and oxidative stress. *Int J Mol Sci*. 2020;21(12):4306.

doi: 10.3390/ijms21124306

53. Song T, Song X, Zhu C, *et al.* Mitochondrial dysfunction, oxidative stress, neuroinflammation, and metabolic alterations in the progression of Alzheimer's disease: A meta-analysis of *in vivo* magnetic resonance spectroscopy studies. *Ageing Res Rev*. 2021;72:101503.

doi: 10.1016/j.arr.2021.101503

54. Nguyen A, Mandavalli A, Diaz MJ, *et al*. Neurosurgical anesthesia: Optimizing outcomes with agent selection. *Biomedicines*. 2023;11(2):372.

doi: 10.3390/biomedicines11020372

55. Bose A, Beal MF. Mitochondrial dysfunction and oxidative stress in induced pluripotent stem cell models of Parkinson's disease. *Eur J Neurosci*. 2019;49(4):525-532.

doi: 10.1111/ejn.14264

56. Jurcau A. Insights into the pathogenesis of neurodegenerative diseases: Focus on mitochondrial dysfunction and oxidative stress. *Int J Mol Sci*. 2021;22(21):11847.

doi: 10.3390/ijms222111847

57. Espay AJ, Aybek S, Carson A, *et al*. Current concepts in diagnosis and treatment of functional neurological disorders. *JAMA Neurol*. 2018;75(9):1132-1141.

doi: 10.1001/jamaneurol.2018.1264

58. Makkar R, Behl T, Bungau S, *et al*. Nutraceuticals in neurological disorders. *Int J Mol Sci*. 2020;21(12):4424.

doi: 10.3390/ijms21124424

59. Kang WY, Wang L, Qiu M, *et al*. Adrenal cavernous hemangioma: A case report and literature review. *Beijing Da Xue Xue Bao Yi Xue Ban*. 2021;53(4):808-810.

doi: 10.19723/j.issn.1671-167X.2021.04.032

60. Jurca CM, Kozma K, Petchesi CD, *et al*. Tuberous sclerosis, type II diabetes mellitus and the PI3K/AKT/mTOR signaling pathways-case report and literature review. *Genes* (*Basel*). 2023;14(2):433.

doi: 10.3390/genes14020433

61. Karageorgiou I, Chandler C, Whyte MB. Silent diabetes mellitus, periodontitis and a new case of thalamic abscess. *BMJ Case Rep.* 2014;2014:bcr2014204654.

doi: 10.1136/bcr-2014-204654

62. Cahyanur R, Setyawan W, Sudrajat DG, Setyowati S, Purnamasari D, Soewondo P. Diagnosis and management of acromegaly: Giant invasive adenoma. *Acta Med Indones*. 2011;43(2):122-128.

63. Ridker PM, MacFadyen JG, Thuren T, *et al.* Effect of interleukin-1β inhibition with canakinumab on incident lung cancer in patients with atherosclerosis: Exploratory results from a randomised, double-blind, placebo-controlled trial. *Lancet*. 2017;390(10105):1833-1842.

doi: 10.1016/S0140-6736(17)32247-X

64. Ha J, Choi DW, Kim KJ, *et al*. Association of metformin use with Alzheimer's disease in patients with newly diagnosed type 2 diabetes: A population-based nested case-control study. *Sci Rep*. 2021;11(1):24069.

doi: 10.1038/s41598-021-03406-5

65. Biag HMB, Potter LA, Wilkins V, *et al*. Metformin treatment in young children with fragile X syndrome. *Mol Genet Genomic Med*. 2019;7(11):e956.

doi: 10.1002/mgg3.956

66. Winship IR, Dursun SM, Baker GB, *et al*. An overview of animal models related to schizophrenia. *Can J Psychiatry*. 2019;64(1):5-17.

doi: 10.1177/0706743718773728

67. Owen MJ, Sawa A, Mortensen PB. Schizophrenia. *Lancet*. 2016;388(10039):86-97.

doi: 10.1016/S0140-6736(15)01121-6

68. Stępnicki P, Kondej M, Kaczor AA. Current concepts and treatments of schizophrenia. *Molecules*. 2018;23(8):2087.

doi: 10.3390/molecules23082087

69. Kane JM, Agid O, Baldwin ML, *et al*. Clinical guidance on the identification and management of treatment-resistant schizophrenia. *J Clin Psychiatry*. 2019;80(2):18com12123.

doi: 10.4088/JCP.18com12123

70. Javitt DC. Cognitive impairment associated with schizophrenia: From pathophysiology to treatment. *Annu Rev Pharmacol Toxicol*. 2023;63:119-141.

doi: 10.1146/annurev-pharmtox-051921-093250

71. Yang AC, Tsai SJ. New targets for schizophrenia treatment beyond the dopamine hypothesis. *Int J Mol Sci*. 2017;18(8):1689.

doi: 10.3390/ijms18081689

72. Donegan JJ, Lodge DJ. Cell-based therapies for the treatment of schizophrenia. *Brain Res*. 2017;1655:262-269.

doi: 10.1016/j.brainres.2016.08.010

73. Tiihonen J, Mittendorfer-Rutz E, Majak M, *et al*. Real-world effectiveness of antipsychotic treatments in a nationwide cohort of 29 823 patients with schizophrenia. *JAMA Psychiatry*. 2017;74(7):686-693.

doi: 10.1001/jamapsychiatry.2017.1322

74. Wu Y, Yang Z, Cui S. Update research advances in the application of transcranial magnetic stimulation in the treatment of schizophrenia. *Scanning*. 2022;2022:5415775.

doi: 10.1155/2022/5415775

75. Maroney M. An update on current treatment strategies and emerging agents for the management of schizophrenia. *Am J Manag Care*. 2020;26(3 Suppl):S55-S61.

doi: 10.37765/ajmc.2020.43012

76. Trivedi MH. Major depressive disorder in primary care: Strategies for identification. *J Clin Psychiatry*. 2020;81(2):UT17042BR1C.

doi: 10.4088/JCP.UT17042BR1C

77. Gu X, Ke S, Wang Q, *et al*. Energy metabolism in major depressive disorder: Recent advances from omics technologies and imaging. *Biomed Pharmacother*. 2021;141:111869.

doi: 10.1016/j.biopha.2021.111869

78. Zhdanava M, Pilon D, Ghelerter I, *et al*. The prevalence and national burden of treatment-resistant depression and major depressive disorder in the United States. *J Clin Psychiatry*. 2021;82(2):20m13699.

doi: 10.4088/JCP.20m13699

79. Dwyer JB, Aftab A, Radhakrishnan R, *et al*. Hormonal treatments for major depressive disorder: State of the art [published correction appears in *Am J Psychiatry*. 2020;177(7):642] [published correction appears in *Am J Psychiatry*. 2020;177(10):1009]. *Am J Psychiatry*. 2020;177(8):686-705.

doi: 10.1176/appi.ajp.2020.19080848

80. Paris J. The mistreatment of major depressive disorder. *Can J Psychiatry*. 2014;59(3):148-151.

doi: 10.1177/070674371405900306

81. Chiriţă AL, Gheorman V, Bondari D, Rogoveanu I. Current understanding of the neurobiology of major depressive disorder. *Rom J Morphol Embryol*. 2015;56(2 Suppl):651-658.

82. Kang SG, Cho SE. Neuroimaging biomarkers for predicting treatment response and recurrence of major depressive disorder. *Int J Mol Sci*. 2020;21(6):2148.

doi: 10.3390/ijms21062148

83. Hofmann SG, Gómez AF. Mindfulness-based interventions for anxiety and depression. *Psychiatr Clin North Am*. 2017;40(4):739-749.

doi: 10.1016/j.psc.2017.08.008

84. Zhang Z, Zhang L, Zhang G, Jin J, Zheng Z. The effect of CBT and its modifications for relapse prevention in major depressive disorder: A systematic review and meta-analysis. *BMC Psychiatry*. 2018;18(1):50.

doi: 10.1186/s12888-018-1610-5

85. Mirchandaney R, Barete R, Asarnow LD. Moderators of cognitive behavioral treatment for insomnia on depression and anxiety outcomes. *Curr Psychiatry Rep*. 2022;24(2):121-128.

doi: 10.1007/s11920-022-01326-3

86. Tondo L, Vázquez GH, Baldessarini RJ. Depression and Mania in bipolar disorder. *Curr Neuropharmacol*. 2017;15(3):353-358.

doi: 10.2174/1570159X14666160606210811

87. Harrison PJ, Geddes JR, Tunbridge EM. The emerging neurobiology of bipolar disorder. *Trends Neurosci*. 2018;41(1):18-30.

doi: 10.1016/j.tins.2017.10.006

88. Solé B, Jiménez E, Torrent C, *et al*. Cognitive impairment in bipolar disorder: Treatment and prevention strategies. *Int J Neuropsychopharmacol*. 2017;20(8):670-680.

doi: 10.1093/ijnp/pyx032

89. Arnold I, Dehning J, Grunze A, Hausmann A. Old age bipolar disorder-epidemiology, aetiology and treatment. *Medicina* (*Kaunas*). 2021;57(6):587.

doi: 10.3390/medicina57060587

90. McCormick U, Murray B, McNew B. Diagnosis and treatment of patients with bipolar disorder: A review for advanced practice nurses. *J Am Assoc Nurse Pract*. 2015;27(9):530-542.

doi: 10.1002/2327-6924.12275

91. Kato T. Current understanding of bipolar disorder: Toward integration of biological basis and treatment strategies. *Psychiatry Clin Neurosci*. 2019;73(9):526-540.

doi: 10.1111/pcn.12852

92. Post RM, Grunze H. The challenges of children with bipolar disorder. *Medicina* (*Kaunas*). 2021;57(6):601.

doi: 10.3390/medicina57060601

93. Maron E, Nutt D. Biological markers of generalized anxiety disorder. *Dialogues Clin Neurosci*. 2017;19(2):147-158.

doi: 10.31887/DCNS.2017.19.2/dnutt

94. Locke AB, Kirst N, Shultz CG. Diagnosis and management of generalized anxiety disorder and panic disorder in adults. *Am Fam Physician*. 2015;91(9):617-624.

95. Muris P, Ollendick TH. Selective mutism and its relations to social anxiety disorder and autism spectrum disorder. *Clin Child Fam Psychol Rev*. 2021;24(2):294-325.

doi: 10.1007/s10567-020-00342-0

96. Ströhle A, Gensichen J, Domschke K. The diagnosis and treatment of anxiety disorders. *Dtsch Arztebl Int*. 2018;155(37):611-620.

doi: 10.3238/arztebl.2018.0611

97. Kaczkurkin AN, Foa EB. Cognitive-behavioral therapy for anxiety disorders: An update on the empirical evidence. *Dialogues Clin Neurosci*. 2015;17(3):337-346.

doi: 10.31887/DCNS.2015.17.3/akaczkurkin

98. Vejux A. Cell death, inflammation and oxidative stress in neurodegenerative diseases: Mechanisms and cytoprotective molecules. *Int J Mol Sci*. 2021;22(24):13657.

doi: 10.3390/ijms222413657

99. Niedzielska E, Smaga I, Gawlik M, *et al*. Oxidative stress in neurodegenerative diseases. *Mol Neurobiol*. 2016;53(6):4094-4125.

doi: 10.1007/s12035-015-9337-5

100. Trist BG, Hare DJ, Double KL. Oxidative stress in the aging substantia nigra and the etiology of Parkinson's disease. *Aging Cell*. 2019;18(6):e13031.

doi: 10.1111/acel.13031

101. Dias V, Junn E, Mouradian MM. The role of oxidative stress in Parkinson's disease. *J Parkinsons Dis*. 2013;3(4):461-491.

doi: 10.3233/JPD-130230

102. Badanjak K, Fixemer S, Smajić S, Skupin A, Grünewald A. The contribution of microglia to neuroinflammation in Parkinson's disease. *Int J Mol Sci*. 2021;22(9):4676.

doi: 10.3390/ijms22094676

103. Miyazaki I, Asanuma M. Neuron-astrocyte interactions in Parkinson's disease. *Cells*. 2020;9(12):2623.

doi: 10.3390/cells9122623

104. Vrijsen S, Houdou M, Cascalho A, Eggermont J, Vangheluwe P. Polyamines in Parkinson's disease: Balancing between neurotoxicity and neuroprotection. *Annu Rev Biochem*. 2023;92:435-464.

doi: 10.1146/annurev-biochem-071322-021330

105. Elsworth JD. Parkinson's disease treatment: Past, present, and future. *J Neural Transm* (*Vienna*). 2020;127(5):785-791.

doi: 10.1007/s00702-020-02167-1

106. Gao C, Liu J, Tan Y, Chen S. Freezing of gait in Parkinson's disease: Pathophysiology, risk factors and treatments. *Transl Neurodegener*. 2020;9:12.

doi: 10.1186/s40035-020-00191-5

107. Pajares M, Rojo AI, Manda G, Boscá L, Cuadrado A. Inflammation in Parkinson's disease: Mechanisms and therapeutic implications. *Cells*. 2020;9(7):1687.

doi: 10.3390/cells9071687

108. Sonntag KC, Song B, Lee N, *et al*. Pluripotent stem cell-based therapy for Parkinson's disease: Current status and future prospects. *Prog Neurobiol*. 2018;168:1-20.

doi: 10.1016/j.pneurobio.2018.04.005

109. Fabbri M, Barbosa R, Rascol O. Off-time treatment options for Parkinson's disease [published correction appears in *Neurol Ther*. 2023]. *Neurol Ther*. 2023;12(2):391-424.

doi: 10.1007/s40120-022-00435-8

110. Radhakrishnan DM, Goyal V. Parkinson's disease: A review. *Neurol India*. 2018;66(Suppl):S26-S35.

doi: 10.4103/0028-3886.226451

111. Pirker W, Katzenschlager R, Hallett M, Poewe W. Pharmacological treatment of tremor in Parkinson's disease revisited. *J Parkinsons Dis*. 2023;13(2):127-144.

doi: 10.3233/JPD-225060

112. Scheltens P, De Strooper B, Kivipelto M, *et al*. Alzheimer's disease. *Lancet*. 2021;397(10284):1577-1590.

doi: 10.1016/S0140-6736(20)32205-4

113. Weller J, Budson A. Current understanding of Alzheimer's disease diagnosis and treatment. *F1000Res*. 2018;7:F1000 Faculty Rev-1161.

doi: 10.12688/f1000research.14506.1

114. Khan S, Barve KH, Kumar MS. Recent advancements in pathogenesis, diagnostics and treatment of Alzheimer's disease. *Curr Neuropharmacol*. 2020;18(11):1106-1125.

doi: 10.2174/1570159X18666200528142429

115. Breijyeh Z, Karaman R. Comprehensive review on Alzheimer's disease: Causes and treatment. *Molecules*. 2020;25(24):5789.

doi: 10.3390/molecules25245789

116. Bondi MW, Edmonds EC, Salmon DP. Alzheimer's disease: Past, present, and future. *J Int Neuropsychol Soc*. 2017;23(9-10):818-831.

doi: 10.1017/S135561771700100X

117. Graff-Radford J, Yong KXX, Apostolova LG, *et al*. New insights into atypical Alzheimer's disease in the era of biomarkers. *Lancet Neurol*. 2021;20(3):222-234.

doi: 10.1016/S1474-4422(20)30440-3

118. Briggs R, Kennelly SP, O'Neill D. Drug treatments in Alzheimer's disease. *Clin Med* (*Lond*). 2016;16(3):247-253.

doi: 10.7861/clinmedicine.16-3-247

119. Rostagno AA. Pathogenesis of Alzheimer's disease. *Int J Mol Sci*. 2022;24(1):107.

doi: 10.3390/ijms24010107

120. Ferrari C, Sorbi S. The complexity of Alzheimer's disease: An evolving puzzle. *Physiol Rev*. 2021;101(3):1047-1081.

doi: 10.1152/physrev.00015.2020

121. Stefaniak O, Dobrzyńska M, Drzymała-Czyż S, Przysławski J. Diet in the prevention of Alzheimer's disease: Current knowledge and future research requirements. *Nutrients*. 2022;14(21):4564.

doi: 10.3390/nu14214564

122. Knapskog AB, Engedal K, Selbæk G, Øksengård AR. Alzheimers sykdom - diagnostikk og behandling [Alzheimer's disease - diagnosis and treatment]. *Tidsskr Nor Laegeforen*. 2021;141(7).

doi: 10.4045/tidsskr.20.0919

123. Stern Y. Cognitive reserve in ageing and Alzheimer's disease. *Lancet Neurol*. 2012;11(11):1006-1012.

doi: 10.1016/S1474-4422(12)70191-6

124. Penney J, Ralvenius WT, Tsai LH. Modeling Alzheimer's disease with iPSC-derived brain cells. *Mol Psychiatry*. 2020;25(1):148-167.

doi: 10.1038/s41380-019-0468-3

125. Chen ZY, Zhang Y. Animal models of Alzheimer's disease: Applications, evaluation, and perspectives. *Zool Res*. 2022;43(6):1026-1040.

doi: 10.24272/j.issn.2095-8137.2022.289

126. Sun BL, Li WW, Zhu C, *et al*. Clinical research on Alzheimer's disease: Progress and perspectives. *Neurosci Bull*. 2018;34(6):1111-1118.

doi: 10.1007/s12264-018-0249-z

127. Toups K, Hathaway A, Gordon D, *et al*. Precision medicine approach to Alzheimer's disease: Successful pilot project. *J Alzheimers Dis*. 2022;88(4):1411-1421.

doi: 10.3233/JAD-215707

128. Ma C, Hong F, Yang S. Amyloidosis in Alzheimer's disease: Pathogeny, etiology, and related therapeutic directions. *Molecules*. 2022;27(4):1210.

doi: 10.3390/molecules27041210

129. Liu S, Gao J, Zhu M, Liu K, Zhang HL. Gut microbiota and dysbiosis in Alzheimer's disease: Implications for pathogenesis and treatment. *Mol Neurobiol*. 2020;57(12):5026-5043.

doi: 10.1007/s12035-020-02073-3

130. Beata BK, Wojciech J, Johannes K, Piotr L, Barbara M. Alzheimer's disease-biochemical and psychological background for diagnosis and treatment. *Int J Mol Sci*. 2023;24(2):1059.

doi: 10.3390/ijms24021059

131. Viña J, Escudero J, Baquero M, *et al*. Genistein effect on cognition in prodromal Alzheimer's disease patients. The GENIAL clinical trial. *Alzheimers Res Ther*. 2022;14(1):164.

doi: 10.1186/s13195-022-01097-2

132. Boespflug EL, Eliassen JC, Dudley JA, *et al*. Enhanced neural activation with blueberry supplementation in mild cognitive impairment. *Nutr Neurosci*. 2018;21(4):297-305.

doi: 10.1080/1028415X.2017.1287833

133. Gonzales MM, Garbarino VR, Marques Zilli E, *et al*. Senolytic therapy to modulate the progression of Alzheimer's disease (SToMP-AD): A pilot clinical trial.

*J Prev Alzheimers Dis*. 2022;9(1):22-29.

doi: 10.14283/jpad.2021.62

134. Losso JN, Finley JW, Karki N, *et al*. Pilot study of the tart cherry juice for the treatment of insomnia and investigation of mechanisms. *Am J Ther*. 2018;25(2):e194-e201.

doi: 10.1097/MJT.0000000000000584

135. Aarsland D, Khalifa K, Bergland AK, *et al*. A randomised placebo-controlled study of purified anthocyanins on cognition in individuals at increased risk for dementia. *Am J Geriatr Psychiatry*. 2023;31(2):141-151.

doi: 10.1016/j.jagp.2022.10.002

136. Rust R, Chien C, Scheel M, *et al*. Epigallocatechin gallate in progressive MS: A randomized, placebo-controlled trial. *Neurol Neuroimmunol Neuroinflamm*. 2021;8(3):e964.

doi: 10.1212/NXI.0000000000000964

137. Qureshi MY, Patterson MC, Clark V, *et al*. Safety and efficacy of (+)-epicatechin in subjects with Friedreich's ataxia: A phase II, open-label, prospective study. *J Inherit Metab Dis*. 2021;44(2):502-514.

doi: 10.1002/jimd.12285

ACCSCIENCE PUBLISHING

Brain & Heart

REVIEW ARTICLE

# Recognition predictive modeling using electroencephalogram

**S. K. B. Sangeetha[1], Sandeep Kumar Mathivanan[2], Saurav Mallik[3,4]*, and Aimin Li[5]**

[1]Department of Computer Science and Engineering, Faculty of Computer Science and Engineering, SRM Institute of Science and Technology, Chennai, Tamil Nadu, India

[2]Department of Computer Science and Engineering, School of Computer Science and Engineering, Galgotias University, Greater Noida, Uttar Pradesh, India

[3]Department of Environmental Health, Harvard T.H. Chan School of Public Health, Boston, Massachusetts, United States of America

[4]Department of Pharmacology and Toxicology, The University of Arizona, Tucson, Arizona, United States of America

[5]School of Computer Science and Engineering, Xi'an University of Technology, Xi'an, Shaanxi, China

(This article belongs to *Special Issue: Deep Learning and Optimization Insight into Cardiovascular Risk Factors, Cognitive Decline*)

## Abstract

A machine learning model that operates on raw electroencephalogram (EEG) signals is essential for accurately discerning the user's current thoughts. Given the difficulty of categorizing EEG signals for use in brain-computer interface (BCI) programs, we adopted a systematic approach in this study to select an optimal predictive model. To enhance the effectiveness of our systematic approach, we extracted features such as band powers, averages, and root-mean-squared values. K-nearest neighbor (KNN), principal component analysis, and dual-layer neural networks were employed to evaluate and validate the effectiveness of the extracted features. The BCI IV competition-I dataset was utilized for analysis and validation. KNN achieved an average classification success rate of 98.02% compared to other methods. Furthermore, our research extends the application of this approach using it to create, test, and evaluate human driving behavior as a case study.

***Keywords:*** Brain-computer interface; Electroencephalogram; Feature extraction; Human-computer interface; Machine learning; Neural network

***Corresponding author:**
Saurav Mallik
(smallik@arizona.edu)

**Citation:** Sangeetha SKB, Mathivanan SK, Mallik S, Li A. Recognition predictive modeling using electroencephalogram. *Brain & Heart.* 2024;2(2):2819. doi: 10.36922/bh.2819

**Received:** January 24, 2024

**Accepted:** March 19, 2024

**Published Online:** May 15, 2024



## 1. Introduction

With recent developments in imaging techniques for the brain and the field of cognitive neuroscience, we now have the ability to directly interface with individuals' minds. Studies of how our thoughts evolve over time may be recorded and monitored in the form of low-power electrical signals using these technologies and cutting-edge sensors. This knowledge has paved the way for brain-computer interfaces (BCIs) and other types of communication systems that allow users to control computers and equipment solely with their minds as opposed to physically moving them.[1] BCIs have moved their attention

from creating devices to creating systems that address the challenges that individuals with physical limitations encounter. In particular, individuals with catastrophic neuromuscular injuries or progressive neurodegenerative diseases, which impair the user's ability to move voluntarily but leave their brain intact, have a pressing need for such systems. Recent advances in BCI research have aligned with trends in other human-computer interaction (HCI) studies in narrowing their attention.[2]

The initial step in building a BCI is acquiring reliable electroencephalogram (EEG) signals. Understanding the brain's physiology and anatomy in depth is crucial. This knowledge aids in pinpointing the optimal spots for sensing nodes and taking the necessary measurements. The human brain contains roughly one hundred billion nerve cells (neurons), each capable of collecting and transmitting electrochemical signals to other neurons, sometimes over very long distances. By relaying signals from the brain to the rest of the body's neurons, the brain directs cognitive and motor processes. The two hemispheres of the brain exhibit differences in specialization and processing styles, with certain functions being more dominant in one hemisphere over the other. However, cognitive tasks typically involve interactions between both hemispheres, highlighting their interconnectedness and collaborative nature.[3] For instance, tasks requiring imagination and creativity, such as recognizing faces, expressing emotions, and reading emotions, tend to be associated with the right brain, while logical and analytical processes, such as critical thinking and reasoning, tend to be associated with the left. Most motor and sensory signals between the brain and the body travel across the cerebral midline, with the right hemisphere sensing and controlling the left side of the body and vice versa.[4]

Recorded signals are the numerical representation of voltage fluctuations caused by the movement of electrochemical currents within the brain's neurons. The term "electroencephalography" describes the method by which this activity is captured along the scalp. Metal disks called electrodes are applied to the scalp and used to record signals. These electrodes are moistened with a conducting gel or liquid to keep them in contact with the underlying electrical signals.[5] Some commercial dry EEG headsets, however, are starting to make an appearance in the BCI world, and these could be used to capture data and transfer it to a computer through a wireless medium. Electrode patterns of EEG signals indicate ongoing brain activity, with the varying signal strengths reflecting the effects of the body's mental and physical states. EEG signals over the brain's surface have been recorded at intensities between 0 and 200 μV.[6]

The brain's signaling rhythms are typically categorized into bands according to their frequencies. Although the names for these frequency ranges are arbitrary, they are commonly used to imply that the rhythmic activity observed at those frequencies holds biological significance and follows a particular pattern of distribution across the scalp.[7] The typical placement of electrodes is presented in Figure 1A and B.[8]

BCIs focus on eliciting brain signals associated with specific types of thought and translating them into machine commands. It represents a form of communication where thoughts, rather than conventional nerves and muscles, serve as the means to transmit information. In the early stages of BCI research and development, researchers concentrated on creating assistive devices for individuals with physical disabilities. However, the demand for BCIs and public awareness surrounding them has surged, leading researchers to explore their potential applications across various fields beyond medicine. Future user-communication systems may require offering input on the user's mental state or intentions in addition to their physical state, representing one of the most discussed possible uses for BCIs.[9]

Both dependent and independent BCIs are common. In dependent BCIs, conventional output pathways in the brain are bypassed, whereas autonomous BCIs operate without reliance on the brain's typical output pathways. In a dependent BCI, such as one utilizing a sample matrix of blinking letters, the eye's gaze direction determines the direction of the EEG signal. In contrast, an independent BCI's EEG signal is based on the user's intention to select a particular letter. To operate BCIs successfully, users must learn and maintain the skill of regulating different types of electrophysiological signals to achieve their desired interaction outcomes. The BCI must then translate this regulation into machine commands that carry out the user's intended action. Consequently, users must train themselves to deliberately control their brain waves.[10]

There are currently two methods for teaching users to regulate their own brain waves. The first type requires users to engage in targeted mental activities, like motor imagery, to produce detectable brain activity. By mentally imagining sequences of rest and movement – for example, raising and lowering one's arms or performing high kicks – the user can send binary data to a computer. The second technique, called operant conditioning, involves providing immediate feedback to the user as they attempt to control the interface. As long as the goal is met, it does not matter what a user is thinking about. Eventually, after multiple sessions, the user will be able to complete the task without thinking about the interface at all. However, many

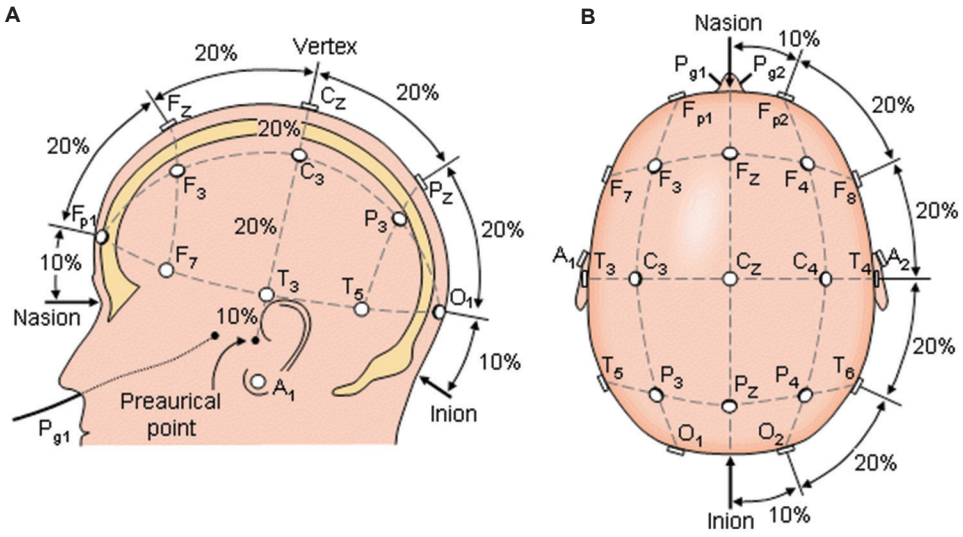


**Figure 1.** Standard electrode positions. (A) Left side view and (B) Top view.

users struggle to master this method. The use of mobile phones, even when hands-free or activated by voice, is just as risky as driving while intoxicated, according to recent studies that analyzed brain imaging results of cell phone use while driving.[11] The purpose of this study is to examine better classifier models to work with EEG data. The main contributions of this study are twofold: (i) to develop an approach for choosing a better predictive model to address EEG data for use in BCI systems, and (ii) to validate this approach through the analysis of human driving behavior.

## 2. Related studies

Data collected and processed in the time domain, the spatial domain, or both can serve as the basis for an EEG-based conversation. Users can manipulate the characteristics of electrophysiological signals on demand with adequate training and practice, making EEG signals widely employed in BCI research. Most current BCIs are built to detect specific patterns of brain activity that can then be translated into physical actions. Many different signal patterns have been studied, and it has been claimed that some of them are particularly easy to recognize and control. There are essentially two types of signals here: (i) visual-evoked potentials and (ii) slow cortical potentials (SCPs). The brain's electrical potentials that are elicited by visual stimuli, such as light, are known as visual evoked potentials. Gaze control is crucial for the effective operation of such signals. Applications currently utilizing these signals aim to generate motor output in robots in response to the user's gaze direction. When an EEG is recorded over the scalp, the lowest frequency components are typically attributed to slow voltage fluctuations in the cortex. SCPs refer to changes in cortical potential that take place over 0.5–10.0 s. As a rule, negative SCPs are linked to motor and other cortically activated functions, while positive SCPs are associated with deactivated cortical regions.[12]

The biopotentials from the scalp's surface are recorded to create an EEG. These recordings capture electrochemical potentials gathered from neurons in the human brain's cerebrum. Initial inspection of EEG data may reveal a chaotic, non-stationary, and noisy signal. To isolate individual brain wave components, cutting-edge signal processing methods are required. After being broken down into their constituent parts, these pieces can be linked to specific regions and functions of the brain. Acquiring potential from a single neuron is extremely inefficient. Instead, the final electrical potential recorded at a single sensor node is sufficient for subsequent signal processing stages. Studies of brain topology have shown that neurons in the same general area will all fire in response to any mental or physical activity that has a localized basis.[13]

In addition, choosing between a non-invasive and an invasive approach to obtaining the signals is crucial. There is no strict rule against using both invasive and non-invasive techniques, as well as both evoked and spontaneous inputs. Electrode signals are collected, amplified, and digitized to make them usable in the subsequent steps. However, eye (EOG: electrooculogram) or muscle (EMG: electromyogram) electrical activity can introduce noise into the acquired EEG data, which can be mitigated by maintaining ideal conditions during the signal acquisition, such as staying in a comfortable, motionless position. However, in real-world scenarios, BCIs cannot mimic laboratory conditions, and such systems are not trusted to control embedded applications like wheelchairs in outdoor

environments. In general, this issue can be fixed by effective pre-processing techniques.[14] With potential applications in the diagnosis and treatment of sleep disorders, the study offers a promising method for enhancing the classification of sleep states using deep learning models and sophisticated signal processing techniques.[15]

In EEG research, segmenting signals into their component frequency bands is crucial because each band is associated with a different type of cognitive process. To isolate the signal components related to the studied physiological action, temporal filters such as low-pass and band-pass filters are used. In the course of signal processing, the alpha and beta rhythms are typically extracted for tasks involving motor imagery. Temporal filtering is facilitated by tools such as the discrete Fourier transform and filters based on the finite impulse response (FIR). Spatial filters serve a similar purpose, removing unwanted information from EEG signals. However, to obtain a comprehensive understanding of the physiological task, recording data from a small number of electrodes in close proximity is necessary. Taking into account a larger number of nodes could lead to complications such as redundancies, channel correlations, features, and increased training data requirements. Noise-free copies of the original signals can be easily generated using spatial filters by defining linear combinations of the original signals.[16]

EEG signal processing and BCI implementations have greatly benefited from the application of independent component analysis (ICA). ICA separates the information coming from various parts of the brain, increasing the likelihood that only signals from the desired areas will be retained, while components likely to be artifacts or noise can be discarded. Subsequently, EEG signals can be reconstructed based on the chosen features. One of the most popular spatial filtering methods in BCI studies is common spatial patterns.[17] This technique entails mapping EEG readings onto spatial patterns, with the patterns selected to increase the dissimilarity between the studied groups, aiding in data categorization. Dimension reduction and appropriate techniques for identifying differences in signals belonging to different classes are crucial, as different physiological actions can produce distinct signal patterns. In some cases, it is not possible to observe the differences simply by inspecting or using classifying techniques on the original signals. Feature extraction is frequently employed to specify an interesting signal and illustrate the similarities and differences between signals belonging to the same class and those belonging to different classes.[18]

A BCI's classification phase is critical, with feature extraction and identification being two of its most crucial components. The BCI will struggle during the test phase to accurately classify the training signals into the appropriate classes if the EEG features retrieved from the data are not pertinent to the associated neurophysiological event. It is advisable to use an effective feature extraction technique to enhance the speed and efficiency of the BCI rather than directly applying classification steps to the raw signals, which could produce results but would take time. The EEG data can be subjected to various simple measurements to glean the necessary information, and transformations can be applied to the signal to provide a new perspective. Machine learning (ML) finds applications in diverse fields, such as spam filtering, computer vision, and weather forecasting. Effective feature extraction separates the extracted features into discrete classes from training datasets, enabling the categorization of test signals according to the various physiological tasks performed.[19]

Most ML systems force you to make a tradeoff between bias and variance due to the inverse relationship between the two. A large proportion of stable classifiers have low variance and high bias, while the unstable ones have high variance and low bias. Given this fact, straightforward models may outperform their complex counterparts. The experimental results must be validated by addressing bias and variance issues, which requires an understanding of the significance of cross-validation. Model selection and performance estimation inspire validation methods. The success of pattern recognition and classification methods typically relies on one or more ad hoc parameters.[20,21] Table 1 below compares and contrasts various ML approaches in terms of their respective levels of difficulty.

Following the model selection process, the model's performance can be estimated by calculating its true error rate, which is the classifier's error rate across the entire dataset. Optimizing the system involves raising the model's complexity and introducing some variance error while simultaneously lowering the bias error to lower the training error. However, there is no guarantee that adding new test data will improve the learned model's performance.[8,22] In this setting, access to validation data, in addition to traditional training and test data, is crucial. Model selection

**Table 1. Comparison of machine learning methods**

| Method | Difficulties |
|---|---|
| Nonlinear regression | Levels of complexity in polynomials |
| Decision trees | The number of levels can be customized |
| Regularized models | Modifying the regularization parameter in various ways |
| K-nearest neighbors | Different choice of k |
| Support vector machine | Different choices of hyperparameter |
| Kernel-based methods | Different choices of kernels |

relies on validation data to check how well various trained models perform. Researchers are increasingly interested in diving into more complex and automated feature extraction methods, suggesting that the field of feature extraction is reaching its point of diminishing returns. For certain biological signals, choosing the optimal feature from extracted features may not always be straightforward since some features may not be equally informative, may lose some important information present in the raw data, or maybe noisy, correlated, or irrelevant.[23] To understand how to represent the data and make complex EEG oscillatory data useful for categorization, ML models were applied.

## 3. System model

Data acquisition, signal processing, and application control are the backbone of any BCI system, as depicted in Figure 2. These parts must all function simultaneously so that the whole can accomplish its goals.

Each component processes data in unison to ensure the system's optimal performance. During system operation, the source module processes data in chunks before sending it to the signal processing block, which then extracts features from the data and converts them into control signals before sending them to the application module. Once the application module transfers event markers to the source module, it stores the signals and associated markers on the disk. This signal pattern could be analyzed offline with the help of this data file.

### 3.1. Proposed systematic approach

BCIs can be designed, prototyped, tested, experimented with, and evaluated with the help of software such as BCILAB and EEGLAB, which are MATLAB toolboxes. The proposed systematic approach includes:

(i) Signal processing is the process of taking unprocessed data and transforming it into a form that can be read and utilized by other devices.
(ii) Feature extraction can create the necessary feature vectors from either embedded or continuous signals.
(iii) Training and test data are fed into a predictive model.
(iv) The BCI paradigms standardize the full computational approach, from data-driven model learning to offline data sets or real-time cognitive state prediction.
(v) It is possible to connect certain pieces of hardware to the BCILAB's data-crunching infrastructure by means of online plug-ins and drivers.

Electrodes are applied to the scalp to record EEG signals. Depending on the application and specific brain regions of interest, various electrode configurations and locations may be utilized. To eliminate noise and artifacts, the acquired EEG signals must be cleaned up in this step. Common preprocessing techniques include re-referencing to a common reference electrode to improve signal quality, artifact removal to remove interference from sources such as eye blinks and muscle activity, and filtering to remove unwanted frequencies (e.g., high-pass, low-pass, or notch filtering). Finding relevant data in the preprocessed EEG signals are part of the feature extraction process. This process can include frequency-domain features such as power spectral density or time-domain features such as amplitude.

### 3.2. Data acquisition

The data acquisition module takes raw EEG data from the hardware (EEG headsets wireless/Bluetooth) and converts it to digital format before sending it to the signal processing

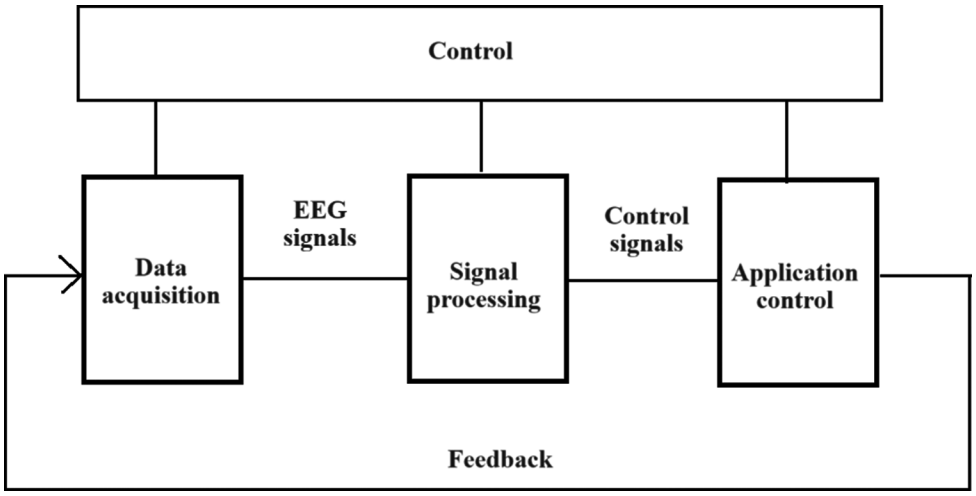


**Figure 2.** Proposed brain-computer interface framework.
Abbreviation: EEG: Electroencephalogram.

module for analysis. It gathers information and saves it in a file.

#### 3.2.1. Feature extraction

Several crucial aspects of the EEG signals have been studied to analyze the motor imagery signals, with each capability proving effective. Band powers, in particular, play a significant role in EEG processing. By selectively utilizing spectral features from the alpha and beta-frequency bands, motor imagery has a profound effect on these regions of the brain during EEG processing. The steps involved in analyzing motor imagery signals using band powers include:

(i) Removing any artifacts from the raw EEG data.
(ii) Selecting the relevant inputs, such as F3 and F4 electrodes.
(iii) Applying 8–12 Hz and 18–35 Hz band-pass filters to each path.
(iv) If N represents a time series, then it can be calculated using Equation I, where $\alpha$ is the number of trails and $\gamma$ is the number of channels.

$$N = \alpha \times \gamma \times 2 \quad \text{(I)}$$

(v) To determine the average band power, an FFT must be used.

The average method involves taking the mean and standard deviation of the time series data from a single experiment, making it the most basic feature extraction method. Due to the oscillating nature of EEG signals and the possibility that averaged values across classes may be similar, this method is not particularly helpful for BCI applications, particularly for motor imaging. On the other hand, the RMS method calculates the average and standard deviation of a signal by squaring it, finding its average, and then evaluating its square root using Equation II to get root-mean-square, where $x$ denotes the mean of the values $x_i^2$.

$$\text{RMS} = \sqrt{x^2} \quad \text{(II)}$$

### 3.3. Signal processing

In two distinct steps – feature extraction and translation – the signal processing module transforms the raw EEG data into categorized results usable by output devices. Each phase is implemented separately from the other and is subdivided into filters. Two filters, one spatial and one temporal, make up the feature extraction phase. In the translation stage, the first filter employed is the linear classifier, followed by a normalizer that adjusts the outputs to maintain a zero mean and a predetermined range of values.

### 3.4. User application

The user application is in charge of regulating the external processes that are affected by the signals sent from the signal processing module. Keystroke filter and connector filter stand out as particularly useful built-in application modules because they allow the control signals to be routed to a different program using automated keystrokes and user datagram protocol (UDP) sockets, respectively. Games can be controlled by accessing the UDP port and using the control signals sent to it.

### 3.5. Operator

The graphical interface is designed to provide users with convenient access to the various modules previously discussed. Users have the ability to start, pause, and restart the process, as well as adjust its settings, all while viewing the system's parameters and real-time analysis results.[24]

## 4. Experimental results

### 4.1. Data set description

The BCI IV Competition-I dataset, accessible through http://www.bbci.de/competition/iv/#dataset1, comprises publicly available EEG signals obtained from a task in which the participants were instructed to focus on the muscles in their left and right hands and feet. Spectral features, including band powers, average power, and RMS power, play a crucial role in deriving valuable information from these EEG signals. These features were probably chosen for the BCI IV Competition-I dataset because they are useful in differentiating between motor imagery tasks such as left- and right-handed movements. These features are extracted by computing them from each trial's or time segment's EEG recordings, which are then fed into ML models that are responsible for either classifying or decoding the intended motor imagery tasks. The dataset comprises data from 15 individuals engaged in cued motor imagery tasks across four classes: left hand, right hand, foot, and tongue. According to a 10-to-20 montage, electrodes were attached to the linked mastoids T7 and T8 through the femoral arteries (F3, F4, FC5, FC6, F7, and F8). The impedance of each electrode was maintained at 10 kΩ or less. The data were digitized at 300 Hz using an A/D converter connected to a personal computer. The dataset includes EEG recordings collected from 15 individuals aged 18 to 36, while they performed cognitive tasks. Each class has 60 trials, and there are a total of 60 channels in this data set. This EEG data feature was sampled at 250 Hz and filtered between 1 and 50 Hz with a Notch filter enabled. Figure 3 depicts the positions of the electrodes that were used to record the experiment's results.

In this experiment, participants were seated in overstuffed armchairs and instructed to visualize

movements of their left or right hand, foot, or tongue in response to randomized cues. The sequence of the indicators was random. This experiment comprised multiple runs of 60 trials each. Each trial began with an auditory stimulus presented at t = 5 s, followed by the appearance of a cross "+" on the screen, which remained visible throughout the trial. At t = 10 s, participants were shown an arrow pointing left, right, up, or down for 2 s, during which they were instructed to imagine moving their left hand, right hand, tongue, or feet. Finally, at t = 12 s, the cross vanished. This experimental paradigm formed the basis for in-house data acquisition trials conducted with the Emotiv EEG headset.

The stimulus presentation software included with BCI2000 serves various purposes, primarily facilitating real-time data acquisition from any headset and the optional integration of this data with feedback applications. In this study, cues were generated with this stimulus presentation software, and EEG data and event markers were recorded in real-time to reflect their association with the cues. Successful data collection requires running a sufficient number of independent experiments. Fifteen normal subjects have been used to collect data for this study through an EEG headset. The BCI2000 stimulation presentation program used visual cues to instruct participants to perform a left motor imagery task, a right motor imagery task, or nothing at all. This resulted in a total of 360 trials, with 60 trials allocated to each of the three activities (left, right, and rest).

Subjects were instructed to maintain a state of activity during data collection, visualizing themselves opening or closing the corresponding hand at a rate of about once per second when the left or right arrow was on screen. The oscillatory nature of the EEG signals has been observed by researchers during motor imagery tasks.

Figure 4 displays the frequency distribution for subject K, providing evidence that the analyzed signals are acquired during motor imagery tasks. Each individual exhibits a unique "sweet spot" in terms of the frequency at which their power output is maximized. In frequency plots for Subject K, it is clear that there are not very many frequencies with significant power. This is because the subject's accuracy on motor imagery tasks is lower. Understanding the timing and frequency characteristics of these signals can be valuable, particularly concerning event-related potential latencies and the synchronization/desynchronization of EEG signals after/during motor imagery tasks.

### 4.2. Predictive models used

The BCI IV Competition-I dataset presents an EEG signal classification task. Various ML models, including k-nearest

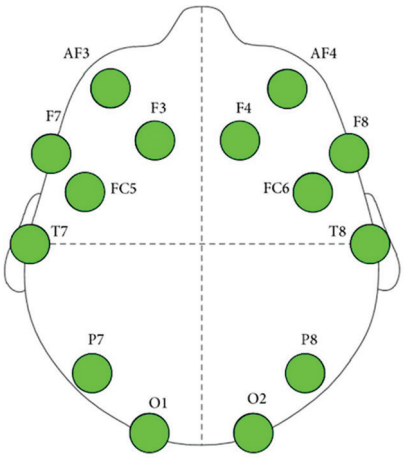


**Figure 3.** Electrode locations.

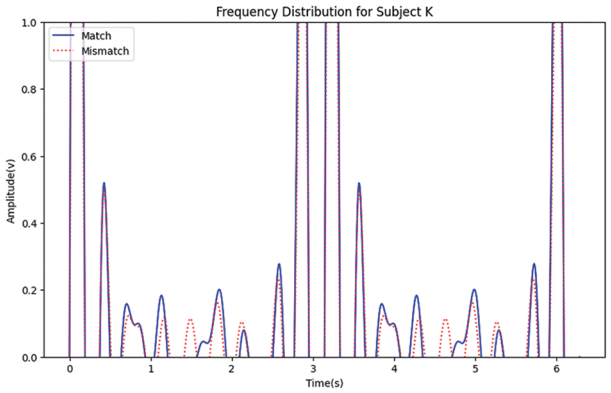


**Figure 4.** Frequency plot (Subject K).

neighbors (KNN), principal component analysis (PCA), and dual-layer neural networks (NN), are selected based on their unique advantages and disadvantages. KNNs are a popular non-parametric algorithm that is easy to use, simple to understand, resilient to noisy data, and appropriate for tasks involving multiple classes. However, its computational requirements can be problematic, particularly when dealing with big datasets. PCA, on the other hand, offers a useful method for reducing dimensionality, which helps to improve computational efficiency and lessen the impact of dimensionality. However, it makes the assumption that the principal components with the highest variance contain the most relevant information, which may limit its application in capturing subtle aspects of EEG signals. Dual-layer NNs, on the other hand, are particularly good at capturing complex nonlinear relationships in the data, making them an attractive option for tasks where complex patterns call for sophisticated modeling. However, given their computational demands, overfitting proneness, and decreased interpretability, they might need to be carefully considered, especially in scenarios where resources are

limited or interpretability is important. Choosing the best model requires careful consideration of the features of the dataset, the computational limitations, and the requirements for interpretability so that the model selected closely matches the particular requirements of the EEG signal processing task.

The BCI IV Competition-I dataset may not be entirely representative of the general population despite offering insightful information on the processing and classification of EEG signals. Thus, to evaluate the generalizability and performance of models trained on such benchmark datasets in real-world applications, comprehensive evaluation and validation, including cross-validation and testing on independent datasets, are necessary. Careful validation is required to determine the best classification technique with better parameters. The k-fold cross-validation strategy is best because it employs all of the data trails for both training and testing, which is especially important given the small sample size. It is possible that using different techniques will result in an insufficiently precise validation error. When there are many variables in the ML method, model selection can be critical. The best model can be selected by tweaking individual features in isolation. However, the accuracy of classification when employing different models may differ from one individual to the next and from one data set to the next. Using solely MATLAB's built-in ML and statistics toolboxes, we conducted the following analysis. All feature vectors were utilized during both the training and testing phases, employing k-fold cross-validation techniques.

#### *4.2.1. K-nearest neighbors*

Table 2 demonstrates that a well-trained classifier for the sorts of signals utilized is often produced using the KNN method to the dataset and extracting features with different k-values.

According to Figure 5, the k-value should be set to 7 to yield optimal results. Following this, the effects of different features, including the Euclidean distance used to calculate the separation between data points, should be tested. It is important to emphasize that each individual has a unique k-value and, as a result, different values for the parameters that are taken into account when choosing a model. It is advised that various models be employed for each subject after a detailed analysis of all signals originating from each one.

#### *4.2.2. Principal component analysis (PCA)*

Table 3 displays the findings from using principal component analysis with various discriminant functions. Linear, kernel, and radial basis function (RBF) kernel are among the many functions tried.

**Table 2. K-size analysis**

| Subject | Components | k=1 | k=4 | k=7 | k=9 | k=11 |
|---|---|---|---|---|---|---|
| Subject 1 | Band power | 47.8 | 54.7 | 58.2 | 60.2 | 62.5 |
| | Average | 34.5 | 42.8 | 44.6 | 50.3 | 52.4 |
| | RMS | 65 | 68.4 | 72.3 | 76.2 | 70 |
| Subject 2 | Band power | 46.2 | 48.4 | 49 | 51.2 | 54.6 |
| | Average | 48.8 | 46.6 | 44.1 | 45.4 | 50 |
| | RMS | 52 | 53.3 | 56.7 | 54.4 | 60.2 |
| Subject 3 | Band power | 64.6 | 62.9 | 61 | 60.1 | 58.2 |
| | Average | 55.2 | 50 | 52.2 | 52.5 | 59.1 |
| | RMS | 62 | 67.2 | 70.2 | 68.3 | 65 |

Abbreviation: RMS: Root-mean square.

**Table 3. Principal component analysis functions analysis**

| Subject | Components | Linear | Kernel | RBF kernel |
|---|---|---|---|---|
| Subject 1 | Band power | 65.2 | 65.2 | 63.1 |
| | Average | 42.3 | 42.3 | 42.5 |
| | RMS | 68.1 | 72.6 | 70.4 |
| Subject 2 | Band power | 52.1 | 52.1 | 48 |
| | Average | 42 | 42 | 46.7 |
| | RMS | 64 | 64 | 62.2 |
| Subject 3 | Band power | 51 | 51 | 48.4 |
| | Average | 56.3 | 56.3 | 47.4 |
| | RMS | 72.2 | 72.2 | 74.6 |

Abbreviations: RBF: Radial basis function; RMS: Root-mean square.

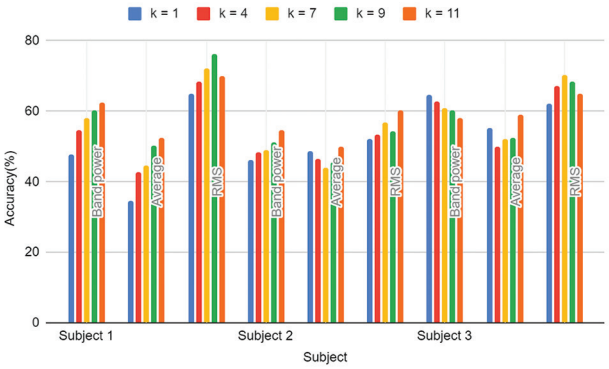


**Figure 5.** Performance metric comparison (k-value analysis).
Abbreviation: RMS: Root-mean square.

From Figure 6, it depicts the comparison of kernel functions used in PCA. When comparing results from using KNN and PCA to classify the data, it is clear that the band power features improve classification accuracy. Although accuracy is straightforward to understand and intuitive, it can be deceptive in datasets that are unbalanced or have a skewed class distribution. In these situations, precision

and recall offer more information about the performance of the classifier but might not be as effective at capturing the overall classification performance as accuracy. The aforementioned tabulated results demonstrate that it would be unrealistic to assume that a single classification model would be effective across multiple datasets obtained from multiple test subjects under multiple experimental conditions and over time. The algorithm may not be able to accurately fit the available data into the model, or a lack of training data may be to blame for some models' low performance for some subjects.

#### *4.2.3. Neural networks*

Through the process of learning a representation of the input at the hidden layers, multilayer neural networks can be utilized for feature learning before being applied to classification or regression. The majority of neural networks will adjust the model's parameters iteratively in response to a training sample. With each iteration, the cost function, or classification error, should get smaller. Figure 7 displays a simplified version of the neural network with just one input layer, two hidden layers, and one output layer. Results, however, have been confirmed through testing with varying densities of hidden layer neurons. Normal data present the network with a 400-element input vector.

The network may not be able to accurately describe a test input vector, even though it has learned a model that correctly characterizes the majority of the data in all of the input vectors. Based on these findings, it is clear that as the number of hidden neurons grows, classification accuracy suffers. Due to the finite number of training input vectors, models with more hidden units are more likely to experience over-fitting issues. Table 4 illustrates NN with different hidden neurons.

### 4.3. Performance analysis

The classification results for the experimental data are presented in Table 5, demonstrating that the KNN algorithm can accurately classify emotional states based on the EEG data. Both PCA and NN also endeavor to categorize samples into subsets based on specific criteria. However, it is possible that the EEG data related to emotional states may be clustered without a clear delineator between the various types of data available to us.

From Figure 8, it can be concluded that the KNN method is the most appropriate for categorizing the data. A test is done to confirm the claim. The first step involved grouping the vehicle parameters gleaned from driving the simulated car into one of four categories representing four distinct human driving styles: cautious, aggressive, inexpert, and relaxed. The second step is to record subjects' electrical brain activity while they operate the vehicle, and

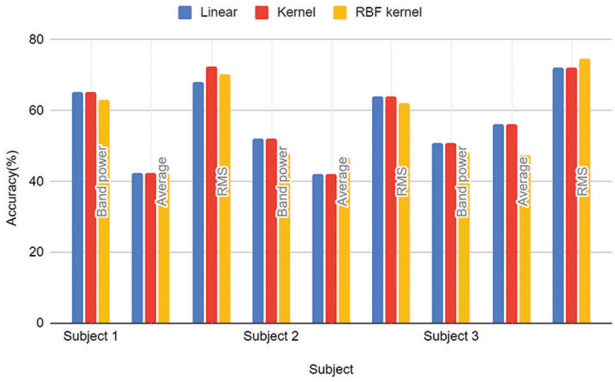


**Figure 6.** Performance metric comparison: Function analysis. Abbreviations: RBF: Radial basis function; RMS: Root-mean square.

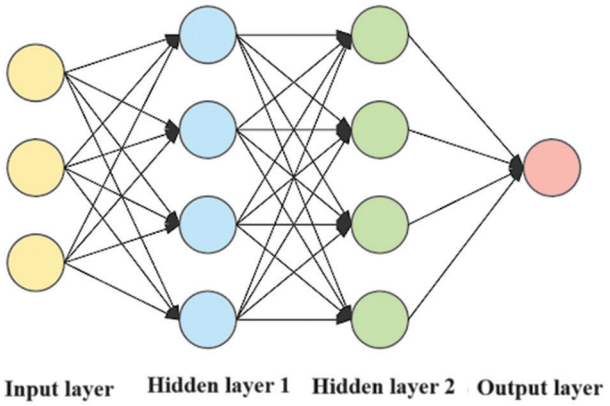


**Figure 7.** Neural network structure.

**Table 4. Neural network with different hidden neurons**

| Hidden units=2 | 400 | 600 | 800 |
|---|---|---|---|
| Subject 1 | 78.3 | 76.2 | 74.5 |
| Subject 2 | 70.1 | 68.6 | 62.8 |
| Subject 3 | 74.4 | 72.9 | 71.2 |

**Table 5. Accuracy analysis**

| Subject | KNN | PCA | NN |
|---|---|---|---|
| Subject 1 | 85.6 | 36.3 | 28.1 |
| Subject 2 | 86.8 | 34.2 | 30.3 |
| Subject 3 | 82.3 | 28.8 | 31 |

Abbreviations: KNN: K-nearest neighbor; NN: Dual-layer neural network; PCA: Principal component analysis.

then use a KNN classifier to assign each recording to one of four possible mental states. High arousal and a favorable valence describe the alert mental state.

An eager or enthusiastic person is viewed as a keen operator. The operator is familiar with the vehicle's

characteristics and will make full use of its dynamics when dealing with the behavior of a keen subject while operating the vehicle. Cars can be maneuvered with lightning speed and pinpoint accuracy. Any unintended responses are promptly adjusted. Attitudes of aggression have been linked to stimuli with a high arousal value but a negative valence. An aggressive operator is one who takes great risks in pursuit of his goals and is known for using forceful methods to achieve them. An inexperienced person's emotional state is low arousal and negative valence, characterized by fatigue and boredom. This causes drivers to veer off course, speed up and slow down unexpectedly, and make clumsy, imprecise maneuvers.

The participants' driving performance was assessed through these simulated road conditions. In every case, data on the driver"s actions and the car's state of motion (including speed, lanes traveled, steering angle, brake and gas pedal positions, and lateral and longitudinal acceleration) were recorded.

### 4.4. Training data to build the classifier

The data on vehicle parameters collected for each human subject were classified using master data to create a classifier. This "master data" was collected solely while an expert driver carried out the same driving maneuvers while under the influence of various psychedelic drugs. Any given driving scenario, such as those listed in Table 6, was created with the intention of eliciting a specific response from the driver. However, this is hardly a given, as drivers vary greatly in their reach. In contrast, the "master data" was gathered from situations in which the driver actively modeled each of the four possible driving styles.

The master data were collected so that a generic classifier could be trained using the values of the vehicle parameters exhibited by the vehicle when the driver was engaging in one of the four behaviors typical of the scenario in question. This "master data" is trained using the KNN, PCA, and NN. Table 7 displays the results of using various ML techniques to determine how accurate each scenario is. When compared to PCA, the classification accuracies for KNN and NN are significantly higher, as shown in Figure 9.

### 4.5. Classification results

As previously noted, using the classifier created from "master data" as test samples, the vehicle parameter data obtained for each subject were classified into one of the four driving tendencies (keen, aggressive, and inexpert). The results for each of the three classifiers – KNN, PCA, and NN – for each of the human participants are listed in Tables 8-10, along with the conclusions/observations reached.

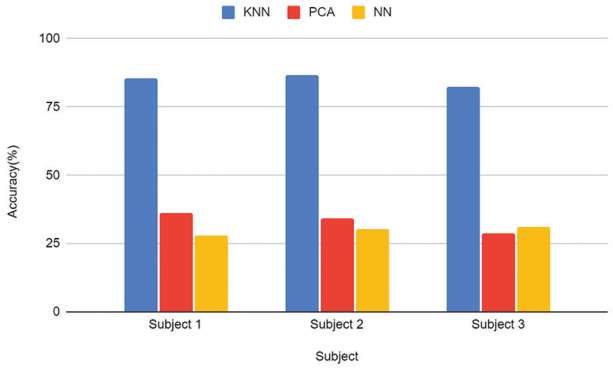


**Figure 8.** Accuracy analysis: K-nearest neighbor (KNN) versus principal component analysis (PCA) versus dual-layer neural network (NN).

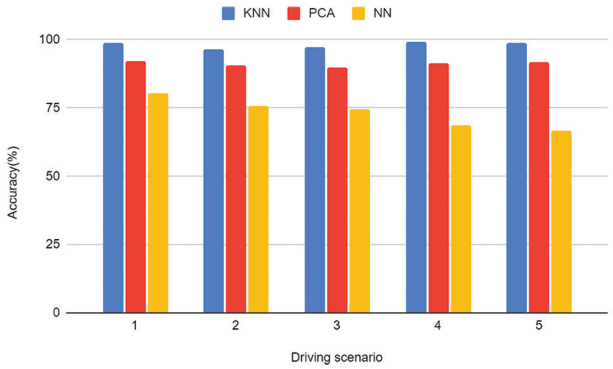


**Figure 9.** Driving scenario analysis: K-nearest neighbor (KNN) versus principal component analysis (PCA) versus dual-layer neural network (NN).

**Table 6. Driving scenario**

| Scenario | Details |
|---|---|
| 1 | A 35-mph speed limit and emergency vehicles are in effect. |
| 2 | A 40-mph speed limit and traffic to contend with. |
| 3 | Sticking to the 30-mph speed limit and waiting behind a slow vehicle. |
| 4 | Stuck behind a snail on a 45-mph, two-lane, curved road |
| 5 | Another sluggish car on a two-lane, winding road with a 50-mph speed limit. |

**Table 7. Accuracy analysis of driving parameters**

| Driving scenario | Classification technique | | |
|---|---|---|---|
| | KNN | PCA | NN |
| 1 | 98.7 | 92.1 | 80.3 |
| 2 | 96.4 | 90.4 | 75.6 |
| 3 | 97.2 | 89.8 | 74.7 |
| 4 | 99.2 | 91.2 | 68.8 |
| 5 | 98.6 | 91.6 | 66.6 |

Abbreviations: KNN: K-nearest neighbor; NN: Dual-layer neural network; PCA: Principal component analysis.

The findings from using all three classifiers together revealed that, in some cases, the classifiers detect different driving modes across all scenarios. This is due to the fact that classifiers' performance varies depending on the scenario and rarely achieves a perfect score. When tested on the dataset, both the KNN and PCA classifiers demonstrated 100% efficiency, and it was discovered that the driving modes observed in these instances by both classifiers are, in most cases, the same. As a result, the collected master data reflects the common characteristics observed across all subjects. There could be a number of factors contributing to the fact that aggressive driving is the least well-defined subtype of driving. The fact that all the drivers are aware that their every move is being recorded could explain this. In addition, the driving scenarios may not effectively stimulate aggressive driving tendencies.

Intriguingly, all classifiers agreed that Subject 1 was the least efficient driver, which aligns with their status as a novice driver in training. The majority of Subject 1's inexpert classifications occurred during turns, revealing a lack of proficiency in this aspect. Conversely, Subject 3 was consistently categorized as perceptive by both KNN and PCA. Subject 2 appeared to possess the most driving experience, as indicated by their consistently accurate classifications by both KNN and PCA. Moreover, it was observed that Scenario 3 was commonly labeled as ineffective by most individuals using reliable classifiers. According to the observations, these incidents occurred when the driver was either too close to or too far from a slower vehicle. Erratic maneuvering led to the observed inexpert mode. Overall, inexpert driving emerged as the most categorized style, possibly influenced by participants' lack of familiarity with the virtual city environment in which they are attempting to drive.

**Table 8. K-nearest neighbor classifier**

| Driving scenario | Subject 1 | Subject 2 | Subject 3 |
|---|---|---|---|
| 1 | Inexpert | Inexpert | Inexpert |
| 2 | Inexpert | Aggressive | Keen |
| 3 | Inexpert | Inexpert | Inexpert |
| 4 | Inexpert | Keen | Keen |
| 5 | Inexpert | Inexpert | Keen |

**Table 9. Principal component analysis classifier**

| Driving scenario | Subject 1 | Subject 2 | Subject 3 |
|---|---|---|---|
| 1 | Inexpert | Keen | Inexpert |
| 2 | Inexpert | Inexpert | Keen |
| 3 | Inexpert | Inexpert | Inexpert |
| 4 | Inexpert | Inexpert | Keen |
| 5 | Inexpert | Keen | Keen |

**Table 10. Dual-layer neural network classifier**

| Driving scenario | Subject 1 | Subject 2 | Subject 3 |
|---|---|---|---|
| 1 | Inexpert | Inexpert | Inexpert |
| 2 | Inexpert | Inexpert | Aggressive |
| 3 | Inexpert | Inexpert | Inexpert |
| 4 | Inexpert | Inexpert | Keen |
| 5 | Inexpert | Keen | Keen |

The results from KNN, PCA, and NN classifiers for the same individual in identical situations exhibit dissimilarities. The built-in classifiers simply lack sufficient accuracy for this purpose. Notably, only KNN achieves a classification success rate of 98.02% on average. Furthermore, KNN once again recognized the least experienced driver as ineffective, while one of the most experienced drivers was recognized as alert. Notably, all the female drivers maintained a relatively stable (and generally upbeat) emotional state throughout the majority of the experiment. Conversely, only drivers fell into the categories of aggressive behavior, negative valence, and high arousal. Incorporating explainable AI techniques into the sleep state classification model could provide valuable insights into the decision-making process and enhance the interpretability of the results.[15] One approach to achieving this is through the use of feature visualization techniques, such as layer-wise relevance propagation (LRP) or saliency maps, which highlight the regions of input data that contribute most to the model's predictions. By visualizing the feature spaces at different layers of the ResNet architecture, researchers can gain a better understanding of how the model extracts and processes information from the multichannel EEG signals.

## 5. Conclusion

This research emphasizes the importance of employing an ML model that processes raw EEG signals to accurately estimate a user's mental state, especially in the context of BCI programs. Our study intends to improve the efficacy of predictive modeling by employing a methodical approach and leveraging features such as band powers, averages, and root-mean-squared extracted from EEG signals. Among the classifiers tested on the BCI IV Competition-I dataset, KNN, PCA, and NN performed the best. Notably, KNN achieved an average classification success rate of 98.02%. In addition, our study expands the application of our methodology to human driving behavior, showcasing its versatility and promise across multiple fields. Further, research into BCI and EEG

signal processing could concentrate on investigating innovative methods for extracting features, merging multimodal data for a profound understanding, carrying out long-term studies to ensure practical application, creating customized and adaptive BCI systems, tackling moral and societal concerns, and creating uniformity for comparative purposes. By tackling these issues, the field can progress toward more effective BCI systems with greater societal impact and applicability. This will ensure responsible deployment, equitable access, and continuous advancement in neurotechnology innovation.

## Acknowledgments

None.

## Funding

None.

## Conflict of interest

The authors declare that they have no competing interests.

## Author contributions

*Conceptualization:* S. K. B. Sangeetha
*Formal analysis:* Saurav Mallik
*Investigation:* S. K. B. Sangeetha
*Methodology:* Sandeep Kumar Mathivanan
*Writing—original draft:* S. K. B. Sangeetha
*Writing—review & editing:* Aimin Li

## Ethics approval and consent to participate

Not applicable.

## Consent for publication

Not applicable.

## Availability of data

Not applicable.

## References

1. Qi G, Zhao S, Ceder AA, Guan W, Yan X. Wielding and evaluating the removal composition of common artefacts in EEG signals for driving behaviour analysis. *Accid Anal Prev*. 2021;159:106223.

   doi: 10.1016/j.aap.2021.106223

2. Zero E, Bersani C, Sacile R. EEG based BCI system for driver's arm movements identification. In: *Automation, Robotics and Communications for Industry 4.0*. Vol. 77. France: International Frequency Sensor Association; 2021.

3. Cao Z, Chuang CH, King JK, Lin CT. Multi-channel EEG recordings during a sustained-attention driving task. *Sci Data*. 2019;6(1):19.

   doi: 10.1038/s41597-019-0027-4

4. Zhang X, Li J, Liu Y, *et al*. Design of a fatigue detection system for high-speed trains based on driver vigilance using a wireless wearable EEG. *Sensors* (*Basel*). 2017;17(3):486.

   doi: 10.3390/s17030486

5. Nader M, Jacyna-Gołda I, Nader S, Nehring K. Using BCI and EEG to process and analyze driver's brain activity signals during VR simulation. *Arch Transp.* 2021;60:137-153.

   doi: 10.5604/01.3001.0015.6305

6. Zhou X, Yao D, Zhu, M, *et al*. Vigilance detection method for high-speed rail using wireless wearable EEG collection technology based on low-rank matrix decomposition. *IET Intell Transp Syst*. 2018;12(8):819-825.

   doi: 10.1049/iet-its.2017.0239

7. He S, Chen L, Yue M. Reliability analysis of driving behaviour in road traffic system considering synchronization of neural activity. *NeuroQuantology*. 2018;16(4):62-68.

   doi: 10.14704/nq.2018.16.4.1209

8. Lawhern VJ, Solon AJ, Waytowich NR, Gordon SM, Hung CP, Lance BJ. EEGNet: A compact convolutional neural network for EEG-based brain-computer interfaces. *J Neural Eng*. 2018;15:056013.

   doi: 10.1088/1741-2552/aace8c

9. Doudou M, Bouabdallah A, Berge-Cherfaoui V. Driver drowsiness measurement technologies: Current research, market solutions, and challenges. *Int J Intell Transp Syst Res*. 2020;18(2):297-319.

   doi: 10.1007/s13177-019-00199-w

10. Haghani M, Bliemer MC, Farooq B, *et al*. Applications of brain imaging methods in driving behaviour research. *Accid Anal Prev*. 2021;154:106093.

    doi: 10.1016/j.aap.2021.106093

11. Murthy GN, Khan ZA. Cognitive attention behaviour detection systems using Electroencephalograph (EEG) signals. *Res J Pharm Technol*. 2014;7(2):238-247.

12. Pal D, Palit S, Dey A. Brain computer interface: A review. In: *Computational Advancement in Communication, Circuits and Systems*. Cham: Springer; 2022. p. 25-35.

    doi: 10.1007/978-3-319-10978-7_1

13. Zero E, Bersani C, Zero L, Sacile R. Towards real-time monitoring of fear in driving sessions. *IFAC-PapersOnLine*. 2019;52(19):299-304.

    doi: 10.1016/j.ifacol.2019.12.068

14. Aricò P, Borghini G, Di Flumeri G, Sciaraffa N, Babiloni F. Passive BCI beyond the lab: Current trends and future directions. *Physiol Meas*. 2018;39(8):08TR02.

doi: 10.1088/1361-6579/aad57e

15. Hasan MJ, Shon D, Im K, Choi HK, Yoo DS, Kim JM. Sleep state classification using power spectral density and residual neural network with multichannel EEG signals. *Appl Sci*. 2020;10:7639.

    doi: 10.3390/app10217639

16. Brouwer AM, Snelting A, Jaswa M, Flascher O, Krol L, Zander T. Physiological Effects of Adaptive Cruise Control Behaviour in Real Driving. In: *Proceedings of the 2017 ACM Workshop on an Application-oriented Approach to BCI out of the Laboratory*. 2017. p. 15-19.

    doi: 10.1145/3038439.3038441

17. Karuppusamy NS, Kang BY. Multimodal system to detect driver fatigue using EEG, gyroscope, and image processing. *IEEE Access*. 2020;8:129645-129667.

    doi: 10.1109/Access.2020.3009226

18. Sangeetha SKB, Kumar MS, Deeba K, Rajadurai H, Maheshwari V, Dalu GT. An empirical analysis of an optimized pretrained deep learning model for COVID-19 diagnosis. *Comput Math Methods Med*. 2022;2022:9771212.

    doi: 10.1155/2022/9771212

19. Khalaf OI, Ogudo KA, Sangeetha SKB. Design of Graph-based layered learning-driven model for anomaly detection in distributed cloud IoT network. *Mob Inf Syst*. 2022;2022:6750757.

    doi: 10.1155/2022/6750757

20. Kanthavel D, Sangeetha SKB, Keerthana KP. An empirical study of vehicle to infrastructure communications-an intense learning of smart infrastructure for safety and mobility. *Int J Intell Netw*. 2021;2:77-82.

    doi: 10.1016/j.ijin.2021.06.003

21. Aggarwal S, Chugh N. Review of machine learning techniques for EEG based brain computer interface. *Arch Comput Methods Eng*. 2022;29:3001-3020.

    doi: 10.1007/s11831-021-09684-6

22. Ahn M, Jun SC, Yeom HG, Cho H. Editorial: Deep learning in brain-computer interface. *Front Hum Neurosci*. 2022;16:927567.

    doi: 10.3389/fnhum.2022.927567

23. Zhu H, Forenzo D, He B. On the deep learning models for EEG-based brain-computer interface using motor imagery. *IEEE Trans Neural Syst Rehabil Eng*. 2022;30:2283-2291.

    doi: 10.1109/TNSRE.2022.3198041

24. Immanuel RR, Sangeetha SKB. Analysis of EEG Signal with Feature and Feature Extraction Techniques for Emotion Recognition Using Deep Learning Techniques. In: *Proceedings of International Conference on Computational Intelligence and Data Engineering*. Singapore: Springer Nature Singapore; 2022. p. 141-154.

    doi: 10.1007/978-981-99-0609-3_10

ACCSCIENCE PUBLISHING

Brain & Heart

ORIGINAL RESEARCH ARTICLE

# Immersive virtual reality for prospective memory and eye fixation recovery following traumatic brain injury: A pilot study

**Kristen Faye Linton[1,2*], Bahareh Abbasi[3], Melissa Gutierrez Jimenez[1], Jaylyn Aragon[1], Anna Gendron[2], Rasmey Gomez[1], Sky Hampton[3], Ben Michael[3], Savanna Monson[1], Nathanael Paulus[3], Vaishnavi Ramprasad[1], and Chrissy Stamegna[2]**

[1]Department Health Sciences, California State University Channel Islands, Camarillo, California, United States of America

[2]Department Administration and Programs, Brain Injury Center of Ventura County, Camarillo, California, United States of America

[3]Department Mechatronics and Computer Science, California State University Channel Islands, Camarillo, California, United States of America

## Abstract

Rehabilitation is crucial for the recoveriy from traumatic brain injuries (TBI); yet, only 77 – 88% of TBI patients are receipients of rehabilitation. Particularly, individuals lacking insurance coverage or facing transportation hurdles, notably within the Hispanic community, are less likely to undergo rehabilitation. Virtual reality (VR), known for its mobility and affordability, is recommended as a rehabilitation alternative. This community-based participatory research project aimed to evaluate the acceptability, feasibility, and potential of VR scenarios in addressing common rehabilitative needs. Focus groups involving TBI patients ($N = 12$) were conducted to identify rehabilitative needs and design VR scenarios. Two novel scenarios were created to enhance prospective memory and eye tracking. The impact of the prospective memory VR scenario was assessed among individuals with brain injuries 1 year post-TBI ($N = 11$), who were divided into intervention and delayed-intervention groups. In addition, six participants underwent the eye-tracking VR scenario to evaluate its effectiveness. Data from memory tests and screen recordings were gathered. In the objective memory test, participants in the VR intervention group (66%) exhibited greater improvement than those in the memory card delayed intervention group (0%) after 12 sessions. However, there was no statistically significant difference in mean scores on a Prospective and Retrospective Memory Questionnaire memory scale between the intervention and delayed-intervention groups after 6 weeks. Nonetheless, all participants demonstrated enhanced eye tracking skills after completing the eye tracking VR scenario between the 6th and 12th sessions. In conclusion, the VR scenarios exhibited promise, acceptability, and feasibility in improving prospective memory and eye tracking for individuals with TBI 1 year post-injury.

***Keywords:*** Virtual reality; Brain injury; Memory; Eye tracking; Eye fixation

***Corresponding author:**
Kristen Linton
(kristen.linton@csuci.edu)

**Citation:** Linton KF, Abbasi B, Jimenez MG, *et al.* Immersive virtual reality for prospective memory and eye fixation recovery following traumatic brain injury: A pilot study. *Brain & Heart.* 2024;2(2):2685.
doi: 10.36922/bh.2685

**Received:** January 9, 2024

**Accepted:** March 12, 2024

**Published Online:** May 8, 2024



## 1. Introduction

Early rehabilitation for traumatic brain injury (TBI) patients is associated with improved functional abilities; however, environmental barriers to accessing rehabilitation services

exist among TBI patients, often based on factors such as race, ethnicity, insurance status, and transportation availability.[1-6] A recent study involving 106,708 TBI patients revealed that 77 – 88% of them did not receive any post-brain injury rehabilitation.[3] Hispanic TBI patients, in particular, are less likely to receive rehabilitation than others, possibly due to cultural and language barriers.[3-4] In addition, individuals with public or no insurance coverage exhibit the lowest rates of discharge to rehabilitation compared to those with private insurance.[3,5] Furthermore, transportation is another environmental barrier to rehabilitation for TBI patients.[6]

Virtual reality (VR) is a recommended option for rehabilitation, offering a solution that addresses geographic and financial constraints.[7] Since transportation to rehabilitation is a challenge for individuals with brain injuries, VR can be conducted at home to prevent this barrier.[6] Studies have linked payer sources, such as self-pay, worker's compensation, and insurance type, to the length of rehabilitation stays, highlighting the importance of tailoring rehabilitation to demographics and injury characteristics.[5] The length of rehabilitation should be determined based on the specific rehabilitation needs arising from injury characteristics, namely, injury severity and functional status at admission. Immersive, interactive VR incorporating headsets, body trackers, and computers enables users to immerse themselves in a virtual world, engage with audio/visual stimuli, and enable eye and body movement tracking. VR has been employed for rehabilitative purposes for decades, but recent technological developments have led to a reduction in both the equipment required and associated costs.

Over a dozen studies have demonstrated the effectiveness of immersive VR in improving outcomes for both adult and child TBI patients, including driving ability, executive function, attention, memory, eye tracking, and visual-motor tasks.[8-16] While some studies found no significant differences between VR and traditional rehabilitation, which commonly consists of physical and occupational therapy,[7,17] others recommend specific parameters for VR interventions, such as 10 – 12 sessions lasting 20 – 40 min each, conducted 2 – 4 times/week to improve cognitive outcomes for TBI patients. [8]

Visual impairment hinders patients' ability to succeed in physical and cognitive rehabilitation. Eye tracking is often assessed with VR, but scant interventions are provided for eye tracking.[17-18] Eye tracking includes quickly and accurately looking (fixations), visually following an object (pursuits), and efficiently moving eyes from point to point (saccades). Specifically, visual eye tracking (ocular motility and oculomotor function) impairments are common in about 30 – 60% of those with acute TBI and 10 – 15% one year post-TBI.[19-20] A systematic review of oculomotor deficit interventions for individuals with brain injury found "few studies overall," with only six of nine total studies having addressed fixation.[21] In another systematic review of 22 studies of visual research on mild TBI, fixation research was focused on the least ($n$ = 3).[22]

Immersive VR involves using a headset equipped with visual, audio, and body-tracking capabilities to immerse participants in virtual scenarios. Consider an individual putting on a headset in their living room. Before them, a virtual scene unfolds: sand on a beach, while the ocean waves crash on the shore. As they look downward, they observe their feet sinking into the virtual sand. The movements of their avatar's feet correspond precisely to their own, mirroring their physical actions. Neurologists posit that our brains process immersive VR scenarios like this in the same way that we process the real world.[23,24] Essentially, the brain perceives the virtual environment as genuine, fostering a sense of presence as if physically standing on the beach. This phenomenon offers distinctive opportunities, enabling users to explore virtual places beyond their physical reach and providing the opportunity to practice physical or cognitive skills.

As the brain perceives the individual's body as the avatar within the VR scenario, they may experience heightened self-efficacy, believing they can move a body part or address a problem that they could not have done without the VR scenario. The skills practiced during the VR scenario can be applied in real-life situations. For example, if a participant can improve the range of motion of their hand in the VR scenario, they have strengthened their brain-to-hand communication as well as their hand muscles. If the participant can improve their ability to remember concepts in VR, they are building muscle memory skills in their brain to apply in real life. However, the VR scenarios and equipment utilized in studies involving United States veterans included bulky, expensive equipment, requiring participants to travel to specific locations to participate in VR activities.[11,25]

## 2. Methods

We received approval from the Institutional Review Board of the California State University Channel Islands before beginning the study (IO5625). This study is a community-based participatory research project conducted in collaboration with TBI patients from a local nonprofit, a trauma hospital, and interdisciplinary students and faculty from a university. Participants provided informed consent before participation. Two focus groups, comprising TBI patients ($N$ = 12), were conducted to assess their interest

in using VR for TBI recovery. Focus groups found that TBI patients desired VR scenarios to assist with eye tracking and prospective memory. Two scenarios were developed using footage captured with a 360° camera during local hiking and a beach walk by the personal instructor (PI); these scenarios were edited using Unity EditorXR (2024, Unity Technologies, San Francisco) by two computer science students. Eleven individuals with brain injuries tested the scenarios in a randomized control, delayed intervention pilot study.

### 2.1. Focus group methods

Focus groups are a qualitative research method ideally suited to gathering rich, descriptive data on individuals' perceptions and experiences. They facilitate an in-depth exploration of a small group of participants' attitudes, beliefs, and reactions, allowing researchers to uncover complex dynamics that quantitative methods might overlook. Focus groups typically include five to seven participants and are guided by a structured discussion. In this study, focus-group members were recruited from a local non-profit organization supporting individuals with brain injuries in Southern California. Two 1-h focus groups were conducted over Zoom to discuss designing a free, immersive VR scenario for individuals with brain injuries was conducted in summer 2021 ($n$ = 6) and spring 2022 ($n$ = 6) with a total of 12 brain injury survivors. The focus group members included 12 adult brain injury survivors (five males and seven females), a certified brain injury specialist, two physical therapists, and an interdisciplinary research team of a computer scientist, a computer science student, a kinesiologist, and a social worker. The first focus group session began with the social worker showing everyone several 360° and VR scenarios and discussing current research on VR and brain injury. The purpose of developing a VR scenario to help individuals with brain injuries with skill development was presented, with the kinesiologist emphasizing the importance of ensuring that movement and skill development are enjoyable. The social worker underscored the project's mission to ensure rehabilitation is accessible and affordable in individuals' homes. The structured discussion guide included prompts such as: (i) What daily challenges do you face that VR might be able to address? (ii) What activities did you enjoy before your injury that you would like to see incorporated into VR? and (iii) Is there anything specific that came to mind when you heard about VR? Each brain injury survivor shared their opinions about VR, how they believed it should be adapted for individuals with brain injuries, what skills they believed it could help them develop, and what scenarios they would find enjoyable. Direct quotes from the focus group discussions were incorporated to improve the design of immersive VR scenarios for individuals with brain injuries.

### 2.2. Focus group findings

The initial focus group resulted in the following themes: accessibility issues, skills, and enjoyable scenario ideas. These themes were utilized to develop a VR scenario, which was shown to members of the second focus group. These themes were confirmed in the second focus group, which confirmed that the scenario met the criteria they had hoped for in the first focus group.

#### *2.2.1. Accessibility issues*

Brain injury survivors reported specific accommodations they require, including adjustments for lighting, visual alignment, and affordability. Concerns were raised regarding blue lighting in VR scenarios, with one member expressing, "Brain injury survivors have issues with the blue light. I have my TV, my phone, and my computer as orange-tinted as possible. As far as VR, is there a way to put in that orange tint so it doesn't cause all the headaches?" In addition, video stability and a minimalist design address a second concern for visual misalignment issues. One member noted, "Impaired perception. You know, a lot of us cannot align ourselves appropriately, so some issues with visual fields shaking and stuff." Furthermore, challenges related to access to rehabilitation due to cost and lack of transportation were discussed. One person mentioned, "I recalled they had a cardboard box that made it (a cell phone) a VR, and you only paid like 10 bucks for it."

#### *2.2.2. Skills*

Five specific skills that brain injury survivors believed could be improved using VR were eye movement and tracking, communication, inhibition control, memory, and balance. One survivor highlighted challenges with eye fixation and pursuit, stating, "I did have a lot of dizziness. It's a lot of eye-movement work. Tracking things." Another individual described undergoing vestibular therapy for eye fixation, recounting, "I was doing vision therapy, and she had me looking at her. We had a big window behind us. Individuals would walk by it. As I focused on her, I could not keep my gaze stable. My eyes started tracking the person walking by. Anything that's crowded. Walking on a sidewalk. Going to the mall. Grocery shopping, navigating parking lots. Anything. Noise." The second reported skill was communication. One person reported, "Conversations from body language to the words and everything. I think a low-pressure VR conversation could really help individuals with that expectation of social performance. I remember the 1st year how exhausted I would be." Inhibition control was also expressed as critically important: The number

of times I've been in (brain injury support) group, and I hear someone say "I knew I shouldn't say something, but I couldn't stop myself." One person reported that memory was a challenge and even thought of an idea for a scenario: "Almost like making a map in our mind. Along the path, there's an apple tree, and under the apple tree, there's an object that you need to remember. And then along the way, there are these objects associated with something along the path to connect concepts." Specifically, prospective memory was reported as a challenge for all members. They provided several examples of going into a room and not remembering why they went there in the first place. All members reported balance and physical skills they would like to develop. One reported, "Although I did go back to a dance class, the balance stuff was really challenging. I danced for 20 years when I was younger. Never had an issue with right and left, especially looking here. It was really challenging. I really enjoyed it, but I found it very challenging to go from left to right. Switch it and use a mirror."

#### *2.2.3. Enjoyable scenario ideas*

Two individuals expressed hiking as an ideal VR scenario. One individual desired to hike in the scenario because she experienced challenges related to these activities after having a brain injury. She shared, "Something I could do before but can't do now is like a day hike. I mean, I could go out for an hour or so, but anything requiring a backpack…my neck is too fragile for a backpack…Being in that position for very long…it causes severe headaches. The balance issue, too." Another participant described, "If I had to picture the perfect scenario, it would be a path similar to a hike; maybe there are obstacles you have to come over, so you're forced to look around."

### 2.3. The VR scenarios

Two initial VR scenarios aimed at improving prospective memory and eye fixation were developed by the authors based on the focus group data. The prospective memory VR scenario developed by the study team lasted 10 min and involved users sitting in a chair while experiencing a first-person scenario of walking up a hill on a mountain hike through an HTC Vive Pro Eye headset. Along the trail, they encountered three hikers. They could turn their head and view their surroundings, including water moving, hillside, and some birds. The users were prompted at the beginning of the scenario to give each hiker specific items as they passed other hikers on the trail. To provide the item to the hiker, the patient must make a throwing motion and press a trigger with a HTC hand controller that is tracked by a HTC body tracker.

The eye-tracking VR scenario developed by the study team lasted 6 min, during which users remained seated in a chair. In a first-person perspective, they strolled down a beach near the shore, where waves crashed, and seagulls flew sporadically yet slowly in front of them. There was a ball positioned at the horizon that they were prompted to focus on, under the guidance of a VR technician. The ball turned green when they were looking at it and turned red when they were not. The HTC Vive Pro Eye headset enables pupil tracking, which is what turns the ball green or red. All relevant equipment is depicted in Figure 1.

### 2.4. VR pilot methods

#### *2.4.1. Participants*

Participants provided informed consent before their participation. A randomized pilot study was conducted with 11 TBI survivors who were at least 1 year post-TBI to evaluate the feasibility, acceptability, and effects of the VR scenarios on prospective memory and eye tracking. Participants were recruited from a local brain injury nonprofit by announcing the study at the beginning of a support group, sending an email to those served by the organization, and posting an announcement on social media. Inclusion criteria comprised individuals who were as follows: (i) 18 years or older, (ii) diagnosed with a TBI defined by any disruption in normal brain function caused by an external mechanical force, such as a blow or jolt to the head or penetrating head injury, ranging from mild, (often referred to as a concussion) characterized by a temporary change in mental status or consciousness, to severe, which may result in an extended period of unconsciousness or amnesia after the injury, (iii) at least 1-year post-TBI, and (iv) have transportation to one of two study locations locally. The 1-year post-TBI criterion was selected for this pilot to ensure participants who had


**Figure 1.** Virtual reality equipment used to assess prospective memory and eye fixation in brain injury survivors.

not recently experienced a TBI, given the novelty of the intervention and potential unknown side effects such as nausea. Exclusion criteria included: (i) Inability to provide consent for the study, (ii) severe vision impairment, (iii) inability to hold and move a VR controller with one hand, and (iv) neck or facial injury preventing the use of a VR headset.

Fourteen participants were recruited to participate in the study (Table 1 and Figure 2). Eligible participants who provided consent ($N$ = 11) were randomized into intervention groups and delayed intervention groups. The intervention group ($n$ = 6) participated in the memory VR scenario twice a week for 20 min each time for 6 weeks. Meanwhile, the control group ($n$ = 5) participated in a memory card game for 20 min twice a week for 6 weeks, followed by participation in the VR memory scenario for the same duration and frequency. In addition, the six participants in the intervention group participated in the eye-tracking scenario. However, not all participants piloted this scenario, as it was developed later in the study. A few participants experienced minor mobility and/or spasticity challenges in their neck and hands, with one participant requiring the use of a wheelchair. One participant had a vision impairment that limited their use of peripheral vision.

### 2.5. Procedures: the delayed intervention groups

The memory card game consisted of 48 outdoor-themed tiles, with each tile forming part of a matching pair, totaling 23 pairs. The VR technician began by explaining the objective of the game to the participant, emphasizing the use of prospective memory to obtain the most matching pairs. They provided a brief overview of the gameplay, which involved flipping two tiles at once to determine if they matched. If the tiles did not match, the other person took a turn, whereas if a match was found, the person would continue taking additional turns until encountering a non-matching pair, at which point the turn rotated back to the other player. Next, the technician shuffled the tiles and spread them face down across the table, typically arranging them into 4 – 5 rows of five or more tiles in each row, depending on the number of tiles used.

When two tiles were flipped over, the participant would verbally describe each tile in one word to aid in remembering their positions. For example, if one tile depicted a flashlight and the other a bear, the participant would say "flashlight" and "bear" before flipping the tiles back over since they did not match. The game continued until all matches were found and paired up. Following a round, the technician offered the participant the option to increase the game's difficulty by adding more tiles or swapping them out for new ones. After receiving feedback from the participant, the technician reshuffled the tiles and continued with one to two additional rounds of matching, based on the participant's preference. Each session of the memory card game typically lasted between 20 and 30 min, depending on factors such as the number of tiles used per round and whether tiles were swapped out.

**Table 1. Description of the sample (*N*=11)**

| Criteria | Mean | Range | Frequency | Percentage |
|---|---|---|---|---|
| Biological sex | | | | |
| Male | | | 3 | 27.27 |
| Female | | | 8 | 72.73 |
| Race | | | | |
| White | | | 9 | 81.82 |
| Latino | | | 1 | 9.09 |
| Black | | | 1 | 9.09 |
| Received rehabilitation | | | | |
| Yes | | | 5 | 45.5 |
| No | | | 6 | 54.55 |
| Age | 46.18 | 29 – 61 | | |
| Severity of TBI | | | | |
| Mild | | | 9 | 81.81 |
| Moderate | | | 2 | 18.18 |
| Total days experienced a loss of consciousness due to TBI | 19.09 | 0 – 150 | | |
| Years since TBI | 21.05 | 2.5 – 61 | | |

Abbreviation: TBI: Traumatic brain injury.

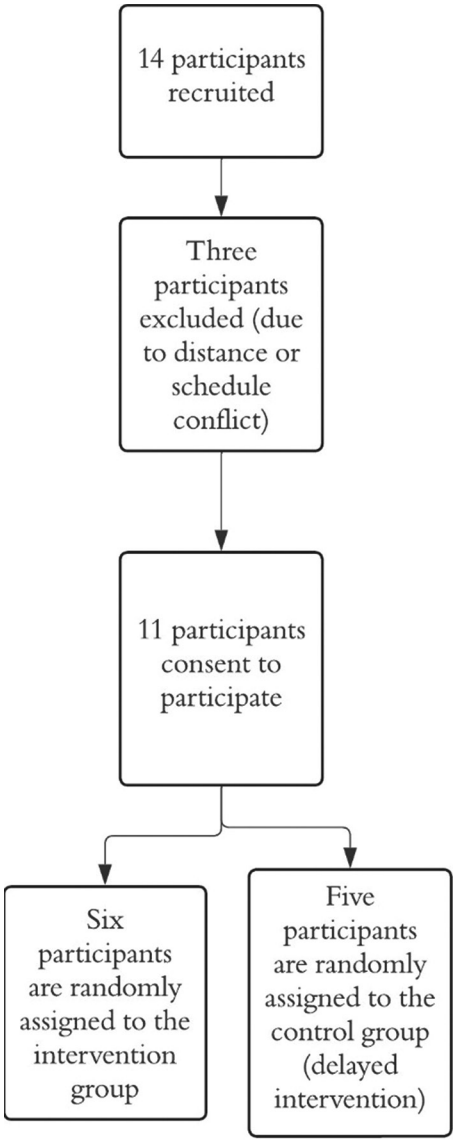


**Figure 2.** Participant flow. The study began with 14 participants recruited, but three chose not to participate due to distance from the study location or scheduling conflicts. Eleven participants continued on in the study. Six of the 11 participants were randomly assigned to the intervention group, and five were assigned to the delayed intervention group.

### 2.6. Procedures: the intervention groups

The VR equipment included the use of a gaming laptop, an HTC Vive Pro Eye headset with a controller, and a sensor to track visual, audio, and body movements. An extendable stand was screwed onto the sensor, and a power cord was connected to the back of it. A USB hub was needed to connect the headset's HDMI cord, and on the other end of it; there are three different ports. These three ports consisted of a power cord to charge the port, a cord to connect to the laptop, and another USB cable to connect to the USB port of the laptop. The HTC Vive Pro Eye headset contained built-in headphones as well as an adjustable head strap and knob to tighten the headset. The headset also included a head strap.

Once the equipment was connected, the participants were sitting in a chair with the controller in their dominant hand, and the headset was adjusted to fit over their heads like a ski mask by the VR technician. The headset gently sat on their forehead, nose, and the strap on the upper back of their head. The headset covered their eyes, and the headphones attached to the headset covered their ears. The technician then began to load the software SteamVR to make sure the base, headset, and controller which were turned on and connected. Once the equipment was connected, the technician started the screen recording for data collection and then began each scenario.

### 2.7. Data collection

Data collection included screen recordings of each session and note taking by the VR technician on qualitative observations. Participants completed an objective prospective memory test before starting and 6 weeks later after VR participation. Participants were asked to inform the researcher if they were left or right-handed after 5 min had passed. Successful completion of the test was determined by whether they remembered what to tell the researcher within the specified timeframe. In addition, participants completed a subjective memory test, Prospective and Retrospective Memory Questionnaire (PRMQ).[26,27] This is a self-report severity measure of prospective and retrospective memory challenges in everyday life. Participants responded to this Likert scale with response options ranging from 1 – 5, with 1 indicating "never" and 5 indicating "very often." Item scores were summed to obtain a total final score, with higher scores indicating severe prospective memory challenges. The data collection for the eye-tracking scenario involved screen recordings of the eye-tracking scenario sessions.

### 2.8. Outcome analysis

Data analysis for the memory outcome focused on comparing differences at the 6-week post-survey data collection time period between the intervention and delayed-intervention groups. This allowed a comparison of the VR to the memory game since the delayed-intervention group had only participated in the memory game at that time. For the memory survey data, bivariate statistical analyses were conducted. Since the objective memory test was a nominal variable, a non-parametric sign test was conducted on the intervention and delayed-intervention group responses to assess group differences in

improvement, staying the same, or declining in their ability to remember something they were told to remember 5 min prior. For the PRMQ, which involves an ordinal variable, the one-way ANOVA was conducted to assess intervention and delayed-intervention group differences in means on the PRMQ.

The screen recordings of eye-tracking sessions were viewed by researchers to assess potential improvements in the participants' eye-tracking ability to keep the ball green. Researchers calculated the proportion of time that the ball was green during the session by watching the screen recordings of each session and using a time watch to calculate the total time that the ball was green. This number was divided by the total time of the scenario, 6 min, providing a proportion of time that the ball was green. The first session was used as the baseline measure of eye tracking, and then a middle session and the last session were used for data analysis to compare participants' ability to focus their eyes over time.

## 3. VR pilot results

### 3.1. Acceptability

All participants expressed enjoyment of both VR scenarios, with the majority describing them as peaceful experiences. One participant said that it was "exactly what I needed" after a stressful week. Another participant who used a wheelchair expressed that she enjoyed seeing the animals and told VR technicians that she was "going on a hike" before putting on the headset to participate each week.

Potential challenges included sleep, mobility, and eye impairments. Although anticipated by mentions of red-light sensitivity in the focus group data, no participants reported motion sickness or sensitivity to red light as they used the scenarios. One participant reported that after completing the scenarios twice, she noticed that she did not sleep as well the nights following her participation. A few participants who had neck and hand mobility struggled more than other participants to complete the memory hiking scenario, which required the neck to turn slightly from side to side to see hikers and the objects they were tasked with passing to the hikers. VR technicians learned about each participant's mobility and were able to prompt participants to move within their ability to engage successfully in the scenario. The beach scenario did not pose any mobility challenges to these participants, as the scenario does not require participants to look around at all; they merely look forward. One participant who had a vision impairment and could not use his peripheral vision in real life successfully completed both scenarios without much challenge at all.

### 3.2. Feasibility

#### *3.2.1. Equipment*

The equipment setup typically requires approximately 10 min due to the various components that need to be attached. Ideally, equipment could be set up and left in place so that setup and takedown are not necessary on a regular basis. However, the ability to move equipment allows for mobility and facilitates meeting patients where they are, whether at home or bedside in a hospital setting.

#### *3.2.2. Space*

Due to the physical movement and use of a sensor on a tripod to detect movement in these VR scenarios, a minimum of a four-foot diameter around the participant is needed to set up equipment, including a chair for the participants to sit in. This study was conducted in two locations. One location was a much smaller space, and the VR technician and participant felt cramped. The "throwing" movement performed by participants during the memory scenario creates a safety challenge for both the participants and the VR technician. They need space to throw the object, and the VR technician should be aware of their throwing motion.

#### *3.2.3. Participant support*

While the long-term goal is for participants to be able to complete VR in the comfort of their homes without support, this study found that a lot of support was needed by the VR technician. The VR technicians provided a lot of technical support, including setup and takedown of equipment, software setup, and ensuring the headset was secure on each participant's head. Second, VR technicians prompted participants to focus on the ball in the eye-tracking scenario, and without giving them an answer as to what to do next, they gave them a gentle reminder that a hiker was coming toward them in the memory scenario. As VR technology and software simplify and ease of use improves, a VR technician may not be needed.

#### *3.2.4. Software*

Each piece of software, including the laptop and VR equipment, needed regular updates, or the VR scenario would begin glitching. Software updates were scheduled to be conducted biweekly to avoid glitching in the VR scenarios.

### 3.3. Outcomes

On the objective memory test, participants in the VR intervention group (66%) improved their memory more often than the memory card delayed-intervention group (0%) after 6 weeks and about 12 sessions on the

objective memory test. Sixty-six percentages of the delayed intervention group also improved their memory after 6 weeks of VR compared to their post-memory game scores on the objective memory test (Table 2). On the subjective PRMQ subjective memory scale, the intervention and delayed-intervention groups did not have statistically significant mean scores after 6 weeks (Table 2). All participants who received Beach Stroll improved between their first and last VR session. From the first to the last session, on average, participants improved their eye fixation by 17%; specifically participants improved between the 6th and 12th session (Table 3 and Figure 3).

## 4. Discussion

The pilot study yielded some notable findings. The VR scenarios developed and tested in this study demonstrated acceptability, feasibility, and promise to improve prospective memory and eye tracking among individuals with TBI one year post-TBI. By leveraging the brain's plasticity, VR interventions can potentially accelerate recovery by reinforcing neural pathways and supporting the development of new compensatory strategies for impaired functions.[8] The scenarios were intentionally designed to offer enjoyable and relaxing experiences, in line with the preferences expressed by focus group participants. Qualitative feedback from participants in the pilot study affirmed that they indeed found the scenarios to be enjoyable and relaxing. The previous studies have designed VR to address anxiety and pain among individuals with TBI.[28] Future research should assess the impact of VR scenarios designed to improve memory and eye tracking with relaxation in mind on anxiety and pain, among other outcomes.

Based on the focus group data, the authors anticipated red light sensitivity and motion sickness among participants but found neither of these issues in the pilot study. In editing the VR scenarios, it is possible to add the option of a blue-light tint, providing a potential solution for individuals who report red-light sensitivity in future studies. Motion sickness was avoided by offering slow movements in the scenarios.

This study designed the treatment sessions in terms of frequency, duration, and weekly schedule based on a systematic review recommending that VR should occur for 10 – 12 sessions, with each session lasting between 20 – 40 min, and conducted 2 – 4 times/week.[8] The study results suggested that a 20-min time frame for VR twice a week may be sufficient to yield positive outcomes. The shorter time frame from the scale of 20 – 40 was chosen to not overwhelm participants with so much information at one time. The authors chose to conduct VR with participants twice per week to prevent overwhelm, scheduling, and travel difficulties. Participants did travel a short driving distance to both locations used by the study. The locations were owned by a local non-profit, which the participants were familiar with and had traveled to before the study. More frequent VR use may have resulted in more challenges for participants to coordinate travel to the study

**Table 2. Virtual reality scenario memory outcomes**

| Statistics | Assessments | Baseline | | 6-week follow-up | | 12-week follow-up | Between-group difference at 6-week follow-up |
|---|---|---|---|---|---|---|---|
| | | Intervention group (*n*=6) | Control group (*n*=5) | Intervention group (*n*=6) | Control group (*n*=5) | Delayed intervention control group (*n*=3) | |
| *n* (%) | Objective memory test | | | | | | Nonparametric sign test* Intervention group: Improved, *n*=3 (50%); Same, *n*=3 (50%); Declined, *n*=0 Control Group: Improved, *n*=0; Same, *n*=5 (100%); Declined, *n*=0 |
| | Remembered | 1 (16.67) | 1 (20) | 4 (66.67) | 1 (20) | 2 (66.66) | |
| | Did not remember | 5 (83.33) | 4 (80) | 2 (33.33) | 4 (80) | 1 (33.33) | |
| *M* (standard deviation) | PRMQ | 3.00 (1.16) | 3.11 (1.15) | 2.67 (0.96) | 2.68 (0.86) | 3.06 (0.82) | One-way ANOVA*: *F*=0.001; *P*=0.971 |

Notes: *A non-parametric sign test was conducted on the intervention and control group to assess group differences in improvement, staying the same, or declining in their ability to remember something they were told to remember 5 min prior. One-way ANOVA was conducted to assess intervention and control group differences in means on the Prospective and Retrospective Memory Questionnaire (PRMQ) during the initial 6-week post-survey data collection time period.

**Table 3. Percentage of time participants were able to successfully fixate their eyes in the eye-tracking virtual reality scenario**

| Session | *M* (standard deviation) |
|---|---|
| Initial | 75% (16%) |
| Middle | 75% (22%) |
| Last | 92% (7%) |

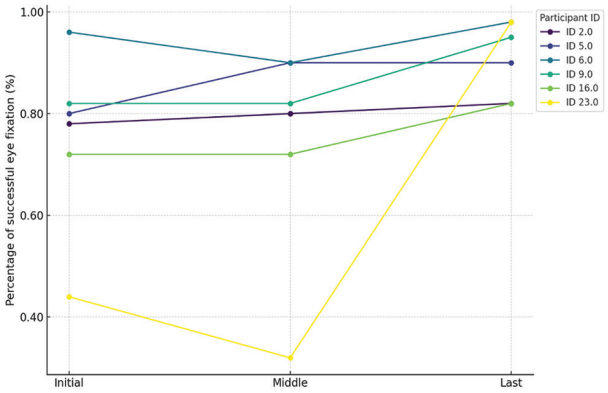


**Figure 3.** Line chart of each participant's percentage of successful eye fixation across the initial, middle, and last sessions ($n = 6$).

location. Future research will assess the same treatment parameters, including frequency of sessions, duration, and weekly schedule in an efficacy study.

## 5. Conclusion

This study is one of the first to use VR eye tracking capabilities as an intervention rather than an assessment tool. According to focus group participants in our study, the inability to fixate one's eyes on another person affected individuals with TBI's ability to have a normal, everyday conversation with others, inhibiting their ability to be social, work, and learn effectively. Few intervention studies have focused on eye fixation.[21,22] VR has been utilized as an assessment tool for eye fixation among individuals with TBI.[29] The literature lacks interventions employing VR to enhance eye fixation for individuals with TBI. Even in research on eye focusing on children with autism, VR is still being used as an assessment rather than an intervention tool.[30] Research on individuals with schizophrenia has included eye-focusing technique interventions as a part of VR social skills training.[31]

While the study's findings have implications for VR use and research, some limitations of the study include a small sample size, participants 1 year post-TBI, and no control group for the eye tracking scenario. An efficacy study with substantial power and randomization to intervention and delayed-intervention groups is needed to draw conclusions about the effectiveness of these VR scenarios. Future research on these scenarios will include individuals with TBI with acute injuries to assess its feasibility, acceptability, and effects on newer injuries and outcomes.

Both the VR scenarios demonstrated promise for improving prospective memory and eye tracking among individuals with TBI. Future research should assess their effects on larger sample sizes to assess their efficacy. VR should be considered as a rehabilitative option for cognitive and vision recovery among individuals with TBI.

## Acknowledgments

The authors would like to acknowledge the support of Lily Zepeda at the Brain Injury Center of Ventura County for helping with scheduling recruitment opportunities.

## Funding

Research, Scholarly, and Creative Award from California State University Channel Islands grant was used to purchase equipment for this study.

## Conflict of interest

The authors declare that they have no competing interests.

## Author contributions

*Conceptualization:* Kristen Linton, Bahareh Abbasi, Melissa Gutierrez Jimenez, Chrissy Stamegna

*Formal analysis:* Kristen Linton

*Investigation:* Jaylyn Aragon, Rasmey Gomez, Sky Hampton, Nathanael Paulus, Savanna Monson, Ben Michael, Vaishnavi Ramprasad

*Methodology:* Anna Gendron, Jaylyn Aragon, Rasmey Gomez, Sky Hampton, Nathanael Paulus, Savanna Monson, Ben Michael, Vaishnavi Ramprasad

*Writing – original draft:* Kristen Linton

*Writing – review & editing:* Kristen Linton, Bahareh Abbasi, Melissa Gutierrez Jimenez, Chrissy Stamegna

## Ethics approval and consent to participate

The California State University Channel Islands Institutional Review Board approved this study (IO5625). Written informed consent was obtained from study participants.

## Consent for publication

The informed consent stated, "study results in aggregate without identifying participants will be published." Participants approved of publishing results.

## Availability of data

The author, Kristen Linton, may be contacted at Kristen.linton@csuci.edu to obtain the data.

## Further disclosure

Part of the findings was presented at the North American Brain Injury Society Conference in March 2024.

## References


1. Dang B, Chen W, He W, Chen G. Rehabilitation treatment and progress of traumatic brain injury dysfunction. *Neural Plast.* 2017;2017:1582182.

   doi: 10.1155/2017/1582182

2. De Luca R, Calabrò RS, Gervasi G, *et al*. Is computer-assisted training effective in improving rehabilitative outcomes after brain injury? A case-control hospital-based study. *Disabil Health J.* 2014;7(3):356-360.

   doi: 10.1016/j.dhjo.2014.04.003

3. Haines KL, Nguyen BP, Vatsaas C, Alger A, Brooks K, Agarwal SK. Socioeconomic status affects outcomes after severity-stratified traumatic brain injury. *J Surg Res.* 2019;235:131-140.

   doi: 10.1016/j.jss.2018.09.072

4. Warren KL, García JJ. Centering race/ethnicity: Differences in traumatic brain injury inpatient rehabilitation outcomes. *PM R*. 2022;14(12):1430-1438.

   doi: 10.1002/pmrj.127371430

5. Lequerica AH, Sander AM, Pappadis MR, *et al*. The association between payer source and traumatic brain injury rehabilitation outcomes: A TBI Model Systems study. *J Head Trauma Rehabil*. 2023;38(1):E10-E17.

   doi: 10.1097/HTR.0000000000000781

6. Ing MM, Vento MA, Nakagawa K, Linton KF. A qualitative study of transportation challenges among intracerebral hemorrhage survivors and their caregivers. *Hawaii J Med Public Health*. 2014;73(11):353-357.

7. Pietrzak E, Pullman S, McGuire A. Using virtual reality and videogames for traumatic brain injury rehabilitation: A structured literature review. *Games Health J.* 2014;3(4):202-214.

   doi: 10.1089/g4h.2014.0013

8. Alashram AR, Annino G, Padua E, Romagnoli C, Mercuri NB. Cognitive rehabilitation post traumatic brain injury: A systematic review for emerging use of virtual reality technology. *J Clin Neurosci.* 2019;66:209-219.

   doi: 10.1016/j.jocn.2019.04.026

9. Caruana N, Seymour K, Brock J, Langdon, R. Responding to joint attention bids in schizophrenia: An interactive eye-tracking study. *Q J Exp Psychol* (*Hove*). 2019;72(8):2068-2083.

   doi: 10.1177/1747021819829718

10. Choi JY, Yi SH, Ao L, *et al*. Virtual reality rehabilitation in children with brain injury: A randomized controlled trial. *Dev Med Child Neurol*. 2021;63(4):480-487.

    doi: 10.1111/dmcn.14762

11. Cox DJ, Davis M, Singh H, *et al*. Driving rehabilitation for military personnel recovering from traumatic brain injury using virtual reality driving simulation: A feasibility study. *Mil Med*. 2010;175(6):411-416.

    doi: 10.7205/MILMED-D-09-00081

12. Dahdah MN, Bennett M, Prajapati P, Parsons TD, Sullivan E, Driver S. Application of virtual environments in a multi-disciplinary day neurorehabilitation program to improve executive functioning using the Stroop task. *NeuroRehabilitation*. 2017;41:721-734.

    doi: 10.3233/NRE-172183

13. Dvorkin AY, Ramaiya M, Larson EB, *et al*. A "virtually minimal" visuo-haptic training of attention in severe traumatic brain injury. *J Neuroeng Rehabil*. 2013;10:92.

    doi: 10.1186/1743-0003-10-92

14. Hougaard BI, Knoche H, Jensen J, Evald L. Spatial neglect midline diagnostics from virtual reality and eye tracking in a free-viewing environment. *Front Psychol*. 2021;12:742445.

    doi: 10.3389/fpsyg.2021.742445

15. Larson EB, Ramaiya M, Zollman FS, *et al*. Tolerance of a virtual reality intervention for attention remediation in persons with severe TBI. *Brain Inj*. 2011;25(3):274-281.

    doi: 10.3109/02699052.2010.551648

16. Sipatchin A, Wahl S, Rifai K. Eye-tracking for clinical ophthalmology with virtual reality (VR): A case study of the HTC vive pro eye's usability. *Healthcare* (*Basel*). 2021;9(2):180.

    doi: 10.3390/healthcare9020180

17. Marklund N, Bellander BM, Godbolt AK, Levin H, McCrory P, Thelin EP. Treatments and rehabilitation in the acute and chronic state of traumatic brain injury. *J Intern Med*. 2019;285(6):608-623.

    doi: 10.1111/joim.12900

18. Fox SM, Koons P, Dang SH. Vision rehabilitation after traumatic brain injury. *Phys Med Rehabil Clin N Am*. 2019;30(1):171-188.

    doi: 10.1016/j.pmr.2018.09.001

19. Glendon K, Desai A, Blenkinsop G, Belli A, Pain M. Recovery of symptoms, neurocognitive and vestibular-ocular-motor function and academic ability after sports-related concussion (SRC) in university-aged student-athletes: A systematic review. *Brain Inj*. 2022;36(4):455-468.

    doi: 10.1080/02699052.2022.2051740

20. Chamelian L, Feinstein A. Outcome after mild to moderate traumatic brain injury: The role of dizziness. *Arch Phys Med Rehabil*. 2004;85(10):1662-1666.

doi: 10.1016/j.apmr.2004.02.012

21. Watabe T, Suzuki H, Abe M, Sasaki S, Nagashima J, Kawate N. Systematic review of visual rehabilitation interventions for oculomotor deficits in patients with brain injury. *Brain Inj*. 2019;33(13-14):1592-1596.

doi: 10.1080/02699052.2019.1658225

22. Stuart S, Parrington L, Martini D, Peterka R, Chesnutt J, King L. The measurement of eye movements in mild traumatic brain injury: A structured review of an emerging area. *Front Sports Act Living*. 2020;2:5.

doi: 10.3389/fspor.2020.00005

23. Bostrom N. Are we living in a computer simulation? *Philos Q*. 2003;53(211):243-255.

doi: 10.1111/1467-9213.00309

24. Tegmark M. *Life 3.0: Being Human in the Age of Artificial Intelligence*. New York: Knopf; 2017.

25. Sessoms PH, Gottshall KR, Collins JD, Markham AE, Service KA, Reini SA. Improvements in gait speed and weight shift of persons with traumatic brain injury and vestibular dysfunction using a virtual reality computer-assisted rehabilitation environment. *Mil Med*. 2015;180(3 Suppl 1):143-149.

doi: 10.7205/MILMED-D-14-00385

26. Crawford JR, Henry JD, Ward AL, Blake J. The prospective and retrospective memory questionnaire (PRMQ): Latent structure, normative data and discrepancy analysis for proxy-rating. *Br J Clin Psychol*. 2006;45:83-104.

doi: 10.1348/014466505X28748

27. Caplan B, Bogner J, Brenner L, *et al*. Compensatory cognitive training for operation enduring freedom/operation Iraqi freedom/operation new dawn veterans with mild traumatic brain injury. *J Head Trauma Rehabil*. 2017;32(1):16-24.

doi: 10.1097/HTR.0000000000000228

28. Felix RB, Rao A, Khalid M, *et al*. Adjunctive virtual reality pain relief following traumatic injury: Protocol for a randomised within-subjects clinical trial. *BMJ Open*. 2021;11(11):e056030.

doi: 10.1136/bmjopen-2021-056030

29. Cogné M, Taillade M, N'Kaoua B, *et al*. The contribution of virtual reality to the diagnosis of spatial navigation disorders and to the study of the role of navigational aids: A systematic literature review. *Ann Phys Rehabil Med*. 2017;60(3):164-176.

doi: 10.1016/j.rehab.2015.12.004

30. Stokes JD, Rizzo A, Geng JJ, Schweitzer JB. Measuring attentional distraction in children with ADHD using virtual reality technology with eye-tracking. *Front Virtual Real*. 2022;3:855895.

doi: 10.3389/frvir.2022.855895

31. Adery LH, Ichinose M, Torregrossa LJ, *et al*. The acceptability and feasibility of a novel virtual reality based social skills training game for schizophrenia: Preliminary findings. *Psychiatry Res*. 2018;270:496-502.

doi: 10.1016/j.psychres.2018.10.014

ACCSCIENCE PUBLISHING

Brain & Heart

ORIGINAL RESEARCH ARTICLE

# Assessment of cerebral venous sinus: Anatomical and functional diagnostic performance of three-dimensional reconstruction models based on venous sinus MRI and CT images

**Xin Liu[1†], Zhenxin Hong[2†], Heyu Ding[3†], Pengfei Zhao[3], Shusheng Gong[4], Dhanjoo Ghista[5], and Zhenchang Wang[3*]**

[1]Guangdong Academy Research on VR Industry, School of Industrial Design and Ceramic Art, Foshan University, Foshan, Guangdong, China

[2]Department of Industrial Robotics, School of Artificial Intelligence, Guangdong Engineering Polytechnic College, Qingcheng, Guangdong, China

[3]Department of Radiology, Beijing Friendship Hospital, Capital Medical University, Beijing, China

[4]Department of Otolaryngology, Head and Neck Surgery, Beijing Friendship Hospital, Capital Medical University, Beijing, China

[5]University 2020 Foundation, San Jose, California, United States of America

*[†]These authors contributed equally to this work.*

***Corresponding author:**
Zhenchang Wang
(cjr.wzhch@vip.163.com)

**Citation:** Liu X, Hong Z, Ding H, *et al*. Assessment of cerebral venous sinus: Anatomical and functional diagnostic performance of three-dimensional reconstruction models based on venous sinus MRI and CT images. *Brain & Heart.* 2024;2(2):2756.
doi: 10.36922/bh.2756

**Received:** January 16, 2024

**Accepted:** April 8, 2024

**Published Online:** May 8, 2024



## Abstract

Venous sinus stenosis is commonly observed in patients presenting with pulsatile tinnitus (PT). While magnetic resonance imaging (MRI) and computed tomography (CT) are commonly used for assessing venous sinus geometries, the preferred modality remains unclear. In this study, we reconstructed the three-dimensional (3D) geometries of the venous sinus using MRI and CT imaging data from 20 PT patients. We conducted comparisons of the anatomical features of the venous sinus through case-wise analysis and anatomic geometrical parameter-wise analysis. Our findings indicate that by taking the geometries from CT as a reference, MRI could provide a better illustration of venous structure, primarily due to a stronger flow signal concentrated in the vascular tree. We observed high agreements in anatomic parameters measured from 3D geometries reconstructed based on CT and MRI in 19 out of 20 cases. Notably, the cross-sectional area of the sinus and segment length displayed the highest consistency, with a mean difference of -5.01% and 6.5% between modalities, respectively. In addition, we noticed that 55% of cases exhibited consistency in analyzing the confluence of the sinus, while variants of connectivity and collateral branching were observed between CT and MRI. Importantly, CT-based geometric reconstruction provided better detail of inflow side branches in the straight sinus, whereas MRI preserved more side branches of outflow in the downstream sinus. It is important to note that CT-based evaluation may be affected by the bone structures surrounding the venous sinus, whereas MRI-based evaluation focuses on blood flow to the segments, potentially indicating both anatomical and functional abnormalities.

***Keywords:*** Cerebral venous sinus; Pulsatile tinnitus (PT); Magnetic resonance imaging (MRI); Computed tomography

## 1. Introduction

Pulsatile tinnitus (PT) is often related to an underlying vascular abnormality, significantly affecting the patient's quality of life.[1] Cerebral venous stenosis-induced PT has gained increasing recognition, with venous sinus stenting (VSS) emerging as an effective treatment option for symptom relief.[2] Transverse sinus stenosis (TSS) is a commonly observed vascular abnormality in patients with PT.[3] The previous studies have highlighted the high diagnostic performance of both computed tomography venography (CTV) and magnetic resonance venography for anatomical analysis of venous sinuses.[4] The choice of modality generally depends on availability, although comparisons between modalities have been rarely assessed.

Anatomical assessment is widely conducted using CTV and Phase-contrast magnetic resonance imaging (MRI).[5,6] Computed tomography (CT) remains the primary approach for differentiating the source of vascular-related tinnitus, due to its high spatial resolution and consequent high diagnostic accuracy.[3] On the other hand, MRI has increasingly been applied for intracranial venous assessment, offering advantages such as superior soft-tissue contrast without interference bone structures, as shown in CT images.[7-9] Therefore, MRI is considered a promising tool for analyzing the vasculature and the defects of surrounding tissues, including vascular interface, meningeal defects, and related malformations.[7,9] However, the previous studies have reported potential false-positive diagnoses due to slow blood flow and artifacts in MRI, leading to ongoing debates regarding abnormalities in unilateral transverse dural sinuses and transverse sinuses (TSs).[10,11]

This study aims to assess the anatomical parameters of the venous sinus based on MRI from patients with PT, with CTV as a reference. For this purpose, three-dimensional (3D) anatomies were reconstructed from medical images for quantitative and qualitative evaluations.

## 2. Methods

### 2.1. Datasets

Patients with PT were retrospectively selected from Beijing Friendship Hospital, Capital Medical University, between March 13, 2019, and August 26, 2019. Inclusion criteria consisted of undergoing CTV and MRI within 3 months of the CTV examination. Exclusion criteria included previous stenting and the presence of venous sinus thrombosis, neoplasms, or arterial/arteriovenous abnormalities. This study was approved by the Institutional Review Board, and informed consent was obtained from all patients. A total of 20 patients, aged between 23 and 60 years with a mean age of 42 ± 12 years, were included in the present study.

### 2.2. Image acquisitions

The MRI data were acquired using a 3.0T MRI unit (Ingenia, Philips Healthcare, Netherlands) equipped with a 16-channel head coil. The MRI examinations employed a 3D phase-contrast technique using a gradient-echo sequence with the following parameters: field of view of $173 \times 173 \times 192$ mm$^3$, repetition time of 17 ms, echo time of 6.2 ms, flip angle of 10°, velocity encoding of 15 cm/s, bandwidth of 230 Hz/pixel, matrix size of $144 \times 108 \times 120$, and acquisition time of 2 min 15 s.

CTV images were acquired using a 256-section CT scanner (Revolution, GE Healthcare, US) with the following parameters: tube voltage of 100 kV, 25mAs (auto-mAs), matrix of $512 \times 512$, collimation of 256×0.625 mm, rotation time of 0.5 s, pitch of 0.992:1, and administration of contrast media (iopamidol, Bracco Diagnostics, UK) at a concentration of 370 mg iodine/ml, 1.5 ml/kg, injected at a rate of 5 ml/s. The average CT dose index (CTDI) was 63.95 mGy, and the average total dose length product (DLP) was 664.3 mGy·cm.

### 2.3. Reconstruction of 3D geometry models

The anatomies of the cases were reconstructed using Mimics 19.0 (Materialise, Belgium). The region of interest was segmented based on the signal intensity distribution of MRI and CTV images. Consultation with clinical technicians was conducted to improve the accuracy of 3D geometric reconstruction. The major segments of the intracranial venous network were evaluated, including the TSs, sigmoid sinuses (SSs), straight sinuses (StSs), inferior sinus, and superior sagittal sinuses (SSSs), as illustrated in Figure 1.

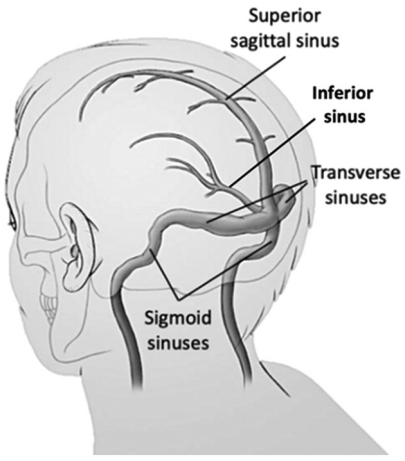


**Figure 1.** Intracranial venous network. The network encompasses superior sagittal sinus, transverse sinuses, sigmoid sinuses, and inferior sinuses.

### 2.4. Anatomical parameters for comparison

The anatomical parameters for comparison included the minimum and maximum cross-sectional area of the segment (CSA), degree of stenosis calculated as the ratio between the minimum and maximum CSA, volume (V) of the segment, segment length of the sinus (SL), the angle of the segment (α), and average curvature of the segment (Equation I):

$$\text{Curvature} = \left| \frac{\text{SL}}{\alpha} \right| \quad \text{(I)}$$

In addition, the length of the venous stenosis (Figure 2) was measured. The number of parameters ranged from 31 to 46, depending on the presence of the segments. Both sinus segment-wise and case-wise analyses were conducted. Intraobserver analysis was conducted to evaluate the consistency of anatomical parameter measurements. Repeated measurements were performed by the same reviewer within 1 week. The diameter ratio (DIAR) between CTV- and MRI-based measurements was used as an indicator for analysis. DIAR was calculated as follows (Equation II):

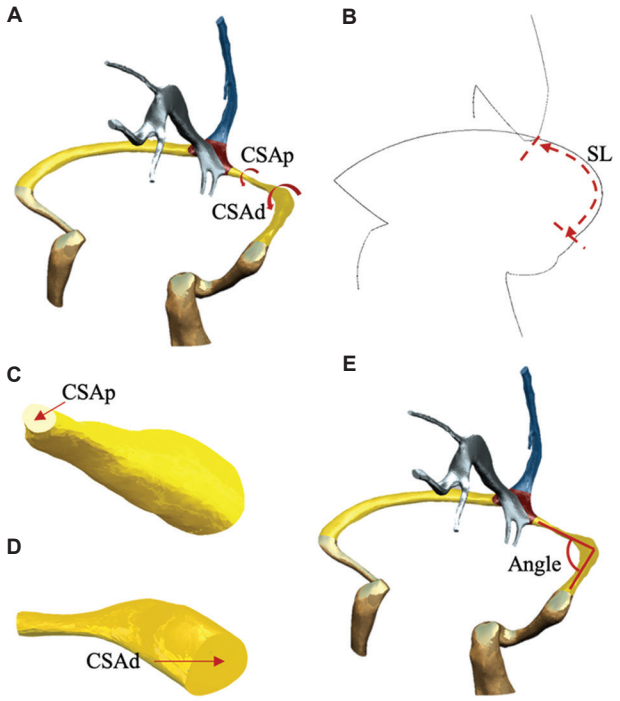


**Figure 2.** A schematic of the anatomical parameter extraction. This schematic illustrates the extraction of anatomical parameters from the 3D reconstructed geometry, specifically focusing on the segment of the transverse sinus. (A) The minimum and maximum cross-sectional areas of the segment are denoted as CSAp and CSAd, as shown in (C) and (D), respectively. (B) The measurement of segment length (SL). (E) The angle of the segment, with the recorded number of angles depending on the number of angles visible in the reconstructed geometry.

$$\text{DIAR} = \frac{\left(\text{CTV}_{\text{Diameter}} - \text{MRI}_{\text{Diameter}}\right)}{\text{CT}_{\text{Diameter}}} \quad \text{(II)}$$

In cases where a segment was absent, its diameter was represented as 0. Specifically, if a segment was absent in the CTV-based geometry, the denominator of DIAR was replaced by $\text{MRI}_{\text{Diameter}}$.

We conducted a sinus-wise analysis by comparing the number of entrances and exits of each sinus and major venous sinuses, including the SSS, inferior sinus, StS, TS, and SS. An agreement number was used to show the difference in collateral branches, which was defined as the ratio of cases with the same number of visible side branches in both CTV and MRI to the number of cases in CTV. A cross-reference analysis was conducted, and the number of missing entrances and exits was recorded.

In addition, we conducted a case-wise analysis of anatomical parameters based on MRI-reconstructed geometries by taking those from CTV-based geometries as references.

The development of the eye ring occurs during the four to 6 months of pregnancy, during which a series of primitive dura mater and dural sinus transitional growth and degeneration patterns occur. Irregular growth patterns can lead to asymmetry of the dural sinuses of varying heights and sizes, mild to obvious irregularities, and even loss of the inner TS.[12,13] The previous studies have illustrated six distinguished types of sinus confluence (connecting points) as follows: Type 1 indicates that the StSs are connected with the left and right TSs and the SSSs. Type 2a and 2b indicate that the StS is connected to the left or right TS. Type 3 is SSS and StS branching to bilateral TS. Types 4a and 4b indicate that the left or right TS is not connected. Types 5a and 5b indicate that an additional connecting vein is found between the StS and the SSS on both sides. Type 6 is the oblique sinus. These confluences are illustrated in Figure 3.[14] As the pattern of confluence sinus could be an important factor for evaluating the drainage of the blood flow in the sinus, a comparison of confluence classification using CTV and MRI was conducted.

### 2.5. Statistical analysis

Data analysis was performed using SPSS24.0 software (SPSS Inc., USA). Continuous variables, when appropriate, are expressed as mean±standard deviation (SD) or median (interquartile range [IQR]). Differences were assessed using the Bland-Altman test for consistency. Categorical variables are expressed as frequencies and percentages. Correlation analysis was conducted to examine the correlation between CTV and MRI anatomical structure parameters using correlation coefficients. $P < 0.01$ was considered statistically significant.

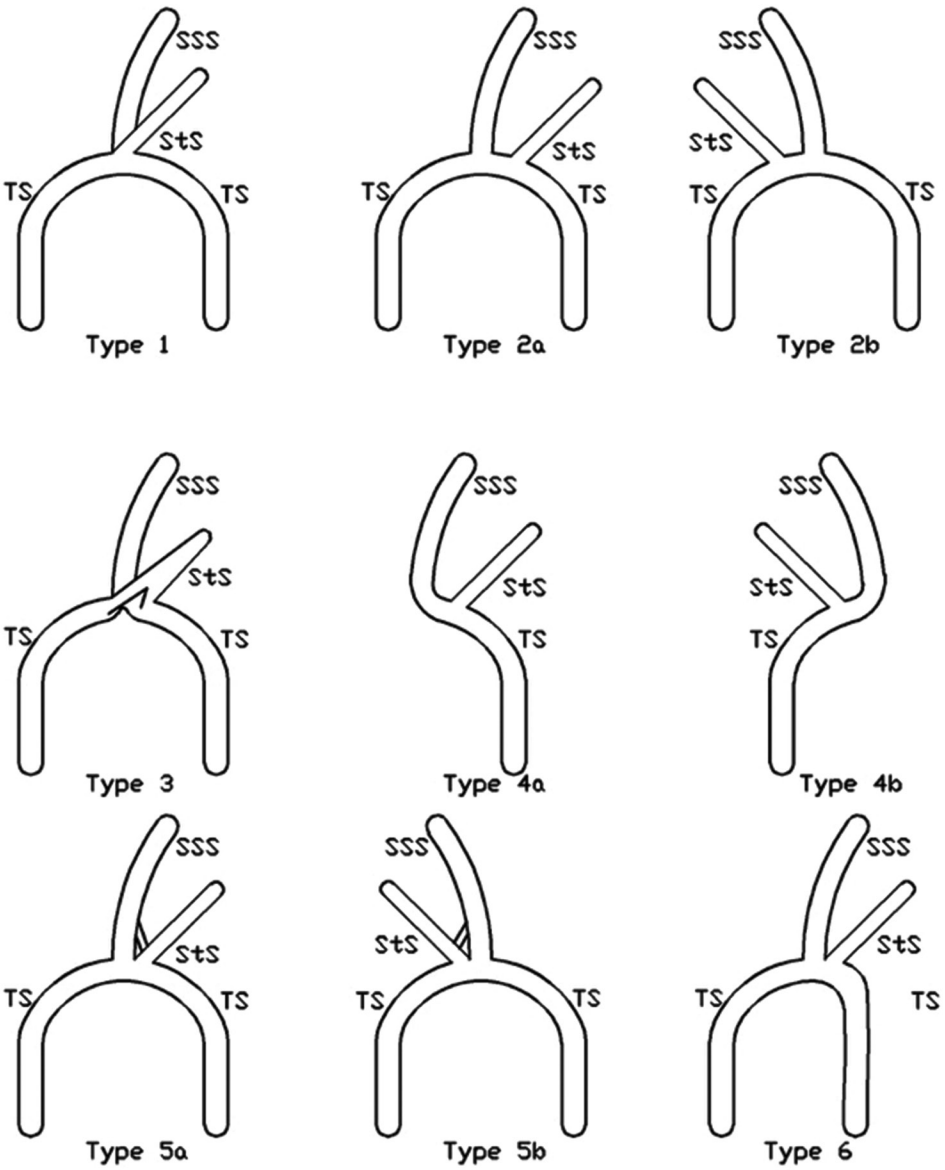


**Figure 3.** The schematics of six types of confluences
Abbreviations: SSS: Superior sagittal sinus; StS: Straight sinus; TS: Transverse sinus.

## 3. Results

In all cases, 3D geometries were successfully reconstructed from both CTV and MRI datasets. Figure 4 illustrates comparisons of segments reconstructed from CTV and MRI data. While the TS was identifiable in both CTV and MRI, the MRI images presented a stronger signal at the left TS (normalized against the surrounding structures) compared to those in the CTV images (A2 and B2). Segments are highlighted in colors. As an example, the comparisons of segments revealed a variation in visually available bifurcation at SSS between the geometric reconstructions based on MRI and CTV.

### 3.1. Comparison of anatomic parameters between CTV and MRI

In the sinus-wise analysis, a high degree of consistency (65%) was observed in SSS, with an average of one visible branch in both CTV and MRI. Compared to MRI, CTV exhibited more entrances to StS, with an agreement rate of 15%. The average number of visible branches in CTV and MRI was 6 and 5, respectively. On the other hand, MRI

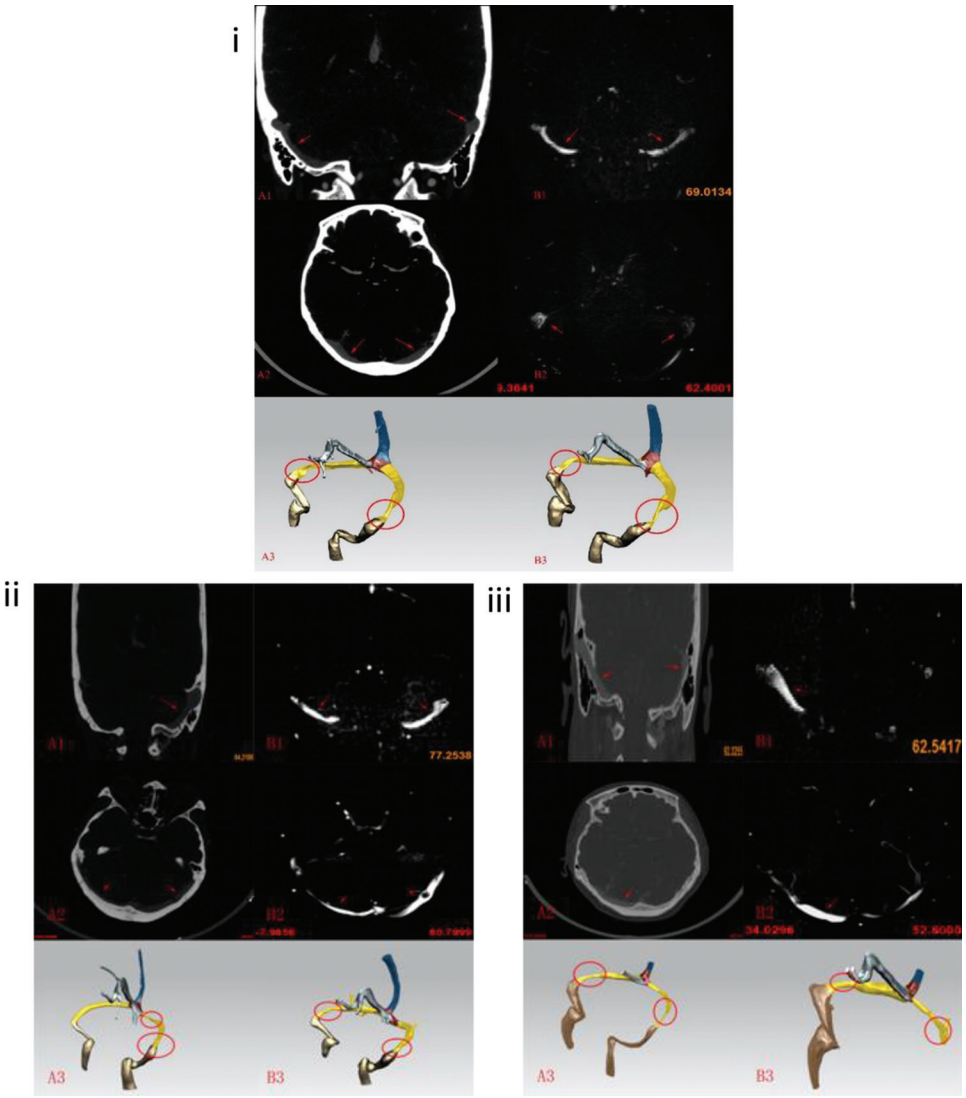


**Figure 4.** Comparison models of computed tomography venography (CTV) (images labeled by A) and magnetic resonance imaging (images labeled by B). A1 and B1 are coronal planes with transverse sinuses (indicated by red arrows); A2 and B2 are axial planes with transverse sinuses (indicated by red arrows); A3 and B3 are geometries reconstructed based on CTV and MRI images, respectively. Segments are highlighted in colors as follows: the superior sagittal sinus (blue), the left and right transverse sinuses (yellow), the left and right sigmoid sinuses (gold), the inferior sinus (silver), and the confluence of the segments (brown). Stenosis is highlighted with red circles. Panels i, ii, and iii represent Cases 3, 2, and 19, respectively.

demonstrated more TS outlets compared to CTV, with an agreement rate of 15% and an average of one and three visible branches in CTV and MRI, respectively. Similarly, MRI displayed more of the SS outlets compared to CTV, with an agreement rate of 25%. Detail distributions of inlets and outlets for CTV- and MRI-based geometric reconstructions are shown in Figure A1.

The case-wise analysis of anatomical parameters for each segment is illustrated in Figure 5. In general, the results demonstrated a robust correlation in ten out of 20 cases (correlation coefficient >0.9), a moderate correlation in nine out of 20 cases (correlation coefficient >0.5), and one case with a poor correlation (correlation coefficient = 0.28). Bland-Altman analysis indicated agreement between MRI- and CTV-based evaluations. Specifically, good consistency was observed in the CSA and segment lengths, while high variations were found in other parameters due to differences in visible-based reconstructions. Figure 6 illustrates the comparison of anatomical parameters in the best- and worst-correlated cases.

The intraobserver analysis showed high consistency of the measurements from geometries reconstructed CTV

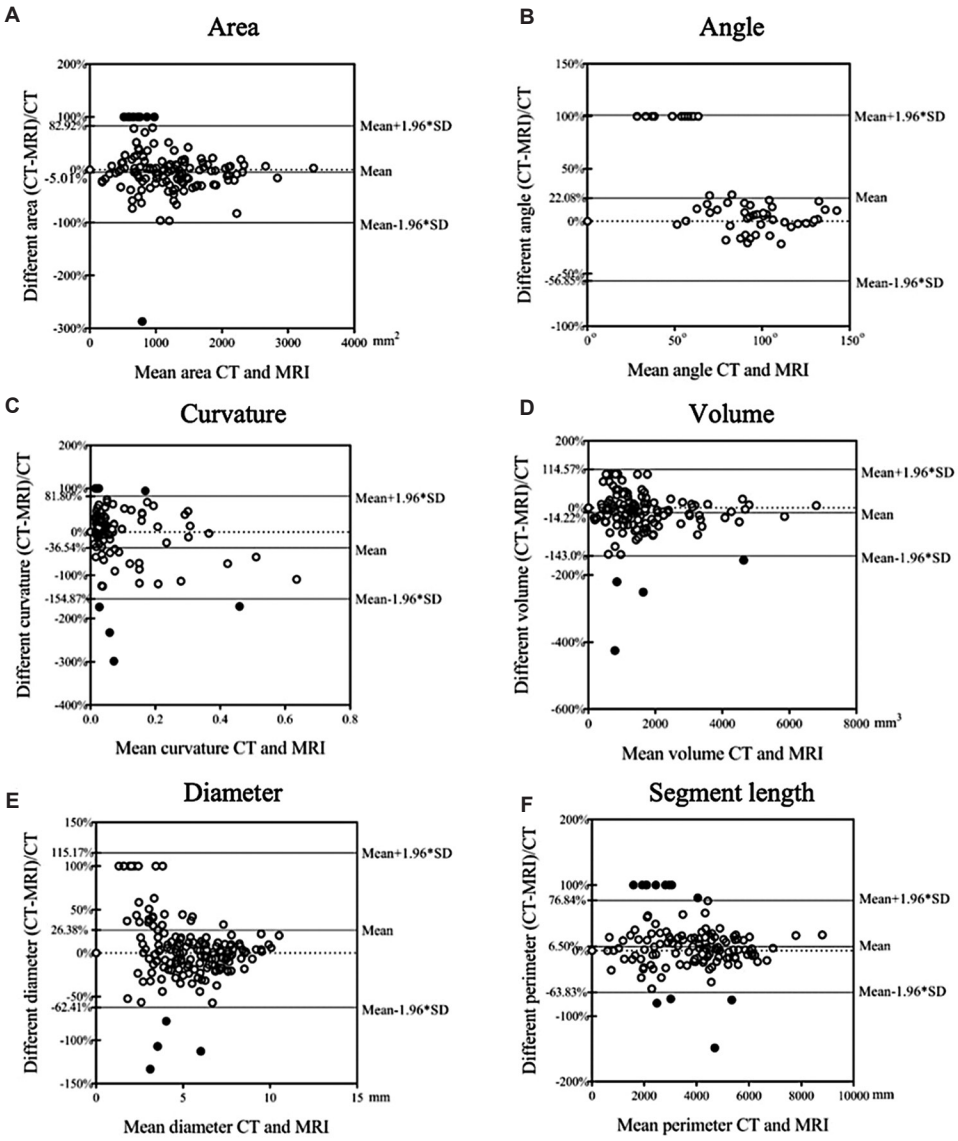


**Figure 5.** The case-wise analysis of anatomical parameters for each segment. This figure presents the geometrical parameters of all cases. (A) Cross-section area: Mean difference (−5.01%) and range of limits (82.92%, −100%). (B) Angle: Mean difference (22.08%) and range of limits (100%, −56.85%). (C) Curvature: Mean difference (−36.54%) and range of limits (81.80%, −154.87%). (D) Volume: Mean difference (−14.22%) and range of limits (114.57%, −143.0%). (E) Diameter: Mean difference (26.38%) and range of limits (115.17%, −62.41%). (F) Segment length: Mean difference (6.50%) and range of limits (76.84%, −63.83%). Abbreviations: CT: Computed tomography; MRI: Magnetic resonance imaging; SD: Standard deviation.

and MRI. Repeated measurements were 1 week after the first measurements. The reviewer was blinded to the recorded results and locations of measurement. The DIAR between CTV- and MRI-based measurements was taken as an indication for the analysis. The indicator segment-wise correlation analysis was conducted for all cases. The results of each venous sinus segment were recorded separately. The correlation analysis is shown in Figure 7, whereas the coefficients are shown in Table 1.

### 3.2. Comparison of the confluence of the sinus

The distribution of confluences in our dataset was determined using the CTV-based analysis as a reference. In general, the patterns of confluence analyzed using MRI images displayed agreement with CTV-based analysis in 55% of cases (11 out of 20). Comparisons between CTV and MRI are illustrated in Figure 8. The majority of the cases fall in the Type 2 category for both CTV- and MRI-

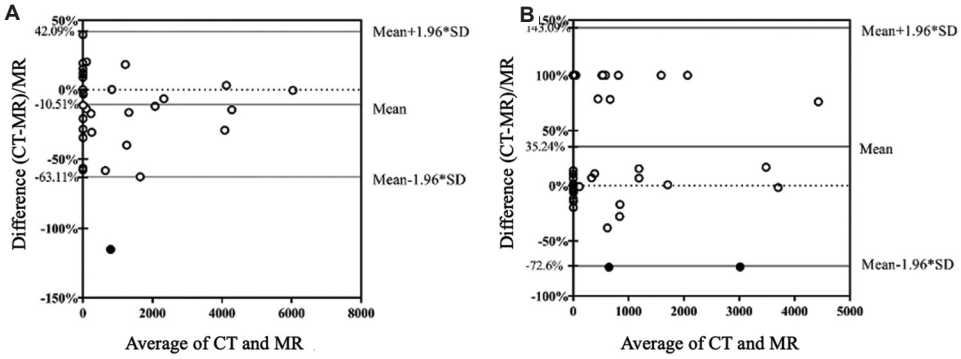


**Figure 6.** The comparison of anatomical parameters in the best- and worst-correlated cases. (A) The best-correlated case displays a Pearson coefficient value of 0.992, with a mean difference of 10.51% and a range of limits of (42.09%, −63.11%). (B) The worst-correlated case displays a Pearson coefficient value of 0.258, with a mean difference of 35.24% and a range of limits of (143.09%, −72.60%). Abbreviations: CT: Computed tomography; MRI: Magnetic resonance imaging; SD: Standard deviation.

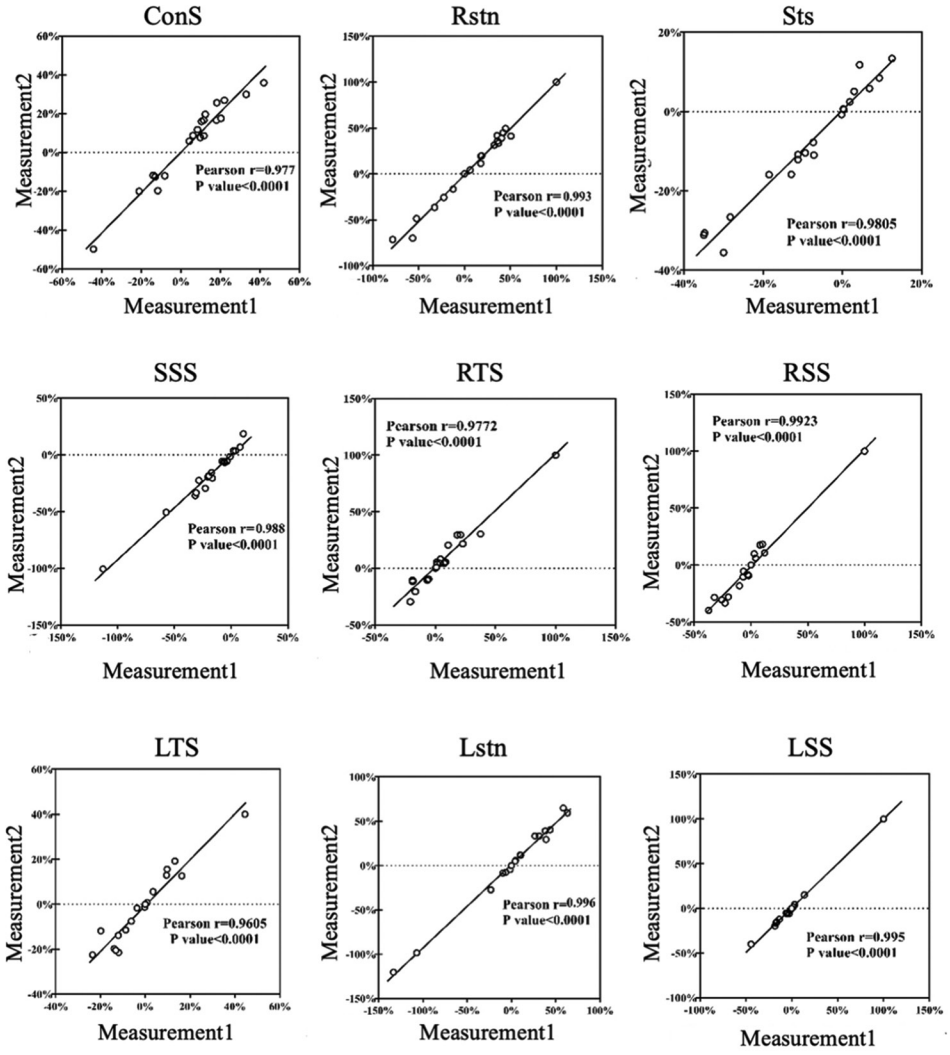


**Figure 7.** Intraobserver analysis using the differences in diameters between computed tomography venography (CTV) – and magnetic resonance imaging (MRI)-based measurements as indications. The correlation plots of repeating measurements for the following segments: Confluence sinus (ConS), right stenosis (Rstn), straight sinus (StS), superior sagittal sinus (SSS), right transverse sinus (RTS), right sigmoid sinus (RSS), left transverse sinus (LTS), left stenosis (Lstn), and left sigmoid sinus (LSS).

**Table 1. Results of the repeated measurement for intraobserver analysis using diameter ratio as an indicator**

| Segments | ConS | Rstn | Sts | SSS | RTS | RSS | LTS | Lstn | LSS |
|---|---|---|---|---|---|---|---|---|---|
| Correlations | 0.977 | 0.993 | 0.9805 | 0.988 | 0.9772 | 0.9923 | 0.9605 | 0.996 | 0.995 |

Abbreviations: ConS: Confluent sinus; LSS: Left sigmoid sinus; Lstn: Left stenosis; LTS: Left transverse sinus; RSS: Right sigmoid sinus; Rstn: Right stenosis; RTS: Right transverse sinus; SSS: Superior sagittal sinus; Sts: Straight sinus.

based analysis (20% and 35%, respectively). The number of cases for Type 4a and Type 6 was consistent between CTV and MRI (Two cases each for Type 4a and 1 case for Type 6). Variations in confluence were observed in other types (Figure 9). Specifically, the Type 3 confluence was identified based on CTV-based analysis in four cases (Cases 1, 7, 9, and 12, as illustrated in Figure A1), while in MRI-based analysis, these cases were identified as Types 4a, 2a, 2b, and 4a. Significant variations in confluence were observed in Cases 2, 11, and 17, where StS joined with the contralateral TS in MRI compared to CTV. Meanwhile, the small side branch originating from SSS was observed in CTV for Case 20, which was absent in MRI.

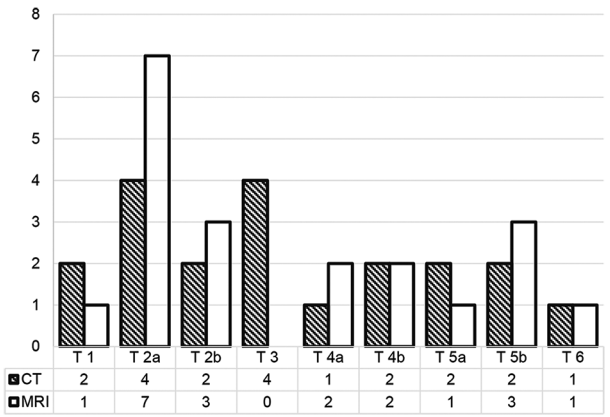


**Figure 8.** The distribution of the confluence variations. Type 1 to Type 6 indicated the nine types of confluence, as shown in **Figure 3**. Abbreviations: CT: Computed tomography; MRI: Magnetic resonance imaging; T: Type.

## 4. Discussion

A robust correlation and good agreement were evident in the sinus geometries when comparing the reconstructed geometries based on CTV and MRI. Sinus-wise analysis indicated that, with few exceptions observed in particular segments, MRI-based geometries preserved more side branches compared to CTV-based ones (Figure A1). However, despite these positive findings, several concerns remain regarding the use of MRI for the assessment of the venous sinus.

### 4.1. Classification of the confluence of the sinus

The previous studies have established the reliability of CT and MRI for vascular imaging. Nevertheless, both methods have limitations. The imaging of blood vessels in CT is affected by bone structures, contrast agents, and blood density,[15] while MRI is affected by the direction of blood flow, signal strength, and artifacts.[10] In addition, the confluence of the sinus is more discernible in CT due to the straightforward blood flow directions from SSS, StS, and TSs to the confluence sinus (Figure A2). Conversely, MRI may not clearly depict this confluence due to the complexity of blood flow directions. Notably, the density difference facilitates the recognition of the confluence sinus in CTV. Similarly, both modalities typically display a Type 1 confluence sinus in cases where the left and right TSs are connected (Figure 2), while Type 4 is observed in cases of unilateral TS and Type 6 in cases of an oblique sinus.[16] In addition, MRI may fail to capture the round Torcular Herophili type (Type 3) in all cases. Variations in geometric reconstruction arise from differences in the visibility of blood flow in images obtained from CTV and MRI (Figure 5). In particular, SS could be captured in CTV images but not in MRI images in certain cases (Figure A2), resulting in a 100% difference, as shown in Figure 4. Importantly, the volume of the geometries is significantly impacted by the absence of the sinus in MRI compared to CTV-based assessment.

Moreover, different patterns of confluent sinuses may introduce variability into the image-based assessment of the venous sinus system. Among these configurations, the circular torcular Herophili type exhibited higher overall accuracy when evaluated using CTV, a finding not significantly recognized by MRI. However, our results indicate that MRI is more adept at evaluating the dominant phenomenon of the TS, in line with previous reports.[13] Although this observation remained consistent in the segment-wise analysis of each venous sinus, other confluent sinus types exhibited a high disagreement rate (45%) when comparing MRI to CTV in our patient population with PT. In addition, Type 4b and Type 6 configurations could be misinterpreted as the same confluent sinus when using MRI. The misinterpretation of the absent TS may stem from challenges in detecting blood flow, which could be either hindered by variations in venous sinus anatomy or masked by surrounding bone structures.

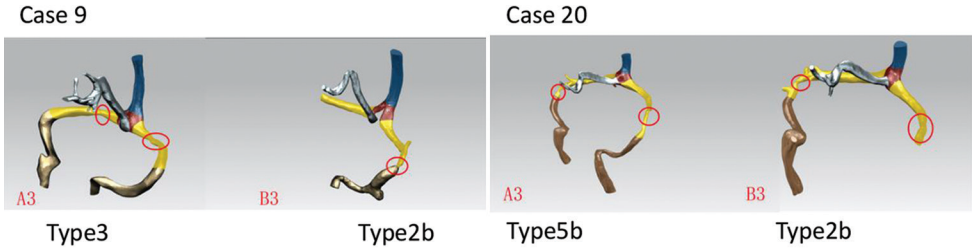


**Figure 9.** An illustration of the Variations in confluences of sinuses that are categorized into different types of patterns: Case 9. Type 3 and Type 2b; Case 20. Type 5b and Type 2b.

### 4.2. Side branch assessment

CTV and MRI have been used to assess venous sinus abnormalities for the diagnosis of PT, including stenosis, collateral sinus, and hypoplastic veins. However, Guryildirim *et al.* demonstrated that the accuracy of identifying blood vessels with a diameter less than 3 mm on CT images ranged 90 – 94%.[17] Conversely, accuracy reached 100% for blood vessels with a diameter exceeding 4 mm.[18] On the other hand, Gao *et al.* stated that MRI exhibited a specificity of over 94% and a sensitivity was 86% for detecting cerebral venous sinus thrombosis.[19] Our results revealed variability in the detection of small side branches between CTV and MRI. Notably, the SSS segment demonstrated the highest level of agreement in side branch detection when comparing MRI to CTV. In addition, MRI detected more side branches in the TS and SS. The signal flow indicated by MRI could enhance the contrast of the vascular tree against surrounding structures, potentially improving the identification of small branches compared to CTV. This enhancement might be attributed to the similar grayscale resolution of the contrast agent in small side branches compared to adjacent tissue.

In instances of complex cerebral venous sinus anatomy, collateral drainage vessels may transform into main venous outflow channels when positioned upright.[20-22] Mazur *et al.* have reported that if ligation of one TS within the venous sinus is necessary, the contralateral sinus must remain patent or exhibit sufficient drainage before surgery.[23] Similarly, Sheth *et al.* noted that a decreased number of collateral circulation vessels correlates with poorer outcomes in patients with dural venous sinus thrombosis.[24] Venous sinus occlusion can exacerbate brain swelling due to interrupted venous drainage, potentially leading to post-operative brain edema.[25,26] Collateral vessels develop through a process known as angiogenesis (the formation of collateral arteries and veins) may serve as a compensatory mechanism as a primary blood vessel gradually becomes obstructed. However, Florisson *et al.* proposed that collateral branches may reflect congenital abnormalities of the venous system rather than compensation mechanisms for increased intracranial pressure.[27] Therefore, evaluating venous sinus collateral circulation is important for supporting spontaneous and therapeutic thrombosis, and accurately identifying side branches could provide further information for the functional compensation of venous sinus stenosis.[28,29] In the present study, MRI-based evaluation allowed for the observation of more detailed collateral vessels, suggesting the potential for enhanced understanding of the functional significance of anatomic abnormalities in the TS and SS.

### 4.3. Clinical application

Computational fluid dynamics (CFD) simulation has emerged as a valuable tool for studying idiopathic intracranial hypertension.[30,31] The accuracy of patient-specific CFD simulations of hemodynamics depends significantly on the geometries. In the present work, we observed variations between CTV- and MRI-based 3D geometric reconstructions that could significantly impact simulations. As a result, hemodynamic analyses may vary, potentially leading to misinterpretation of sinus drainage in transient flow simulations. Our results of geometric reconstructions indicated a high degree of similarity between the geometries derived from CTV and MRI. While the distributions of stenosis exhibited high consistency between CTV and MRI, notable variations were observed in anatomical parameters. Although advanced MRI can visualize intracranial venous hemodynamics in patients with and without PT,[32] a more comprehensive understanding of hemodynamics is not solely attainable through MRI assessment, as invasive examinations remain the gold standard for measuring trans-stenotic pressure. Further, evaluation of the impact of geometries on hemodynamics is necessary to determine the optimal choice of imaging modalities for subsequent CFD simulations.

### 4.4. Limitations

Several limitations were identified in this study. First, the sample size was small, potentially compromising statistical power. Our analysis primarily focused on patients with PT to evaluate additional anatomical variations related to stenosis. While this approach may introduce clinical bias, our results

underscored the potential impact of non-invasive imaging modalities on anatomical analysis. Further investigation is warranted to justify the prevalence of such variations to facilitate the more convenient diagnosis of venous abnormalities related to PT. Second, digital subtraction angiography (DSA) was not incorporated in this study. Despite its utility in detecting vascular abnormalities in PT patients, the invasiveness of DSA has restricted its use exclusively to guide interventional radiology procedures.[33] However, DSA has demonstrated superior performance in assessing collateral venous drainage. Hence, further evaluation is required to evaluate the impact of additional drainage on comprehensively understanding PT diagnosis.[32] Thirdly, CTV data and visual-based vein segmentation served as the reference in the present study. To mitigate human error, geometric reconstruction was conducted with input from experts. In addition, repeated measurements were conducted to assess the consistency of visual-based evaluations, revealing a high correlation between measurements.

## 5. Conclusion

MRI has demonstrated high efficacy in assessing venous sinus stenosis when compared to CTV as a reference. In addition, MRI offers enhanced visualization of collateral vessels, thereby potentially facilitating a more accurate diagnosis of the functional significance of venous sinus stenosis based on anatomical analysis. While CTV-based evaluations may be affected by the bone structures surrounding the venous sinus, MRI-based evaluations primarily focus on blood flow within the segments, thus enabling the detection of both anatomical and functional abnormalities.

## Acknowledgments

None.

## Funding

This study is supported by the National Natural Science Foundation of China (grant nos.: 82202098, 61931013, and 82001910) and the Natural Science Foundation of Guangdong Province, China (2019A1515011463).

## Conflict of interest

The authors declare that they have no competing interests.

## Author contributions

*Conceptualization:* Xin Liu, Heyu Ding, Zhenchang Wang
*Formal analysis:* Pengfei Zhao, Shusheng Gong
*Investigation:* Xin Liu, Zhenxin Hong, Heyu Ding
*Methodology:* Xin Liu, Zhenxin Hong, Heyu Ding
*Writing – original draft:* Xin Liu, Zhenxin Hong
*Writing – review & editing:* Xin Liu, Dhanjoo Ghista

## Ethics approval and consent to participate

The Research Ethics Committee of Beijing Friendship Hospital, Capital Medical University, approved this study (Ethics approval code: 2023-P2-095-01). Data were collected retrospectively, and no further procedure was performed; hence, informed consent was waived.

## Consent for publication

All images used in this study were anonymized; hence, consent for publication was waived.

## Availability of data

The data used in this study will be made available on request after publication.

## References

1. Essibayi MA, Oushy SH, Lanzino G, Brinjikji W. Venous causes of pulsatile tinnitus: Clinical presentation, clinical and radiographic evaluation, pathogenesis, and endovascular treatments: A literature review. *Neurosurgery*. 2021;89(5):760-768.

   doi: 10.1093/neuros/nyab299

2. Nicholson P, Brinjikji W, Radovanovic I, *et al*. Venous sinus stenting for idiopathic intracranial hypertension: A systematic review and meta-analysis. *J Neurointerv Surg*. 2019;11(4):380-385.

   doi: 10.1136/neurintsurg-2018-014172

3. Zhao P, Ding H, Lv H, *et al*. CT venography correlate of transverse sinus stenosis and venous transstenotic pressure gradient in unilateral pulsatile tinnitus patients with sigmoid sinus wall anomalies. *Eur Radiol*. 2021;31(5):2896-2902.

   doi: 10.1007/s00330-020-07415-2

4. Zhao P, Lv H, Dong C, Niu Y, Xian J, Wang Z. CT evaluation of sigmoid plate dehiscence causing pulsatile tinnitus. *Eur Radiol*. 2016;26:9-14.

   doi: 10.1007/s00330-015-3827-8

5. Li Y, Chen H, He L, *et al*. Hemodynamic assessments of venous pulsatile tinnitus using 4D-flow MRI. *Neurology*. 2018;91(6):e586-e593.

   doi: 10.1212/WNL.0000000000005948

6. Heyu D, Pengfei Z, Han L, *et al*. A new method for assessing transverse sinus stenosis with CT venography based on the venous trans-stenotic pressure gradient. *J Neurointerv Surg*. 2023;15(10):1034-1038.

   doi: 10.1136/jnis-2022-019270

7. Patel D, Machnowska M, Symons S, *et al*. Diagnostic performance of routine brain MRI sequences for dural venous sinus thrombosis. *AJNR Am J Neuroradiol*. 2016;37(11):2026-2032.

doi: 10.3174/ajnr.A4843

8. Ghoneim A, Straiton J, Pollard C, Macdonald K, Jampana R. Imaging of cerebral venous thrombosis. *Clin Radiol*. 2020;75(4):254-264.

   doi: 10.1016/j.crad.2019.12.009

9. Dmytriw AA, Song JS, Yu E, Poon CS. Cerebral venous thrombosis: State of the art diagnosis and management. *Neuroradiology*. 2018;60:669-685.

   doi: 10.1007/s00234-018-2032-2

10. Provenzale JM, Kranz PG. Dural sinus thrombosis: Sources of error in image interpretation. *Am J Roentgenol*. 2011;196(1):23-31.

    doi: 10.2214/AJR.10.5323

11. Lansley JA, Tucker W, Eriksen MR, Riordan-Eva P, Connor SE. Sigmoid sinus diverticulum, dehiscence, and venous sinus stenosis: Potential causes of pulsatile tinnitus in patients with idiopathic intracranial hypertension? *Am J Neuroradiol*. 2017;38(9):1783-1788.

    doi: 10.3174/ajnr.A5277

12. Sarma A, Martin D, Pruthi S, Jones R, Little SB. Imaging the cerebral veins in pediatric patients: Beyond dural venous sinus thrombosis. *Radiographics*. 2023;43(2):e220129.

    doi: 10.1148/rg.220129

13. Pallewatte AS, Tharmalingam T, Liyanage N. Anatomic variants and artefacts in non enhanced MRV-Potential pitfalls in diagnosing cerebral venous sinus thrombosis (CVST). *Sri Lanka J Radiol*. 2016;2(1):40.

    doi: 10.4038/sljr.v2i1.23

14. Kobayashi K, Matsui O, Suzuki M, Ueda F. Anatomical study of the confluence of the sinuses with contrast-enhanced magnetic resonance venography. *Neuroradiology*. 2006;48:307-311.

    doi: 10.1007/s00234-006-0065-4

15. Buyck PJ, Zuurbier SM, Garcia-Esperon C, *et al*. Diagnostic accuracy of noncontrast CT imaging markers in cerebral venous thrombosis. *Neurology*. 2019;92(8):e841-e851.

    doi: 10.1212/WNL.0000000000006959

16. Vymazal J, Rulseh AM, Keller J, Janouskova L. Comparison of CT and MR imaging in ischemic stroke. *Insights Imaging*. 2012;3:619-627.

    doi: 10.1007/s13244-012-0185-9

17. Guryildirim M, Kontzialis M, Ozen M, Kocak M. Acute headache in the emergency setting. *Radiographics*. 2019;39(6):1739-1759.

    doi: 10.1148/rg.2019190017

18. Pereira VM, Cancelliere NM, Najafi M, *et al*. Torrents of torment: Turbulence as a mechanism of pulsatile tinnitus secondary to venous stenosis revealed by high-fidelity computational fluid dynamics. *J Neurointerv Surg*. 2021;13(8):732-737.

    doi: 10.1136/neurintsurg-2020-016636

19. Gao L, Xu W, Li T, *et al*. Accuracy of magnetic resonance venography in diagnosing cerebral venous sinus thrombosis. *Thromb Res*. 2018;167:64-73.

    doi: 10.1016/j.thromres.2018.05.012

20. Ruíz DS, Gailloud P, Rüfenacht DA, Delavelle J, Henry F, Fasel JH. The craniocervical venous system in relation to cerebral venous drainage. *Am J Neuroradiol*. 2002;23(9):1500-1508.

21. Boddu S, Dinkin M, Suurna M, Hannsgen K, Bui X, Patsalides A. Resolution of pulsatile tinnitus after venous sinus stenting in patients with idiopathic intracranial hypertension. *PLoS One*. 2016;11(10):e0164466.

    doi: 10.1371/journal.pone.0164466

22. Farrag A, Irfan M, Guliani GK, *et al*. Occurrence of post-acute recanalization and collateral formation in patients with cerebral venous and sinus thrombosis. A serial venographic study. *Neurocrit Care*. 2010;13:373-379.

    doi: 10.1007/s12028-010-9394-6

23. Mazur MD, Cutler A, Couldwell WT, Taussky P. Management of meningiomas involving the transverse or sigmoid sinus. *Neurosurg Focus*. 2013;35(6):E9.

    doi: 10.3171/2013.8.FOCUS13340

24. Sheth SA, Trieu H, Liebeskind DS, *et al*. Venous collateral drainage patterns predict clinical worsening in dural venous sinus thrombosis. *J Neurointervent Surg*. 2018;10(2):171-175.

    doi: 10.1136/neurintsurg-2016-012941

25. Tanaka M, Imhof HG, Schucknecht B, Kollias S, Yonekawa Y, Valavanis A. Correlation between the efferent venous drainage of the tumor and peritumoral edema in intracranial meningiomas: Superselective angiographic analysis of 25 cases. *J Neurosurg*. 2006;104(3):382-388.

    doi: 10.3171/jns.2006.104.3.382

26. Inamura T, Nishio S, Takeshita I, Fujiwara S, Fukui M. Peritumoral brain edema in meningiomas--influence of vascular supply on its development. *Neurosurgery*. 1992;31(2):179-185.

    doi: 10.1227/00006123-199208000-00002

27. Florisson JM, Barmpalios G, Lequin M, *et al*. Venous hypertension in syndromic and complex craniosynostosis: The abnormal anatomy of the jugular foramen and collaterals. *J Craniomaxillofac Surg*. 2015;43(3):312-318.

28. Huang YC, Lee JD, Pan YT, Weng HH, Yang JT, Lin LC. Perfusion defects and collateral flow patterns in acute small subcortical infarction: A 4D dynamic MRI study. *Transl Stroke Res*. 2022;13:339-409.

doi: 10.1007/s12975-021-00953-x

29. Venema SM, Dankbaar JW, Wolff L, *et al*. Collateral status and recanalization after endovascular treatment for acute ischemic stroke. *J Neurointerv Surg*. 2023;15(6):531-538.

doi: 10.1136/neurintsurg-2021-018545

30. Hatami H, Danesh N, Shojaei M, Hamedani AR. Evaluation of diagnostic values in NCCT and MRI of the patients with cerebral venous or sinus thrombosis in loghman hakim Hospital in Tehran 2014-2018. *Int Clin Neurosc J*. 2019;6(1):17-21.

31. Stoumpos S, Tan A, Hall Barrientos P, *et al*. Ferumoxytol MR angiography versus duplex US for vascular mapping before arteriovenous fistula surgery for hemodialysis. *Radiology*. 2020;297(1):214-222.

doi: 10.1148/radiol.2020200069

32. Bonatti M, Valletta R, Lombardo F, *et al*. Accuracy of unenhanced CT in the diagnosis of cerebral venous sinus thrombosis. *Radiol Med*. 2021;126:399-404.

doi: 10.1007/s11547-020-01263-2

33. Qiu X, Zhao P, Li X, *et al*. The relationships among transverse sinus stenosis measured by CT venography, venous trans-stenotic pressure gradient and intracranial pressure in patients with unilateral venous pulsatile tinnitus. *Front Neurosci*. 2021;15:694731.

doi: 10.3389/fnins.2021.694731

## Appendix

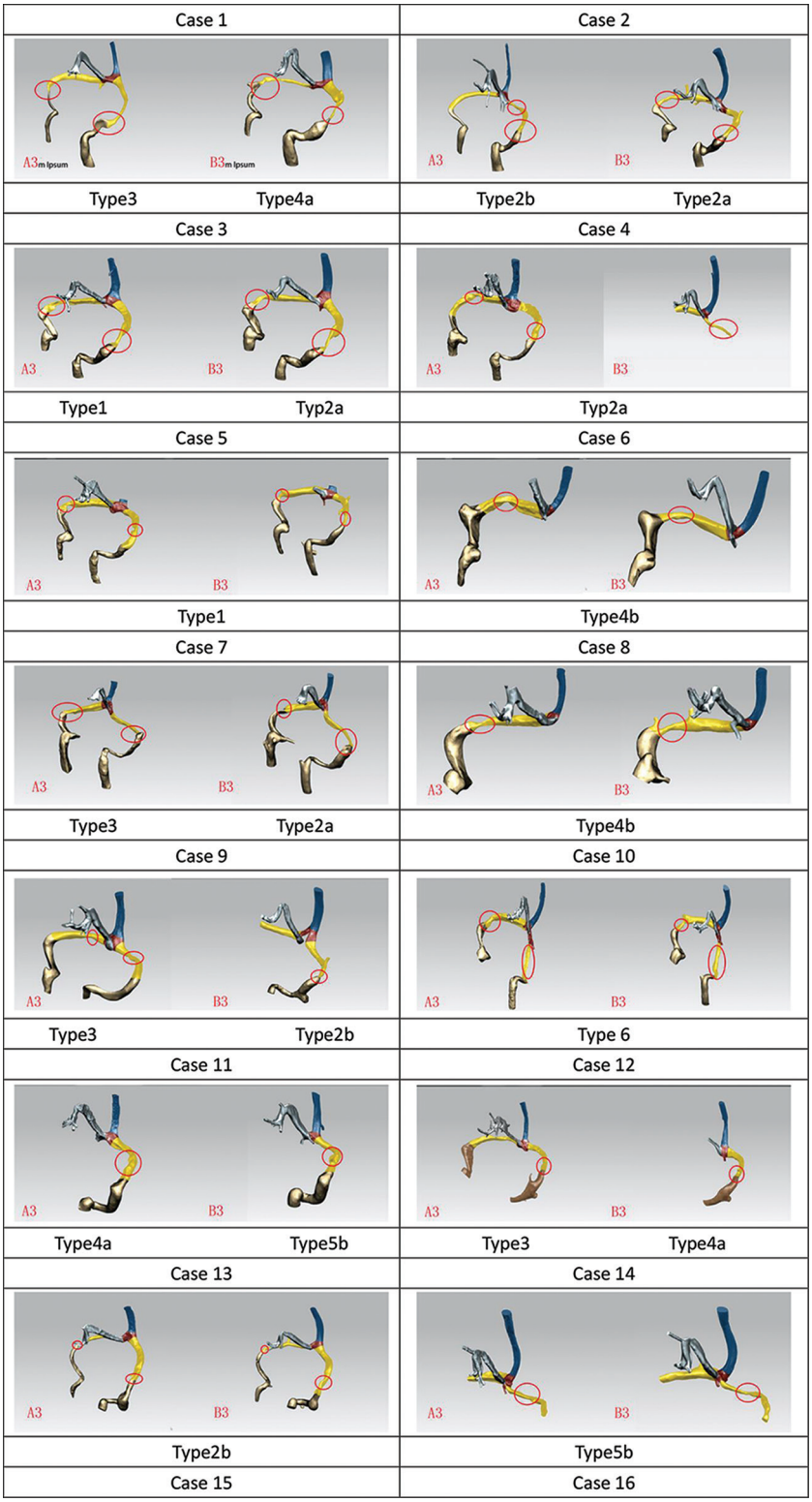


**Figure A1.** *(Cont'd...).*

*(Continued)*

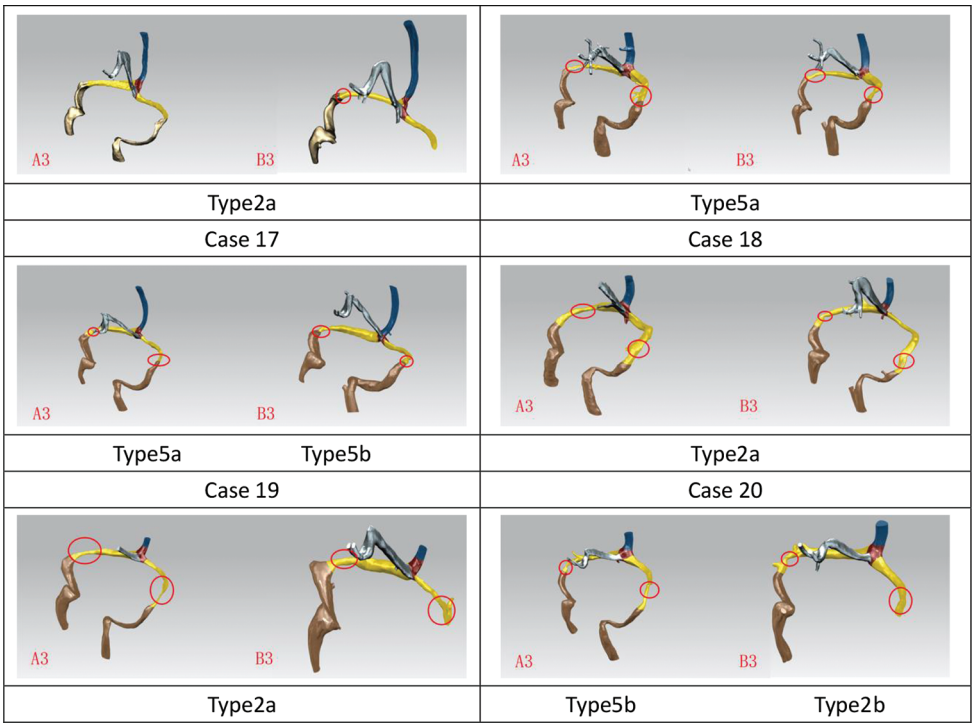


**Figure A1.** Sinus-wise analysis to compare the number of inlets and outlets between computed tomography (CT)-and magnetic resonance imaging (MRI)-based geometric reconstructions. In general, more inlets were observed at the superior sagittal sinus in CT-based geometric reconstructions, with the exception of Cases 7, 10, 15, 16, 18, and 19. Conversely, additional outlets were detected at the sigmoid sinus (SS) in MRI-based reconstructions for Cases 1, 5, 7, 8, 9, 10, 13, 15, 16, 17, 18, and 19.

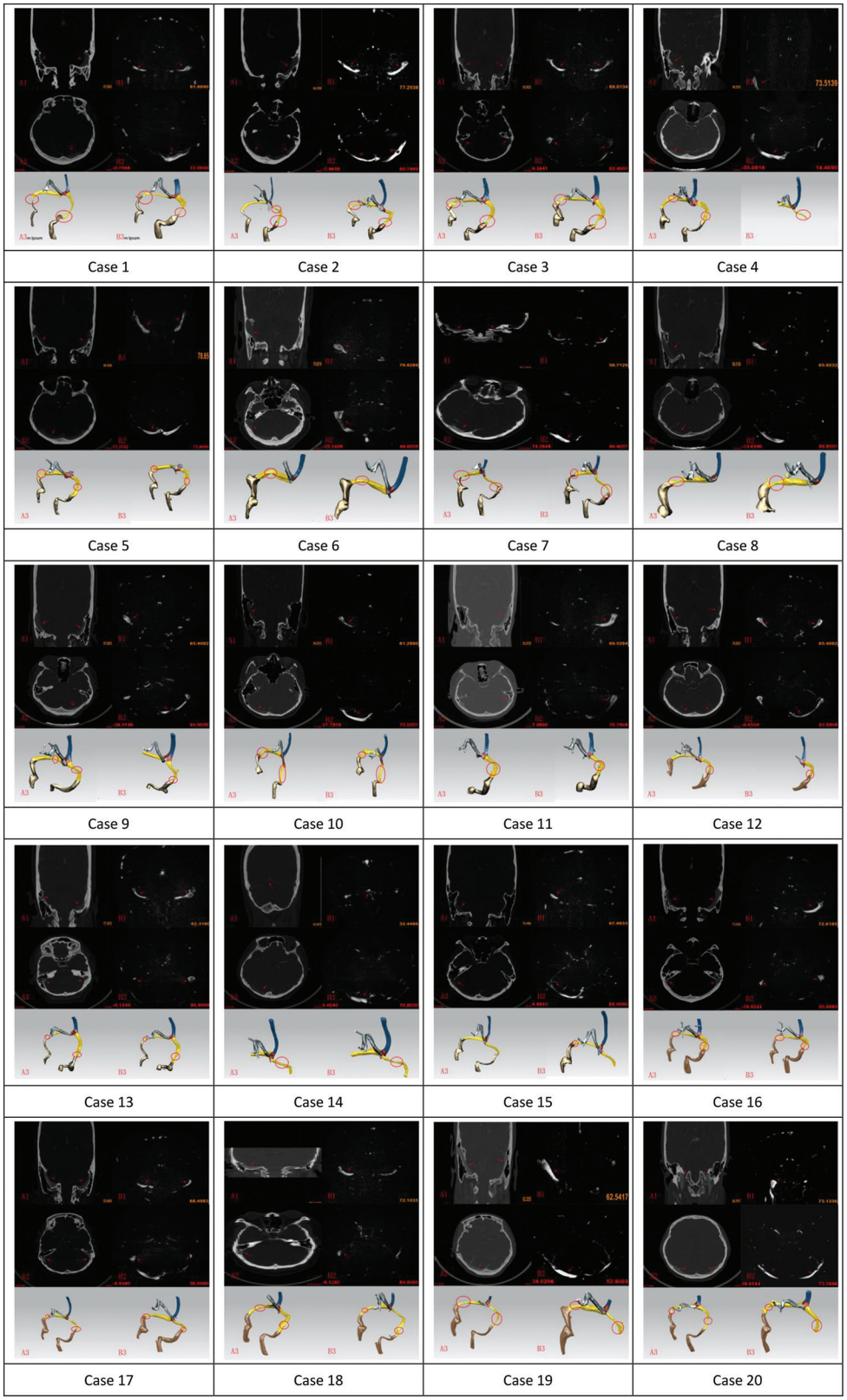


**Figure A2.** The case analysis in the present study. For each case, the left column illustrates the computed tomography-based results, while the right column presents the magnetic resonance imaging-based analysis. The first row displays the coronary plane relative to the transverse sinus. The second row depicts the transverse plane relative to the beginning of the sigmoid sinus. The third row showcases the three-dimensional geometric reconstructions based on the images.

ACCSCIENCE PUBLISHING

Brain & Heart

ORIGINAL RESEARCH ARTICLE

# Examining the relationship between Life's Essential 8 and atherosclerotic cardiovascular disease among Adults in the United States: Insights from the National Health and Nutrition Examination Surveys (2017-2020)

**Abraham M. Enyeji[1]* and David L. Wetzell[2]**

[1]Division of Community Medicine, Mercer University School of Medicine, Columbus Georgia, United States of America

[2]Division of Economics, Michigan State University, East Lansing, Michigan, United States of America

## Abstract

The American Heart Association recently updated the assessment of cardiovascular health (CVH) with the Life's Essential 8 (LE8) score. Our cross-sectional analytical study utilized data from 5042 adults in the United States (US) from the 2017 to 2020 NHANES surveys to examine the relationship between CVH assessed by LE8 metrics and the prevalence of atherosclerotic cardiovascular disease (ASCVD). Multivariate linear regressions were utilized to explore the relationship between CVH metrics and ASCVD, while linear probability models were used to predict ASCVD prevalence based on achieved LE8 scores. Controlling for relevant covariates revealed an inverse association between LE8 metrics and ASCVD prevalence. Improvements in LE8 were linked to a 29% reduction in ASCVD prevalence, with transitions to higher LE8 quartiles predicting a 4.8% reduction in ASCVD prevalence. Subgroup analysis indicated significant effects of age, education, and gender on ASCVD prevalence, with younger age, college education, and the female gender being associated with lower prevalence ($P < 0.05$). Higher LE8 scores correlated with decreased ASCVD prevalence, while factors such as younger age, college education, and the female gender were also associated with lower ASCVD prevalence. Conversely, transitioning from married to divorced/widowed/separated status was linked to increased ASCVD prevalence ($P < 0.01$).

***Keywords:*** Cardiovascular disease; Cardiovascular health; Non-Hispanic; Life's Simple 8; Healthy Eating Index

***Corresponding author:**
Abraham M. Enyeji
(enyeji_a@mercer.edu)

**Citation:** Enyeji AM, Wetzell DL. Examining the relationship between Life's Essential 8 and atherosclerotic cardiovascular disease among Adults in the United States: Insights from the National Health and Nutrition Examination Surveys (2017-2020). *Brain & Heart.* 2024;2(2):2915. doi: 10.36922/bh.2915

**Received:** February 12, 2024

**Accepted:** April 9, 2024

**Published Online:** May 14, 2024



## 1. Introduction

Atherosclerotic cardiovascular disease (ASCVD) continues to pose a significant burden, both in the United States of America (USA) and globally. In 2020 in the USA, coronary heart disease (CHD) deaths constituted the most prevalent cause of cardiovascular deaths (41.3%), followed by stroke (17.2%), other cardiovascular diseases (CVDs) (17.3%), hypertension (11.7%), cardiac insufficiency (9.9%), and artery diseases

(2.8%).[1] This condition is expected to contribute to a rising number of ASCVD-related deaths, reaching 20 million worldwide by 2030. Over the previous century, ASCVD has consistently been identified as a significant contributor to mortality rates in the USA. Given the generally low heritability of cardiovascular health (CVH) traits,[2] the role of behavioral and environmental factors as ASCVD risk factors is crucial. Emphasis on improvements of behavioral measures and health factors from a young age becomes critical for preserving ideal CVH into middle age and minimizing ASCVD. Therefore, the American Heart Association (AHA) has instituted a set of CVH metrics to improve the CVH on both individual and population scales, which should be assessed and tracked across groups. Recognizing the importance of a multifactorial approach in the prevention of CVD, the AHA introduced an updated set of metrics in 2022, known as Life's Essential 8 (LE8). These metrics are designed to guide and enhance the efforts to reduce the prevalence of ASCVD in the overall popuation.[3]

Prior investigations have revealed elevated stroke mortality rates within the African American population compared to whites, attributable to an increased incidence of comorbidities, such as hypertension, diabetes mellitus, and obesity. These findings, particularly those from cohorts of individuals free of prevalent cardiovascular disease at baseline, with over a 26-year temporal span, align with analogous conclusions posited by other scholars.[4,5] Concurrently, the prevalence of individuals attaining optimal CVH scores among whites marginally fell below 40%, while the corresponding rates for Mexican and black Americans markedly registered at 25%.[5]

While previous work mostly addressed individuals free of CVD, scant attention has been given to assessing the association of CVH metrics in adults with ASCVD, which includes stroke and CHD, the primary contributors to global cardiovascular mortality.[1] By utilizing nationally representative data from 2017 to 2020, this research seeks to examine the existing relationship between the AHA's LE8 scores and the prevalence of ASCVD among non-Hispanic (NH) white individuals in the USA.

## 2. Methods

### 2.1. Study design

This research utilized aggregated cross-sectional, secondary data from the National Health and Nutrition Examination Survey (NHANES), conducted between 2017 and 2020. The NHANES study is derived from a nationally representative survey administered every 2 years, covering the nonmilitary, non-institutionalized United States (US) population. Employing a complex multistage-probability sampling design, the survey aims to capture a diverse and comprehensive view of the population's health. The survey systematically gathers self-reported and directly measured data from participants, including health conditions, behaviors, dietary intake, physical examination, and laboratory tests. A comprehensive description of NHANES has been previously published.[6]

### 2.2. Study population

Adults aged 20 and above, identified as NH white, both with and without ASCVD, and participating in the NHANES conducted from 2017 to 2020 were considered. The final sample of 5042 participants was derived from various datasets using essential variables, including questionnaires, dietary, and demographic data.

ASCVD was determined through participant self-report, as individuals were asked to respond to inquiries such as, "Have you ever received confirmation from a medical professional indicating the presence of stroke, angina, myocardial infarction, or CHD?" The designation of having ASCVD was attributed to participants providing an affirmative response to any of the specified conditions. This extensively utilized criterion has been previously recorded in the literature.[7-10]

### 2.3. Assessment of LE8

In 2022, the AHA unveiled a new framework for measuring health, known as LE8, which builds on and extends the concepts introduced in Life's Simple 7 (LS7).[11] The LE8 framework employs a more intricate algorithm for the quantification of each metric and incorporates sleep health as an additional parameter[3] (Table S1). The LE8 includes eight components: four behavioral health measures (diet, sleep health, physical activity, and exposure to nicotine), and four health factors (normalized plasma glucose levels, body mass index [BMI], blood lipids, and blood pressure).

The LE8 scores were conceived on a continuous scale from 0 to 100, which increased the sensitivity of the metrics.[12] Consequently, in this study, individual LE8 metrics were computed as the mean of its eight constituent components, each graded on a scale from 0 to 100. Scores falling within the ranges of ≤49, 50 – 79, and ≥80 were, respectively, classified as indicative of poor, intermediate, or ideal CVH.

#### *2.3.1. Health behavior assessment*

Standardized questionnaires administered during study visits assessed the participants' self-reported health behaviors. The evaluation of dietary intake utilized the Automated Self-Administered 24-h (ASA24) Dietary Assessment Tool, where participants reported their food consumption exclusively for the preceding 24-h period,

specifically on the initial day of the study. The Healthy Eating Index-2015 (HEI-2015), serving as a metric for diet quality, was computed with a scale ranging from 0 to 100, where elevated scores signify improved diet quality.[13] The HEI-2015 scores were utilized as a surrogate for evaluating healthy dietary patterns, derived from a 1st-day 24-h dietary recall. HEI-2015 scores, constituting a 13-component index, spanned from 0 to 100, with elevated scores reflecting greater adherence to a healthy diet. The components comprised various dietary elements, including total fruit, whole fruit, grains, total vegetables, beans, dairy, whole grains, plant protein, total protein foods, seafood, fatty acids, refined grains, sodium, and empty calories. Participants were stratified based on their HEI-2015 score: ≤50 for poor health, 51 – 80 for intermediate health, and >80 for ideal health.[14] Certain variables necessary for calculating these components were directly sourced from the Food Patterns Equivalents Database (FPED) and NHANES totals files. The FPED and NHANES Total Nutrient Intake datasets provided the following components directly used in computing HEI-2015: data on total fruit, whole grains, dairy, refined grains, and added sugars, as well as sodium and saturated sats (Table S2).

Physical activity was assessed through a 3-day scale, transforming activity duration into weekly minutes of moderate- or higher-intensity physical activity. Sleep health was evaluated by self-reported usual sleep duration. Tobacco use, aligned with the AHA's nicotine exposure definition, included inquiries about current/former/non-cigarette-smoker status and cohabitation with regular cigarette smokers (Table S1).[15]

#### *2.3.2. Health factors assessment*

Health factors underwent assessment following NHANES protocols. BMI (kg/m²) was calculated by dividing the weight (kg) by the square of the standing height (m²). Systolic and diastolic blood pressure values were determined as the mean of all available measurements at the baseline assessment. Enzymatic methods were employed to measure serum cholesterol, while non-high-density lipoprotein (HDL) cholesterol was determined by subtracting HDL cholesterol from the total cholesterol value. Glycated hemoglobin levels were measured using high-performance liquid chromatography methods. Comprehensive details regarding each CVH metric, including the scoring algorithm, are available in the supplementary file and in previous studies.[15]

### 2.4. Main outcome measure

The assessment of ASCVD prevalence involved participants completing a self-administered questionnaire, where the diagnoses of any myocardial infarction, angina pectoris, congestive heart failure, stroke, or CHD were reported.

### 2.5. Covariates

During home interviews, demographic characteristics, such as age, ethnicity, highest level of education, self-reported sex, race, marital status, and annual household income, were collected. Participants were categorized into four age groups: 20 – 39 (young adulthood), 31 – 50 (middle age), 51-65, or ≥66 years (older age). Race and ethnicity information, as reported by the participants, followed NHANES protocols and included categories, such as NH Asian, NH black, NH white, Mexican American, or multiracial groups. Family income level was assessed using a monthly poverty level index, where participants reported the total family income for the previous month in dollars. This variable indicated the ratio of reported monthly income to the poverty threshold. Household poverty status was established by comparing monthly family income to poverty thresholds set by the Department of Health and Human Services and is classified into very low income (<1.0), low income (1.01 – 2.0), low middle income (2.01 – 3.0), middle income (3.01 – 4.0), and high income (>4.0).

### 2.6. Statistical analysis

Descriptive statistics were utilized to summarize the frequency distributions, employing corresponding weighted proportions and stratified by ASCVD and non-ASCVD status. The statistical analyses followed NHANES analysis and reporting standards, incorporating sample weights, stratification, and clustering considerations as stipulated. Continuous variables were expressed as mean (95% confidence interval [CI]), while categorical variables were delineated as counts (percentages). Baseline characteristics between the two groups based on CVH were compared using a *t*-test for continuous variables and a $\chi^2$ test for categorical variables, respectively. The relationship between LE8 and ASCVD was assessed using multivariate linear regression. All statistical analyses were performed using Stata SE, version 18, and a two-sided *p*-value of <0.05 was deemed statistically significant.

## 3. Results

### 3.1. Characterization of the sample

The study population consisted of 5042 individuals, representing a total of 102,388,285 individuals, with and without ASCVD. Within the ASCVD subgroup, the average age was 66.1 years (95% confidence interval [CI]: 65.44 – 66.90), while in the non-ASCVD subgroups, it was 32.40 years (95% CI: 32.0 – 32.80), with females

comprising 50.38% of the population. Table 1 provides a comprehensive breakdown of demographic characteristics for the study population.

The ASCVD subgroup had a mean age of 69.4 years (95% CI: 68.4 – 70.4), while the non-ASCVD subgroups had a mean age of 34.6 years (95% CI: 33.9 – 35.4), with 50.38% being female. These numbers were slightly higher than the average ages for the combined race sample, which were 66.1 (95% CI: 65.4 – 66.8) and 32.3 (95% CI: 31.9 – 32.7), respectively.

In Table 1, it is evident that males constituted a larger proportion of the ASCVD subgroup relative to the non-ASCVD subgroup. Those achieving some college education but without a 4-year degree completion were overrepresented in the ASCVD subgroup relative to those in the non-ASCVD subgroup (35.5% [95% CI: 31.6 – 39.[5] vs. 21.3% [95% CI: 20.1 – 22.[5]; $p<0.001$). A similar statistically significant difference in the proportions of college graduates did not exist between the two ASCVD subgroups. However, there is consistently a statistically significant difference between the proportions of individuals in different age groups between the two ASCVD subgroups. There is no consistent difference between the five income groups. The second lowest income group has a statistical difference, with a higher proportion of them being in the ASCVD subgroup. There are statistical differences between the two marital status subgroups, with the ASCVD subgroup being both older and more likely to be married or formerly married than the non-ASCVD subgroup.

Only 11.33% of participants in the current sample met the ideal diet criteria (Table 2). The frequency of participants meeting the ideal level for the remaining CVH metrics in the present sample was as follows: HbA1c (weighted, 94.6%), physical activity (weighted, 91.80%), cigarette smoking (weighted, 70.79%), total cholesterol level (weighted, 42.42%), BMI (weighted, 41.6%), blood pressure (weighted, 38.5%), and sleep health (weighted, 30.25%).

While fewer than 5% of the entire sample displayed subpar metric scores in the specific components related to sleep health, glycated hemoglobin A1c, and physical activity, approximately 60% of the population is classified as obese (BMI > 25 kg/m$^2$). In addition, 34% adhered to a poor diet, and 32% had a total cholesterol level exceeding 222 mg/dL. The assessment revealed that 13.64% of individuals currently engage in some form of smoking (Table 2).

The first regression (Table 3) compared poor and moderate LE8 levels versus an ideal LE8 level of 80 or

**Table 1. Descriptive statistics, comparison of non-Hispanic whites with (*n*=566 [11.23%]) and without (*n*=4,476 [88.77%]) ASCVD**

| Parameter | ASCVD (%) (95% CI) | Non-ASCVD (%) (95% CI) | *P* | Combined sample (%) (95% CI) |
|---|---|---|---|---|
| Gender | | | | |
| Male | 60.9 (56.6 – 64.6) | 48.9 (47.5 – 50.4) | <0.001 | 50.3 (48.9 – 50.6) |
| Age category | | | | |
| 20 – 30 | 1.1 (0.2 – 1.9) | 9.5 (8.6 – 10.3) | <0.001 | 8.5 (7.7 – 9.3) |
| 31 – 50 | 7.8 (5.6 – 10.0) | 18.1 (17.0 – 19.3) | <0.001 | 17.0 (15.9 – 18.0) |
| 51 – 65 | 22.4 (19.0 – 25.9) | 14.1 (13.1 – 15.1) | <0.001 | 15.0 (14.0 – 16.0) |
| 66+ | 67.5 (63.6 – 71.4) | 16.6 (15.5 – 17.7) | <0.001 | 22.3 (21.2 – 23.5) |
| Household income | | | | |
| Very low income (<1.0) | 10.8 (8.2 – 13.3) | 15.9 (14.8 – 16.9) | 0.002 | 15.3 (14.3 – 16.3) |
| Low income (1.01 – 2.0) | 32.2 (28.3 – 36.0) | 23.6 (22.3 – 24.8) | <0.001 | 24.6 (23.4 – 25.7) |
| Low middle income (2.01 – 3.0) | 17.7 (14.5 – 20.8) | 15.1 (14.0 – 16.1) | 0.105 | 15.4 (14.4 – 16.3) |
| Middle income (3.01 – 4.0) | 9.2 (6.8 – 11.6) | 10.1 (9.2 – 11.0) | 0.486 | 10.0 (9.2 – 10.8) |
| High income (>4.0) | 29.5 (25.7 – 33.3) | 35.1 (33.7 – 36.5) | 0.009 | 34.4 (33.1 – 35.7) |
| Education | | | | |
| Some college | 35.5 (31.6 – 39.5) | 21.3 (20.1 – 22.5) | <0.001 | 22.9 (21.7 – 24.1) |
| College graduate | 18.6 (15.3 – 21.8) | 16.8 (15.7 – 17.9) | 0.296 | 17.0 (16.0 – 18.0) |
| Marital status | | | | |
| Married | 52.5 (48.3 – 56.6) | 36.5 (35.1 – 37.9) | <0.001 | 38.3 (36.9 – 39.6) |
| Divorced, widowed, or separated | 42.0 (38.0 – 46.1) | 13.6 (12.6 – 14.6) | <0.001 | 16.8 (15.7 – 17.8) |

Abbreviations: ASCVD: Atherosclerotic cardiovascular disease; CI: Confidence interval.

**Table 2. Distribution of ideal, intermediate, and poor CVH across metrics among non-Hispanic white adults (*n*=4,459) without ASCVD, NHANES 2017 – 2020**

| Metric | Number of participants (*n* [%]) |
|---|---|
| Body mass index (kg/m$^2$) | |
| <25 (ideal) | 1,854 (41.58) |
| 25 – 29.9 (intermediate) | 881 (19.76) |
| ≥30 (poor) | 1,724 (38.66) |
| Smoking | |
| Never or quit for >12 months (ideal) | 3,228 (70.79) |
| Former smoker; quit for ≤12 months (intermediate) | 710 (11.46) |
| Current (poor) | 622 (13.64) |
| Physical activity | |
| ≥150 min/d moderate intensity; ≥75 min/d vigorous intensity; or≥150 min/d moderate and vigorous intensity (ideal) | 4,109 (91.80) |
| 1 – 149 min/d moderate intensity; 1 – 74 min/d vigorous intensity; or 1 – 149 min/d moderate and vigorous intensities (intermediate) | 367 (8.20) |
| None (poor) | 17 (0.4) |
| Healthy diet score* (healthy eating index [HEI]-2015) | |
| ≥80 (ideal) | 493 (11.33) |
| 50 – 79 (intermediate) | 2,406 (55.28) |
| <49 (poor) | 1,453 (33.39) |
| Total cholesterol (non-HDL cholesterol [mg/dL]) | |
| <130 (ideal) | 1,883 (42.42) |
| 131 – 220 (intermediate) | 1,169 (26.33) |
| >220 (poor) | 1,387 (31.25) |
| Blood pressure (mm Hg) | |
| SBP<120; DBP<80 (ideal) | 1,724 (38.56) |
| SBP: 120 – 139; DBP: 80 – 89; or treated to a goal (intermediate) | 914 (20.44) |
| SBP≥140 or DBP ≥90 (poor) | 1,833 (41.00) |
| Glycated hemoglobin A1c (%) | |
| <5.7 (ideal) | 4,236 (94.68) |
| 5.7 – 6.4 (intermediate) | 49 (1.10) |
| >6.4 (poor) | 174 (4.22) |
| Sleep health (h of sleep) | |
| 7 – 9 (ideal) | 1,208 (30.25) |
| 4 – 9 or>10 (intermediate) | 2,757 (69.05) |
| <4 (poor) | 28 (0.70) |

Note: *HEI-2015, validated as a representative measure of diet quality in the population, was employed as a proxy for the American Heart Association (AHA)'s healthy diet score.
Abbreviations: DBP: Diastolic blood pressure; SBP: Systolic blood pressure; CVH: Cardiovascular health; ASCVD: Atherosclerotic cardiovascular disease; NHANES: National Health and Nutrition Examination Survey.

higher, following adjustments for potential confounding variables that included income relative to poverty level, race/ethnicity, educational attainment, sex, age, and marital status. LE8 is then used with a square and then a cubic polynomial specification with similar controls (Table 3). The polynomial specification utilizes all data in LE8, enabling systematic variation of the marginal impact on the probability of ASCVD with the level of LE8. Finally, a linear probability model was constructed by individually incorporating all eight components of LE8, aiming to discern their distinct effects on ASCVD. In addition, significant correlations at the 5% level between the components were considered.

In Table 3, we demonstrated that the use of LE8 controls for poor and intermediate categories did not predict the prevalence of ASCVD. The coefficients on both identification variables were not significantly different from zero. The next column revealed that a quadratic function of the LE8 metric predicted the incidence of ASCVD. The fourth column illustrated that a cubic polynomial did not improve on the quadratic polynomial, as evidenced by the non-statistically significant difference of $R^2$ and the cube of LE8 from zero, as its 95% confidence interval contains zero.

Furthermore, as indicated in Table 3, age categories predominantly predicted a higher ASCVD probability, while being college-educated with a 4-year diploma reduced the prediction probability by 6%, or raised by 4% if self-identified as male. The emergence of diverse results across different age groups aligns with findings from a prior study, where young adults with CVD tended to be older and had lower LS7 scores compared to their CVD-free counterparts in the same age range. Potential explanations for these differences include factors associated with awareness, behavior, and socioeconomic status leopold.[16] In addition, an elevated prevalence of ASCVD of almost 5% was observed among those who were widowed, divorced, or separated, compared to married individuals, as can be calculated by taking the difference between the widowed/divorced/separated coefficient minus the married coefficient in Table 3.

## 4. Discussion

The non-linear relationship between the new LE8 score and ASCVD was investigated using a multivariate linear probability model in a nationwide survey. Our findings indicate that higher LE8 scores are generally associated with lower ASCVD prevalence. Our findings align with prior studies indicating a decrease in the prevalence of CVD associated with higher LE8 scores.[17] Recent research conducted on a group of South Asian American adults with suboptimal (poor) CVH, as evaluated by LE8 scores,

**Table 3. Results from the linear probability model's prediction of the prevalence of ASCVD among non-Hispanic whites from the pre-pandemic NHANES dataset**

| Predictors | Categorical LE8 (95% CI) | LE8+square (95% CI) | LE8, square+cube (95% CI) |
|---|---|---|---|
| CVH | | | |
| Constant | −0.010 (−0.11 – 0.10) | 1.00* (0.39 – 1.6) | 0.521 (-1.1 – 2.14) |
| Poor | 0.043 (−0.14 – 0.23) | - | - |
| Intermediate | −0.032 (−0.10 – 0.03) | - | - |
| LE8 score | | | |
| /10 | - | −0.29* (−0.5 – [−0.1]) | 0.007 (−0.08 – 0.07) |
| squared/100 | - | 0.020* (0.007 – 0.03) | −0.014 (−0.13 – 0.10) |
| cubed/1000 | - | - | 0.0001 (−0.0004 – 0.0007) |
| $R^2$ | 0.120 | 0.129 | 0.130 |
| Age | | | |
| 20 – 30 | 0.040* (−0.01 – 0.10) | 0.051* (0.01 – 0.10) | 0.050* (0.01 – 0.10) |
| 31 – 50 | 0.069* (0.01 – 0.12) | 0.078* (0.01 – 0.14) | 0.076* (0.01 – 0.14) |
| 51 – 65 | 0.196* (0.11 – 0.28) | 0.203* (0.11 – 0.30) | 0.035 (−0.07 – 0.14) |
| 66+ | 0.310* (0.19 – 0.42) | 0.329* (0.22 – 0.44) | 0.329* (0.22 – 0.44) |
| Income/poverty line | | | |
| 1.01 – 2.0 | 0.042 (−0.07 – 0.15) | 0.051 (−0.06 – 0.16) | 0.056 (−0.06 – 0.18) |
| 2.01 – 3.0 | 0.007 (−0.090 – 0.10) | 0.012 (−0.09 – 0.13) | 0.030 (−0.07 – 0.14) |
| 3.01 – 4.0 | 0.018 (−0.09 – 0.12) | 0.026 (−0.08 – 0.13) | 0.056 (−0.11 – 0.22) |
| >4.01 | −0.018 (−0.09 – 0.06) | −0.006 (−0.10 – 0.08) | −0.004 (−0.08 – 0.10) |
| Education | | | |
| Some college (no B.A.) | −0.012 (−0.07 – 0.04) | −0.001 (−0.04 – 0.05) | 0.003 (−0.04 – 0.05) |
| College grad | −0.072* (−0.14 – 0.01) | −0.062* (−0.13 – 0.00) | −0.063* (−0.13 – [−0.003]) |
| Marital status | | | |
| Married | −0.017 (−0.05 – 0.01) | −0.011 (−0.07 – 0.05) | −0.011 (−0.07 – 0.05) |
| Divorced, widowed, or separated | 0.042 (−0.04 – 0.13) | 0.040 (−0.05 – 0.13) | 0.036 (−0.05 – 0.12) |
| Gender | | | |
| Male | 0.040* (0.01 – 0.06) | 0.042* (0.00 – 0.08) | 0.040* (−0.00 – 0.08) |

Note: *denotes significance at a two-sided 5% level.
Abbreviations: B.A.: Bachelor's degree; CVH: Cardiovascular health; LE8: Life's Essential 8; ASCVD: Atherosclerotic cardiovascular disease; NHANES: National Health and Nutrition Examination Survey; CI: Confidence interval.

indicated that a higher LE8 score correlated with lower odds of any coronary artery calcium (CAC), which serves as a marker for ASCVD. In addition, higher LE8 scores were associated with decreased 10-year and lifetime risks of ASCVD.[18-20]

Subgroup analyses among NH whites indicated significant effects of age, college education, and gender on ASCVD, with younger individuals, college graduates, and women having lower probabilities of ASCVD.

The quadratic polynomial in Table 3 enables the calculation of the predicted impact of incremental changes in LE8 metric scores. Improvements in LE8 scores from the 25$^{th}$ to the 75$^{th}$ percentile were marginally associated with a reduction of 4.8% in the likelihood of experiencing ASCVD. These findings align with prior research outcomes.[21,22] It should also be noted that the unconditional probability of ASCVD in our sample is 7.8%. Participants transitioning from a LE8 metric score of 50 – 72.5 during 2017 – 2020, specifically NH whites, would be predicted to have lowered their probability of ASCVD by a maximum of 10%. This sizable reduction in prevalence is in accordance with the previous studies that predict sizeable percent reductions in the probability of a disease for a shift from poor to ideal CVH management. Olson *et al.*[23] noted that individuals classified with ideal and intermediate LS7 categories exhibited a 44% and 38% reduced risk of venous thromboembolism, respectively, in contrast to those categorized as inadequate or poor.[23]

Likewise, in a study conducted within a community setting, individuals characterized by a healthy lifestyle, as denoted by an ideal LS7 score, exhibited a 55% decreased risk of heart failure in comparison to those with an inadequate LS7 score.[24] Moreover, a separate investigation involving older British men illustrated the benefits of LS7 indicators on the incidence of stroke.[25] At present, only a few studies have utilized LE8 to assess CVH, and there have been no investigations into the relationship between LE8 and ASCVD among pre-pandemic adults in the USA. Many studies have focused on significant enhancements in LS7 or individual LS7 metrics with ASCVD, and our findings are consistent with those of previous studies.[26,27]

Using NHANES data and multivariate linear probability regression analysis, we revealed a negative association between enhanced CVH, as defined by LE8, and the prevalence of ASCVD in the NH white population subgroup. While the original LS7 metrics have been extensively utilized to examine the mechanisms, influences, development, and outcomes of CVD across different populations, subsequent evidence has highlighted the limitations of this score. Notably, compared to LS7 metrics, LE8 offers increased sensitivity in the aggregate assessment of adult CVH. Unlike LS7, LE8 metrics range from 0 to 100 and include a refined assessment of components, such as adult physical activity, which now comprises seven categories instead of the previous three.

Moreover, HEI, employed for evaluating the alignment of a food set with the Dietary Guidelines for Americans (DGA), is regularly updated to correspond with each new edition of the DGA. For this study, the version linked with the 2015 – 2020 DGA was utilized, where HEI-2015 maintains the same components as the HEI-2010, except for the substitution of saturated sat and added sugars for empty calories.[28] Thus, LE8 metrics have been established as a new conceptualization of CVH, which expands on the initial seven health behaviors and factors by including sleep health, a component absent in the previous LS7 construct.

In a subsequent analysis, we illustrated that despite the NH white population showcasing commendable efforts and displaying ideal metric scores in specific components related to sleep health, glycated hemoglobin A1c, and physical activity, there are notable concerns. Around 60% of this population, comprising individuals without an ASCVD event, fall into the category of obesity (BMI > 25 kg/m$^2$). In addition, 34% follow a suboptimal diet, and 32% have total cholesterol levels surpassing 222 mg/dL. These findings seem to tie in with findings by Trivedi *et al.*, revealing that increased obesity rates, lack of physical activity, and inadequate dietary habits are more prevalent among rural residents. Hence, adults continue to face a heightened risk of obesity.[29]

Our research also highlights the considerable health burdens posed by diet-related obesity and hyperlipidemia in ASCVD and the critical need to prioritize nutrition in clinical care, health policy, and advocacy in research.[30] In addition, considering previous research indicating a link between high-cholesterol diets and exogenous obesity, as evidenced by elevated BMI,[31] it is essential to emphasize nutritional strategies in the clinical management of individuals at risk of ASCVD.

Our study possesses notable strengths and limitations. The substantial sample size enhances the likelihood of identifying statistically significant results and reduces the confidence intervals in our findings. In addition, NHANES ensures rigorously conducted interviews and study designs, incorporating multilevel verification of participant information. Continuous NHANES data collection is advantageous, allowing for the prompt addressing of emerging public health issues and offering objective data on health conditions for the US population. When interpreting our findings, it is essential to consider the following limitations: our study, being cross-sectional in nature, precludes the establishment of causal inferences between LE8 score and ASCVD events. Second, physical activity, healthy diet, smoking habits, and sleep patterns were self-reported and could be subject to recall bias. The method of scoring utilized in our research may have been prone to errors due to a substantial number of individuals not providing their glycated hemoglobin A1c values (90%). As a result, assumptions were made to classify them into the <5.7% category (non-diabetic range). Importantly, these errors could potentially lead to exposure misclassification bias toward null values, resulting in an underestimated association between LE8 and ASCVD events.

## 5. Conclusion

In this NHANES study (2017 – 2020), we identified an inverse association between the AHA-updated LE8 score and prevalent ASCVD, particularly among young women and college graduates. Therefore, enhancing the domains of the new LE8 score to maintain optimal CVH status carries considerable implications for preventing ASCVD among the adult NH-white population in the USA. It is crucial to emphasize the importance of nutrition in clinical practice, policy, and research, particularly for individuals at risk of acquiring an ASCVD event.

## Acknowledgments

We would like to thank Dr. Georgeta Vaidean for reviewing and making insightful suggestions for improving this article.

## Funding

None.

## Conflict of interest

The authors declare that they have no competing interests.

## Author contributions

*Conceptualization:* All authors
*Investigation:* Abraham Enyeji
*Methodology:* All authors
*Writing – original draft:* All authors
*Writing – review & editing:* All authors

## Ethics approval and consent to participate

Not applicable.

## Consent for publication

Not applicable.

## Availability of data

Data used in the study can be obtained from: NHANES Questionnaires, Datasets, and Related Documentation (https://wwwn.cdc.gov/nchs/nhanes/Default.aspx)

## References

1. Tsao CW, Aday AW, Almarzooq ZI, *et al*. Heart disease and Stroke statistics-2022 update. A report from the American heart association. *Circulation*. 2022;145:e153-e639.

   doi: 10.1161/CIR.0000000000001052

2. Lin CC, Peyser PA, Kardia SL, *et al*. Heritability of cardiovascular risk factors in a Chinese population--taichung community health study and family cohort. *Atherosclerosis*. 2014;235(2):488-495.

   doi: 10.1016/j.atherosclerosis.2014.05.939

3. Lloyd-Jones DM, Ning H, Labarthe D, *et al*. Erratum: Status of cardiovascular health in US adults and children using the American heart association's new "life's essential 8" metrics: Prevalence estimates from the national health and nutrition examination survey (NHANES), 2013 through 2018. *Circulation*. 2022;146:822-835.

   doi: 10.1161/CIRCULATIONAHA.122.060911

4. Enyeji AM, Barengo NC, Ibrahimou B, Ramirez G, Arrieta A. Association between Non-Dietary cardiovascular health and expenditures related to acute coronary syndrome in the US between 2008-2018. *Int J Environ Res Public Health*. 2023;20(9):5743.

   doi: 10.3390/ijerph20095743

5. Brown AF, Liang LJ, Vassar SD, *et al*. Trends in racial/ethnic and nativity disparities in cardiovascular health among adults without prevalent cardiovascular disease in the United States, 1988 to 2014. *Ann Intern Med*. 2018;168:541-549.

   doi: 10.7326/M17-0996

6. Stierman B, Afful J, Carroll MD, *et al*. *National Health and Nutrition Examination Survey 2017-March 2020 Prepandemic Data Files-Development of Files and Prevalence Estimates for Selected Health Outcomes. National Health Statistics Reports Series No 158*; 2021.

   doi: 10.15620/cdc:106273

7. Chobufo MD, Regner SR, Zeb I, Lacoste JL, Virani SS, Balla S. Burden and predictors of statin use in primary and secondary prevention of atherosclerotic vascular disease in the US: From the National Health and Nutrition Examination Survey 2017-2020. *Eur J Prev Cardiol*. 2022;29(14):1830-1838.

   doi: 10.1093/eurjpc/zwac103

8. Al Rifai M, Blaha MJ, Nambi V, *et al*. Determinants of incident atherosclerotic cardiovascular disease events among those with absent coronary artery calcium: Multi-ethnic study of atherosclerosis. *Circulation*. 2022;145(4):259-267.

   doi: 10.1161/CIRCULATIONAHA.121.056705

9. Jain V, Al Rifai M, Turpin R, *et al*. Evaluation of factors underlying sex-based disparities in cardiovascular care in adults with self-reported premature atherosclerotic cardiovascular disease. *JAMA Cardiol*. 2022;7(3):341-345.

   doi: 10.1001/jamacardio.2021.5430

10. Roth GA, Mensah GA, Johnson CO, *et al*. Global burden of cardiovascular diseases and risk factors, 1990-2019: Update from the GBD 2019 study. *J Am Coll Cardiol*. 2020;76(25):2982-3021.

    doi: 10.1016/j.jacc.2020.11.010

11. Lloyd-Jones DM, Hong Y, Labarthe D, *et al*. Defining and setting national goals for cardiovascular health promotion and disease reduction. The American Heart Association's strategic Impact Goal through 2020 and beyond. *Circulation*. 2010;121(4):586-613.

    doi: 10.1161/CIRCULATIONAHA.109.192703

12. Perak AM, Ning H, Khan SS, *et al*. Associations of late adolescent or young adult cardiovascular health with premature cardiovascular disease and mortality. *J Am Coll Cardiol*. 2020;76:2695-2707.

    doi: 10.1016/j.jacc.2020.10.002

13. Reedy J, Lerman JL, Krebs-Smith SM, *et al*. Evaluation of the healthy eating index-2015. *J Acad Nutr Diet*. 2018;118(9):1622-1633.

    doi: 10.1016/j.jand.2018.05.019

14. Chen W, Shi S, Jiang Y, *et al*. Association of sarcopenia with ideal cardiovascular health metrics among US adults: A cross-sectional study of NHANES data from 2011 to 2018.

*BMJ Open*. 2022;12(9):e061789.

doi: 10.1136/bmjopen-2022-061789

15. Shay CM, Ning H, Allen NB, *et al*. Status of cardiovascular health in US adults: Prevalence estimates from the national health and nutrition examination surveys (NHANES) 2003-2008. *Circulation*. 2012;125(1):45-56.

doi: 10.1161/CIRCULATIONAHA.111.035733

16. Leopold JA, Antman EM. Ideal cardiovascular health in young adults with established cardiovascular diseases. *Front Cardiovasc Med*. 2022;9:814610.

doi: 10.3389/fcvm.2022.814610

17. Li X, Ma H, Wang X, Feng H, Qi L. Life's essential 8, genetic susceptibility, and incident cardiovascular disease: A prospective study. *Arterioscler Thromb Vasc Biol*. 2023;43(7):1324-1333.

doi: 10.1161/ATVBAHA.123.319290

18. Shah NS, Talegawkar SA, Jin Y, Hussain BM, Kandula NR, Kanaya AM. Cardiovascular health by life's essential 8 and associations with coronary artery calcium in South Asian American adults in the MASALA study. *Am J Cardiol*. 2023;199:71-77.

doi: 10.1016/j.amjcard.2023.05.004

19. Herraiz-Adillo Á, Higueras-Fresnillo S, Ahlqvist VH, *et al*. Life's essential 8 and life's simple 7 in relation to coronary atherosclerosis: Results from the population-based SCAPIS project. *Mayo Clin Proc*. 2024;99(1):69-80.

doi: 10.1016/j.mayocp.2023.03.023

20. Jin C, Li J, Liu F, *et al*. Life's essential 8 and 10-year and lifetime risk of atherosclerotic cardiovascular disease in China. *Am J Prev Med*. 2023;64(6):927-935.

doi: 10.1016/j.amepre.2023.01.009

21. Zhang N, Wei Z, Zhang Y, *et al*. Association of life's essential 8 with incident atherosclerotic cardiovascular disease in cancer patients: The Kailuan prospective cohort study. *Eur J Prev Cardiol*. 2023;30(17):e78-e80.

doi: 10.1093/eurjpc/zwad256

22. McLaughlin MM, Durstenfeld MS, Gandhi M, *et al*. Cardiovascular health among persons with HIV without existing atherosclerotic cardiovascular disease. *AIDS*. 2023;37(14):2179-2183.

doi: 10.1097/QAD.0000000000003666

23. Olson NC, Cushman M, Judd SE, *et al*. American heart association's life's simple 7 and risk of venous thromboembolism: The reasons for geographic and racial differences in stroke (REGARDS) study. *J Am Heart Assoc*. 2015;4(3):e001494.

doi: 10.1161/JAHA.114.001494

24. Uijl A, Koudstaal S, Vaartjes I, *et al*. Risk for heart failure: The opportunity for prevention with the American heart association's life's simple 7. *JACC Heart Fail*. 2019;7(8):637-647.

doi: 10.1016/j.jchf.2019.03.009

25. Ahmed S, Creanga AA, Gillespie DG, Tsui AO. Economic status, education and empowerment: Implications for maternal health service utilization in developing countries. *PLoS One*. 2010;5(6):e11190.

doi: 10.1371/journal.pone.0011190

26. Ogunmoroti O, Michos ED, Aronis KN, *et al*. Life's simple 7 and the risk of atrial fibrillation: The multi-ethnic study of atherosclerosis. *Atherosclerosis*. 2018;275:174-181.

doi: 10.1016/j.atherosclerosis.2018.05.050

27. Douglas PS, McCallum S, Lu MT, *et al*. Ideal cardiovascular health, biomarkers, and coronary artery disease in persons with HIV. *AIDS*. 2023;37(3):423-434.

doi: 10.1097/QAD.0000000000003418

28. Krebs-Smith SM, Pannucci TR, Subar AF, *et al*. Update of the healthy eating index: HEI-2015. *J Acad Nutr Diet*. 2018;118(9):1591-1602.

doi: 10.1016/j.jand.2018.05.021

29. Trivedi T, Liu J, Probst J, Merchant A, Jones S, Martin AB. Obesity and obesity-related behaviors among rural and urban adults in the USA. *Rural Remote Health*. 2015;15(4):3267.

doi: 10.22605/rrh3267

30. Mozaffarian D. Dietary and policy priorities for cardiovascular disease, diabetes, and obesity. A comprehensive review. *Circulation*. 2016;133(2):187-225.

doi: 10.1161/CIRCULATIONAHA.115.018585

31. David CJ, Rajapriya R, Veena V, Kumaresan G. High cholesterol diet induces obesity in Zebrafish. *Int J Adv Sci Eng*. 2016;2(4):197-201.

ACCSCIENCE PUBLISHING

Brain & Heart

MINI-REVIEW

# Intrinsic cardiac neurons as the consulate general of the brain in the heart: A review

**Meha Fatima Aftab***

Human Electrophysiology Lab, Dow Institute of Medical Technology, Dow University of Health Sciences, Karachi, Sindh, Pakistan

## Abstract

Contrary to the prevailing understanding about one-way communication from brain to heart, recent research has unveiled a two-way communication pathway between these two organs, featuring the delivery of signals from the cardiac afferents to the brain. While the medulla oblongata is known to send autonomic signals for cardiac function regulation, 80% of the vagal afferents send signals to the brain for cardiac regulation. The vagus nerve receives these signals from the intrinsic cardiac neurons, often referred to as "the little brain of the heart." Intrinsic cardiac neurons are neuronal structures with the same biochemical profile as neurons, communicating with the vagus nerve through acetylcholine and expresses markers of neuronal function such as tyrosine hydroxylase and others. Intrinsic cardiac neurons also influence the autonomic system, which can be studied through heart-rate variability measures. Heart rate variability (HRV) is altered in many types of cardiac disorders and is a well-known measure for studying short- and long-term disease-related variations in cardiac function. Some psychiatric disorders such as post-traumatic stress disorder, schizophrenia, and major depression also exhibited alterations in HRV. HRV is related to heartbeat-evoked potentials (HEPs) and electrical potentials in the brain that are influenced by the heart. HEPs are altered in disease states and can be impacted by environmental factors. This paper reviews the existing literature concerning intrinsic cardiac neurons and their possible role in heart-brain communication.

***Keywords:*** Intrinsic cardiac ganglia; Neurocardiology; Heartbeat-evoked potentials; Cardiovascular disease; Psychiatric disorders

***Corresponding author:**
Meha Fatima Aftab
(meha.fatima@duhs.edu.pk)

**Citation:** Aftab MF. Intrinsic cardiac neurons as the consulate general of the brain in the heart: A review. *Brain & Heart.* 2024;2(2):2901. doi: 10.36922/bh.2901

**Received:** February 7, 2024

**Accepted:** April 23, 2024

**Published Online:** May 2, 2024



## 1. Introduction

Heart-brain communication has recently gained traction due to the discovery regarding the bi-directionality of this communication. The conventional understanding about the heart-brain communication dictates that the brain sends signals to the heart to control cardiac functions.[1] Nevertheless, an early clue suggesting the heart's ability to communicate with the brain opened the door to understanding the bidirectional nature of this communication, ultimately leading to the discovery of intrinsic cardiac ganglia or intrinsic cardiac nervous system (ICNS)[2,3] colloquially known as the brain inside the heart. Since then, rigorous research in physiological and pathological processes has been conducted. Yet, the mechanisms of heart-brain communication remain to be clarified. For instance, the molecular characterization of ICNS led to the discovery of both cardiac and neuronal

markers in the ICNS,[4] but the molecular signaling between heart and brain has yet to be deciphered. Heartbeat-evoked potentials (HEPs), which are brain electrical potentials arising from cardiac activity,[5] offer an overview of the physiological crosstalk between brain and heart, but the molecular or hormonal implications of these physiological potentials remain unknown. In this review, we highlight the role of intrinsic cardiac ganglia (ICNS) as a potential relay center for heart-brain communication and discuss the putative link between ICNS and HEP, which reflect the cortical response to the signals originating from the heart.

## 2. Intrinsic cardiac ganglia during embryogenesis

Neural crest cells migrate to the developing heart in the 5th week of gestation and later give rise to different types of neurons including sensory, sympathetic, and parasympathetic neurons.[6] The eight distinct groups of cardiac ganglia at the same anatomical position that would later be identified at the location of intrinsic cardiac ganglia become distinguishable on the 21st day of gestation in rodents, with the exception of ganglia located in the aortic region which are present until the 18th day of gestation and disappear afterward.[7] Postnatal development of cardiac ganglia in rodent models occurs in the 1st month, during which a great number of tyrosine hydroxylase (TH)- and protein gene product 9.5 -rich neurons are detected,[8] differentiating into neurons with microtubule-associated protein-, neuropeptide-Y (NPY)- and acetylcholine transferase (ChAT)-positive neurons.[8] However, evidence suggests that cardiac neurons, especially those serving the conduction system, do not necessarily arise from the neural crest.[9] This finding opens the arena for active exploration of the origin of non-neural crest neurons.

## 3. Anatomical aspects and biochemical pathway of heart-brain communication

An anatomical projection of ICNS to vagal ganglia has been characterized using a zebrafish model,[10] where expression of TH, ChAT, and vasoactive intestinal peptide (VIP) were detected.[10] TH is a rate-limiting enzyme in the production of catecholamines and plays a crucial role in dopamine synthesis.[11] The release of catecholamines through neurohumoral response influences the depolarization of the sinoatrial node,[12] thereby influencing the heart rhythm. The ChAT specifies parasympathetic innervation, while VIP is known to be released from intrinsic and extrinsic cardiac nerves, in addition to the vagus nerve, and modulate heart rhythm.[13] Other neurotransmitters have also been identified in ICNS with a predominance of NPY and cocaine and amphetamine-regulated transcript in the neuronal somata.[4] Despite the occasional expression of vesicular glutamate transporter 2, GABAergic transmission has not been verified in the ICNS thus far.

A computational modeling of the vagus nerve-ICNS communication postulated that signals from vagal efferent flow to ICNS, resulting in the release of acetylcholine from ICNS that eventually inhibit the oscillatory firing of the sinoatrial node.[14] However, intrinsic cardiac ganglia are able to sustain beat-to-beat cardiac indices in the absence of central stimulation,[15] a property that makes ICNS important players in cardioprotection. The mechanism underlying this cardioprotective role involves significantly increased release of acetylcholine from post-ganglionic parasympathetic neurons,[16] which leads to classical ischemic conditioning. This suggests that a feedback signal from the heart to the brain direct or indirect remains largely unexplored.

## 4. Molecular pathways in ICNS

Cholinergic activity in ICNS involves activation of post-junctional M2 muscarinic receptors, coupled to $G\alpha_i$ protein which results in negative dromotropic responses.[17] Most sympathetic activity in the heart originates in the stellate ganglia from the intrathoracic extrinsic cardiac ganglia, prompting the release of norepinephrine (NE), but the cholinergic ICNS possess an integrative network which has sensitive neurons and interneurons that also release NE.[18] In addition to the expression of noradrenergic neurotransmitters, the noradrenergic trophic factors such as tropomyosin-related kinase A and p75 neurotrophin receptors are also detected in the ICNS, reflecting both cholinergic and adrenergic nature of these neurons, even though instances of colocalization of these markers are occasional.[19] While the exact molecular mechanisms of heart-brain communication remain to be elucidated, this communication is putatively underpinned by the involvement of M2 and NE receptors, which act through G protein-coupled receptor (GPCR) signaling. Expression of neuropeptides such as NPY, dynorphine B, substance P, and nitric oxide synthase in ICNS[20] highlights the presence of phosphatidyl inositol 3 kinase and GPCR signaling pathways in ICNS (Figure 1). However, their exact molecular mechanism and cellular outcomes in intrinsic cardiac ganglia remain to be elucidated. Substance P specially has different roles in cardiac modeling following acute and chronic ischemia, where it exerts positive effects in the acute phase but adversely affects myocardial remodeling in the chronic phase.[21] Despite the presence of these neuropeptides, surprisingly, cholinergic somata are devoid of the functions for storage and vesicular release, due to the lack of vesicular monoamine transporter protein,[19] a feature that distinctly differentiates them from the typical parasympathetic neurons.

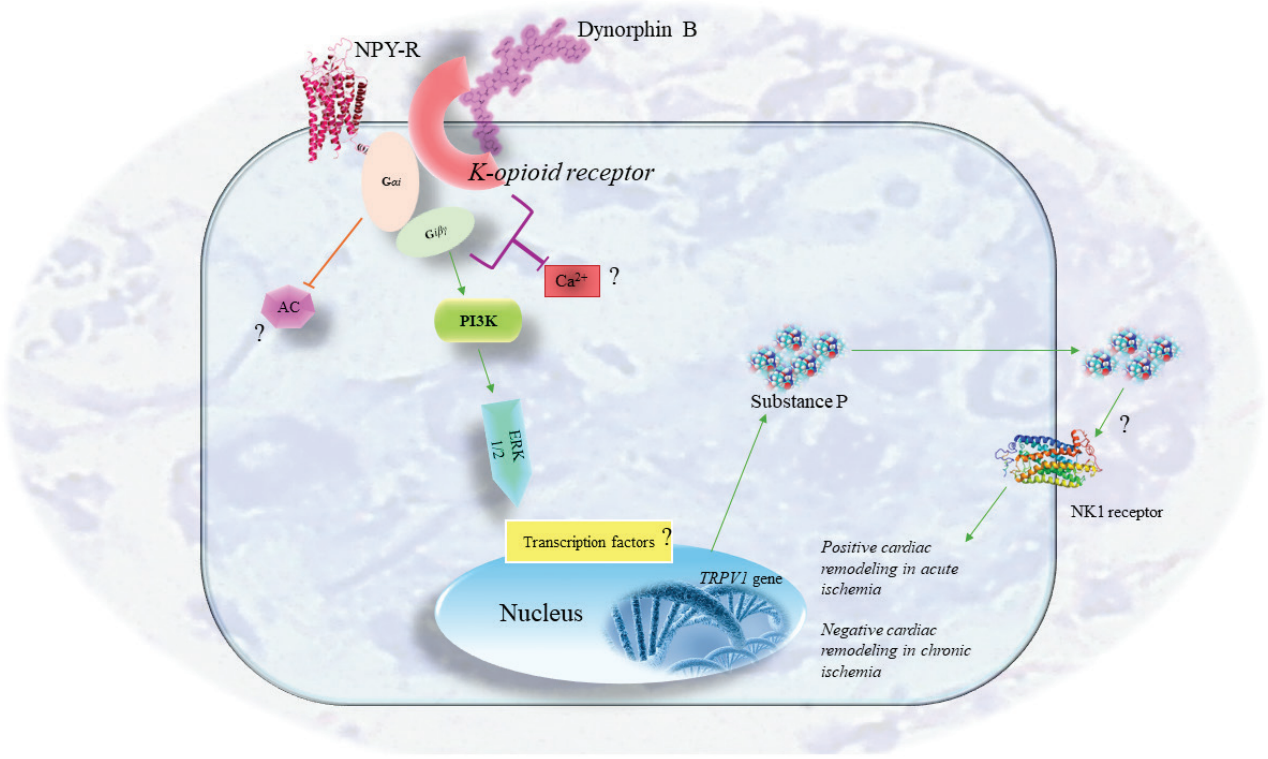


**Figure 1.** Postulated signaling pathways of the neuropeptides discovered in intrinsic cardiac nervous system (ICNS). NPR-Y signaling involves the activation of Gi proteins, which dismantles and activates its α subunit, resulting in the inhibition of adenyl cyclase. B and γ subunit of Gi protein leads to activation of phosphatidyl inositol 3 kinase and extracellular signal-regulated kinase 1, which induces various transcription factors, but their exact target genes in ICNS are currently unknown. Neuropeptide dynorphin B is a kappa opioid receptor agonist and acts through κ receptors, thereby inhibiting the release of intracellular calcium. Substance P is also expressed in ICNS but its mechanism of action remains unclear. Whether they are produced intrinsically via *TRPV1* gene and work in an autocrine fashion or produced by other sensory neurons and work in a paracrine fashion remains unexplored. The "?" in the schematic signifies mechanisms postulated in this figure, which currently lack scientific evidence. This schematic diagram is adapted from multiple sources including.[22-25]

## 5. A possible putative connection between ICNS and heart rate variability (HRV)

The activity of intrinsic cardiac ganglia is mostly cholinergic in nature, resulting in both chronotropic and dromotropic effects.[26] Cholinergic transmission predominantly occurs through vagus nerve,[27] which contributes to autonomic function in the body.[28] Measuring HRV is a novel and useful approach toward understanding the changes in the autonomic function in response to physiological and psychological influences.[29,30] HRV measures the beat-to-beat variation in the heart rhythm. Intrinsic cardiac ganglia are hypothesized to play a role in beat-to-beat coordination of the sinoatrial and atrioventricular node function.[31] The activity of these intrinsic cardiac ganglia can be influenced by epicardial touch, rendering almost 80% of the ICGs active as compared to extracardiac neurons, while both types of neurons can be equally activated through epicardial chemical stimulation.[32] Despite the well-researched role of intrinsic cardiac ganglia in maintaining heart rhythm,[6] there is no direct evidence of the relationship between intrinsic cardiac ganglia and HRV. Intrinsic cardiac ganglia have been implicated in the pathophysiology of atrial fibrillation.[33] On the other hand, HRV also provides indices that could serve as potential indicators of atrial fibrillation[34] This gap of knowledge in the direct relationship between intrinsic cardiac ganglia and HRV measures opens a new research avenue where techniques such as RNA silencing, gene sequencing, and pharmacological inhibition of cardiac ganglia-specific markers can be used to study changes in the HRV indices.

## 6. Pathogenic mechanisms of ICNS and diagnostic efficiency of HRV in cardiac disorders

Selective ablation of ganglionated plexus of atria remarkably improves the symptoms of paroxysmal atrial fibrillation,[35] an evidence that corroborates the role of ICNS in arrhythmias. Myocardial ischemia has also been

established as a modulator of cardiac arrhythmias where arrhythmic signals can arise from the insular cortex[36] and intrinsic cardiac neurons.[37] Myocardial ischemia leads to the formation of large inclusion bodies and induces degenerative changes in the dendrites and axons of these ICNS.[38] While myocardial infarction induces hyperexcitability and altered synaptic efficacy,[39] activation of inflammatory pathways leads to the production of nerve growth factor, which promotes neuronal sprouting leading to sympathetic hyperinnervation.[40] In response to the ischemic insult, an intrinsic adrenal system of the heart increases the production of catecholamines,[6] leading to increased sympathetic tone. It has been hypothesized that both catecholamine release and activation through a feedback system are implicated in ICNS-mediated ischemia remodeling.[37] While the feedback mechanism involves modulation of reflex control,[33] it is likely that activity of ICNS could be translated and observed through measurements of HRV, which has been proposed to predict the lifetime risk of cardiac disorders.[41]

HRV is a predictor of autonomic function[42] and can be obtained to assess short-term or long-term variability. Short-term variability, which can be analyzed using 5-min-long recordings, is commonly utilized to study autonomic function and baroreceptor reflex activity, while long-term variability analysis provides insights to a variety of physiological processes such as circadian rhythms, metabolism, renin-angiotensin-aldosterone system, and vagal activity.[43] HRV is studied using various indices that are broadly categorized into time domain and frequency domain measures, where a higher range in the time and frequency domain reflects increased parasympathetic activity while decreases in time or frequency domain measures are usually linked to disease states.[44,45] Non-linear measures such as entropy represent an underexplored area of HRV analysis,[43] but they have been shown to be decreased in patients with Takotsubo cardiomyopathy or broken-heart syndrome.[46,47] Non-linear measures have shown 90% accuracy, 86% specificity, and 95% sensitivity for predicting real-life stress situations,[48] which make them potential diagnostic tools of other psychological disorders.

## 7. HRV trends in psychiatric disorders

Among the frequency domain measures of HRV, high-frequency (HF) HRV reflects breathing patterns and has shown the most association with altered breathing patterns in psychiatric illnesses[49] as compared to vagal tone.[43] Association of HF domain of HRV has been rigorously studied in many psychiatric illnesses; for instance, impaired parasympathetic autonomic modulation leads to altered cortical and subcortical processing in post-traumatic stress disorder (PTSD)[50] where a decrease in BOLD functional magnetic resonance imaging signal is associated with HF-HRV. Several other studies have also shown reduced resting-state HF-HRV in depression[51,52] and schizophrenia,[53] where severity of symptoms is correlated with reduced HRV.[54] Although psychiatric medication could reduce HRV,[55] medication-free schizophrenic patients still exhibit altered HRV complexity.[56] Apart from HF-HRV, time domain measures like R-R intervals show a declining pattern in depression[57] while SDNN and RMSSD demonstrate a negative correlation with the severity of psychotic symptoms in schizophrenia.[58] Both time domain and frequency domain measures suggest altered vagal activity, but the loss of efferent vagal activity has been established in schizophrenia.[54] Apart from psychiatric disorders, altered HRV in patients of coronary artery disease also leads to abnormal circadian rhythm,[59] which in turn predict severity of symptoms seen in psychiatric disorders, such as major depressive disorder, anxiety, bipolar disorder, and schizophrenia.[60,61] These symptoms, which have been postulated as the schema of associations between HRV, quantitative encephalograms, and cognitive function where altered brain signals are detected through quantitative electroencephalogram, cause cognitive dysfunction, impacting autonomic activity and thereby altering HRV.[61]

## 8. HEPs as the language of cardiac afferents to brain

HEPs, first described by Jones *et al.*,[2] are electrical potentials in the brain influenced by cardiac activity, reflecting the interoceptive ability.[62,63] HEPs are time-locked to the R wave of the electrocardiogram signal. Changes in the electrical activity of the brain in response to cardiac afferents are observed during 50 – 550 ms in 1 s epoch.[64] Differences in HEP are evident in high and low arousal states.[5] Apart from interoceptive ability reflected by heartbeat perception through mental tracking task,[65] where good heartbeat perceivers reflect positive HEP peaks during attention as compared to poor heartbeat perceivers. The interoceptive-exteroceptive integration is also reflected by HEP.[66] HEPs emerge as a new index of heart-brain communication. A case report[67] has shown reduced HEP in near-death experience in the absence of a bidirectional control in a patient with ventricular fibrillation. The molecular mechanism behind the HEP is largely unknown but can be reflected through its interaction with HRV, where HRV modulates the HEP amplitude at N250[68] during emotional states and resonant breathing. Resonant breathing exerts its effects through biofeedback mechanism, where it improves interoceptive capacity and reduces sympathetic overload[69] Similarly, exercise, which serves as another biofeedback mechanism, improves interoceptive capacity in physically fit individuals;[70] however, since exercise training induces sinus bradycardia

and alters HRV, further investigations are warranted to understand the impact of exercise on HEP. Since HRV modulation can be affected by environmental factors such as PM2.5 (particulate matter <2.5 μm) through mitochondrial deoxyribonucleic acid methylation,[71] investigations on HEP changes can be extended to other environmental factors such as radiations and magnetic fields due to two closely linked factors: (i) High-strength geomagnetic field of the Earth is related with the incidence of ST-segment elevation myocardial infarction,[72] and (ii) HEP can be influenced by cardiac activity. Whether intrinsic cardiac ganglia exert a direct effect on HEP can therefore uncover mysteries of heart-brain interactions and shed light on the environmental influence on this interaction (Video A1).

## 9. Conclusion

Residing inside the heart, intrinsic cardiac neurons have a distinct role, working independently and in coordination with the autonomic nervous system to control heart activity during physiological and pathological conditions. It is widely perceived that the brain acts as a master regulator, governing the functioning of the heart, all based on the putative one-way communication from the brain to the heart. The recent discoveries in neurocardiology have highlighted the role of ICNS in maintaining a two-way communication through which the heart receives from the brain and additionally reciprocates by sending signals to the brain through parasympathetic transmission. This loop of communication is critical in both healthy and disease states, with the latter category, which encompasses heart and brain diseases, featuring significant alterations in the morphology and physiology of the ICNS.

The current paper offers a review of the molecular and clinical aspects of heart-brain communication but does not shed light on the cellular and molecular mechanisms underlying the intricate heart-brain communication in detail due to a dearth of relevant scientific evidence. Furthermore, there remains a need for population-based studies, including systematic reviews and meta-analysis, for defining norms and patterns of heart-brain communication in healthy and diseased populations. This article provides a precise discussion on the biochemical and electrophysiological mechanisms of heart-brain communication, which could be studied in various psychiatric disorders, thereby paving a roadmap for future research on the heart-brain communication in the disease states. For instance, biomarkers associated with ICNS can provide a valuable diagnostic tool for debilitating conditions such as arrhythmia and atrial fibrillation. They can also be used to clarify the abnormal autonomic functioning under debilitating psychological disorders such as PTSD. The development of ICNS-specific drugs for controlling symptoms of such psychological conditions represents an interesting area of neuropharmacology research. In addition, establishing a link between ICNS and clinico-physiological parameters such as HRV and HEP can provide a promising arena of research as both parameters have been implicated in both cardiac and psychiatric disorders. It is also noteworthy that the discovery of a heart-brain axis, following that of the well-studied gut-brain axis, underlines the possible existence of such communication serving as the "consulate general of the brain" in respective organs.

## Acknowledgments

None.

## Funding

None.

## Conflict of interest

The author declares that she has no competing interests.

## Author contributions

This is a single-authored article.

## Ethics approval and consent to participate

Not applicable.

## Consent for publication

Not applicable.

## Availability of data

Not applicable.

## References

1. Gordan R, Gwathmey JK, Xie LH. Autonomic and endocrine control of cardiovascular function. *World J Cardiol*. 2015;7(4):204-214.

   doi: 10.4330/wjc.v7.i4.204

2. Jones GE, Leonberger LT, Rouse CH, Caldwell JA, Jones KR. Preliminary data exploring the presence of an evoked potential associated with cardiac visceral activity. *Psychophysiology*. 1986;23:445.

3. Armour JA. Intrinsic cardiac neurons. *J Cardiovasc Electrophysiol*. 1991;2:331-341.

   doi: 10.1111/j.1540-8167.1991.tb01330.x

4. Lizot G, Pasqualin C, Tissot A, Pagès S, Faivre JF, Chatelier A. Molecular and functional characterization of the mouse intrinsic cardiac nervous system. *Heart Rhythm*. 2022;19(8):1352-1362.

   doi: 10.1016/j.hrthm.2022.04.012

5. Luft CD, Bhattacharya J. Aroused with heart: Modulation of heartbeat evoked potential by arousal induction and its oscillatory correlates. *Sci Rep.* 2015;5:15717.

doi: 10.1038/srep15717

6. Fedele L, Brand T. The intrinsic cardiac nervous system and its role in cardiac pacemaking and conduction. *J Cardiovasc Dev Dis*. 2020;7(4):54.

doi: 10.3390/jcdd7040054

7. Keh-Min Liu SI. Topographical and morphological studies of the cardiac Ganglia in the prenatal rat. *Showa Univ J Med Sci*. 1989;1(1.2):7-22.

8. Horackova M, Slavikova J, Byczko Z. Postnatal development of the rat intrinsic cardiac nervous system: A confocal laser scanning microscopy study in whole-mount atria. *Tissue Cell*. 2000;32(5):377-88.

doi: 10.1054/tice.2000.0126

9. Hildreth V, Webb S, Bradshaw L, Brown NA, Anderson RH, Henderson DJ. Cells migrating from the neural crest contribute to the innervation of the venous pole of the heart. *J Anat*. 2008;212(1):1-11.

doi: 10.1111/j.1469-7580.2007.00833.x

10. Stoyek MR, Croll RP, Smith FM. Intrinsic and extrinsic innervation of the heart in zebrafish (*Danio rerio*). *J Comp Neurol*. 2015;523(11):1683-1700.

doi: 10.1002/cne.23764

11. Daubner SC, Le T, Wang S. Tyrosine hydroxylase and regulation of dopamine synthesis. *Arch Biochem Biophys*. 2011;508(1):1-12.

doi: 10.1016/j.abb.2010.12.017

12. MacDonald EA, Rose RA, Quinn TA. Neurohumoral control of sinoatrial node activity and heart rate: Insight from experimental models and findings from humans. *Front Physiol*. 2020;11:170.

doi: 10.3389/fphys.2020.00170

13. Accili EA, Redaelli G, DiFrancesco D. Activation of the hyperpolarization-activated current (if) in sino-atrial node myocytes of the rabbit by vasoactive intestinal peptide. *Pflugers Arch*. 1996;431(5):803-805.

doi: 10.1007/BF02253849

14. Huffman WJ, Musselman ED, Pelot NA, Grill WM. Measuring and modeling the effects of vagus nerve stimulation on heart rate and laryngeal muscles. *Bioelectron Med*. 2023;9(1):3.

doi: 10.1186/s42234-023-00107-4

15. Armour JA. Physiology of the intrinsic cardiac nervous system. *Heart Rhythm*. 2011;8(5):739.

doi: 10.1016/j.hrthm.2011.01.033

16. Pickard JMJ, Burke N, Davidson SM, Yellon DM. Intrinsic cardiac ganglia and acetylcholine are important in the mechanism of ischaemic preconditioning. *Basic Res Cardiol*. 2017;112(2):11.

doi: 10.1007/s00395-017-0601-x

17. Habecker BA, Anderson ME, Birren SJ, *et al*. Molecular and cellular neurocardiology: Development, and cellular and molecular adaptations to heart disease. *J Physiol*. 2016;594(14):3853-3875.

doi: 10.1113/JP271840

18. Owji A, Varudkar N, Ebert SN. Therapeutic potential of Pnmt+ primer cells for neuro/myocardial regeneration. *Am J Stem Cells*. 2013;2(3):137-154.

19. Hoard JL, Hoover DB, Mabe AM, Blakely RD, Feng N, Paolocci N. Cholinergic neurons of mouse intrinsic cardiac ganglia contain noradrenergic enzymes, norepinephrine transporters, and the neurotrophin receptors tropomyosin-related kinase A and p75. *Neuroscience*. 2008;156(1):129-142.

doi: 10.1016/j.neuroscience.2008.06.063

20. Steele PA, Gibbins IL, Morris JL, Mayer B. Multiple populations of neuropeptide-containing intrinsic neurons in the guinea-pig heart. *Neuroscience*. 1994;62(1):241-250.

doi: 10.1016/0306-4522(94)90327-1

21. Dehlin HM, Levick SP. Substance P in heart failure: The good and the bad. *Int J Cardiol*. 2014;170(3):270-277.

doi: 10.1016/j.ijcard.2013.11.010

22. Canaider S, Facchin F, Tassinari R, *et al*. Intracrine endorphinergic systems in modulation of myocardial differentiation. *Int J Mol Sci*. 2019;20(20):5175.

doi: 10.3390/ijms20205175

23. Melendez GC, Li J, Law BA, Janicki JJ, Supowit SC, Levick SP. Substance P induces adverse myocardial remodelling via a mechanism involving cardiac mast cells. *Cardiovasc Res*. 2011;92(3):420-429.

doi: 10.1093/cvr/cvr244

24. Tan CMJ, Green P, Tapoulal N, Lewandowski AJ, Leeson P, Herring N. The role of neuropeptide Y in cardiovascular health and disease. *Front Physiol*. 2018;9:1281.

doi: 10.3389/fphys.2018.01281

25. Chottova Dvorakova M, Mistrova E, Paddenberg R, Kummer W, Slavikova J. Substance P receptor in the rat heart and regulation of its expression in long-term diabetes. *Front Physiol*. 2018;9:918.

doi: 10.3389/fphys.2018.00918

26. Allen E, Coote JH, Grubb BD, *et al*. Electrophysiological effects of nicotinic and electrical stimulation of intrinsic cardiac ganglia in the absence of extrinsic autonomic nerves in the rabbit heart. *Heart Rhythm*. 2018;15(11):1698-1707.

doi: 10.1016/j.hrthm.2018.05.018

27. Lund DD, Oda RP, Pardini BJ, Schmid PG. Vagus nerve stimulation alters regional acetylcholine turnover in rat heart. *Circ Res*. 1986;58(3):372-377.

doi: 10.1161/01.res.58.3.372

28. McCorry LK. Physiology of the autonomic nervous system. *Am J Pharm Educ*. 2007;71(4):78.

doi: 10.5688/aj710478

29. Duong HTH, Tadesse GA, Nhat PTH, *et al*. Heart rate variability as an indicator of autonomic nervous system disturbance in tetanus. *Am J Trop Med Hyg*. 2020;102(2):403-407.

doi: 10.4269/ajtmh.19-0720

30. Ferreira M Jr., Zanesco A. Heart rate variability as important approach for assessment autonomic modulation. *Motriz Rev Educ Fis*. 2016;22(2):3-8.

doi: 10.1590/S1980-65742016000200001

31. Randall DC. Towards an understanding of the function of the intrinsic cardiac ganglia. *J Physiol*. 2000;528(Pt 3):406.

doi: 10.1111/j.1469-7793.2000.00406.x

32. Armour JA, Collier K, Kember G, Ardell JL. Differential selectivity of cardiac neurons in separate intrathoracic autonomic ganglia. *Am J Physiol*. 1998;274(4):R939-R949.

doi: 10.1152/ajpregu.1998.274.4.R939

33. Beaumont E, Salavatian S, Marie Southerland E, *et al*. Network interactions within the canine intrinsic cardiac nervous system: Implications for reflex control of regional cardiac function. *J Physiol*. 2013;591(18):4515-4533.

doi: 10.1113/jphysiol.2013.259382

34. Kim SH, Lim KR, Seo JH, *et al*. Higher heart rate variability as a predictor of atrial fibrillation in patients with hypertension. *Sci Rep*. 2022;12(1):3702.

doi: 10.1038/s41598-022-07783-3

35. Pokushalov E, Romanov A, Shugayev P, *et al*. Selective ganglionated plexi ablation for paroxysmal atrial fibrillation. *Heart Rhythm*. 2009;6(9):1257-1264.

doi: 10.1016/j.hrthm.2009.05.018

36. Uther JB, Hunyor SN, Shaw J, Korner PI. Bulbar and suprabulbar control of the cardiovascular autonomic effects during arterial hypoxia in the rabbit. *Circ Res*. 1970;26(4):491-506.

doi: 10.1161/01.res.26.4.491

37. Armour JA. Myocardial ischaemia and the cardiac nervous system. *Cardiovasc Res*. 1999;41(1):41-54.

doi: 10.1016/s0008-6363(98)00252-1

38. Hopkins DA, Macdonald SE, Murphy DA, Armour JA. Pathology of intrinsic cardiac neurons from ischemic human hearts. *Anat Rec*. 2000;259(4):424-436.

doi: 10.1002/1097-0185(20000801)259:4<424:AID-AR60>3.0.CO;2-J

39. Hardwick JC, Southerland EM, Ardell JL. Chronic myocardial infarction induces phenotypic and functional remodeling in the guinea pig cardiac plexus. *Am J Physiol Regul Integr Comp Physiol*. 2008;295(6):R1926-R1933.

doi: 10.1152/ajpregu.90306.2008

40. Hardwick JC, Ryan SE, Beaumont E, Ardell JL, Marie Southerland E. Dynamic remodeling of the guinea pig intrinsic cardiac plexus induced by chronic myocardial infarction. *Auton Neurosci*. 2014;181:4-12.

doi: 10.1016/j.autneu.2013.10.008

41. Kubota Y, Chen LY, Whitsel EA, Folsom AR. Heart rate variability and lifetime risk of cardiovascular disease: The Atherosclerosis Risk in Communities Study. *Ann Epidemiol*. 2017;27(10):619-625.e2.

doi: 10.1016/j.annepidem.2017.08.024

42. Evans S, Seidman LC, Ci Tsao J, Lung KC, Zeltzer LK, Naliboff BD. Heart rate variability as a biomarker for autonomic nervous system response differences between children with chronic pain and healthy control children. *J Pain Res*. 2013;6:449-457.

doi: 10.2147/JPR.S43849

43. Shaffer F, Ginsberg JP. An overview of heart rate variability metrics and norms. *Front Public Health*. 2017;5:258.

doi: 10.3389/fpubh.2017.00258

44. Tiwari R, Kumar R, Malik S, Raj T, Kumar P. Analysis of heart rate variability and implication of different factors on heart rate variability. *Curr Cardiol Rev*. 2021;17(5):e160721189770.

doi: 10.2174/1573403X16999201231203854

45. McCraty R, Shaffer F. Heart rate variability: New perspectives on physiological mechanisms, assessment of self-regulatory capacity, and health risk. *Glob Adv Health Med*. 2015;4(1):46-61.

doi: 10.7453/gahmj.2014.073

46. Cruciani G, Cavicchioli M, Tanzilli G, Tanzilli A, Lingiardi V, Galli F. Heart rate variability alterations in takotsubo syndrome and related association with psychological factors: A systematic review and meta-analysis. *Sci Rep*. 2023;13(1):20744.

doi: 10.1038/s41598-023-47982-0

47. Evdokimov D, Boldueva SA, Feoktistova VS, Baeva TA. Features of heart rate variability in patients with takotsubo syndrome. *Eur Heart J Acute Cardiovasc Care*. 2021;10(Suppl 1):zuab020.187.

doi: 10.1093/ehjacc/zuab020.187

48. Melillo P, Bracale M, Pecchia L. Nonlinear Heart Rate Variability features for real-life stress detection. Case study: Students under stress due to university examination. *Biomed Eng Online*. 2011;10:96.

doi: 10.1186/1475-925X-10-96

49. Quintana DS, Elstad M, Kaufmann T, *et al*. Resting-state high-frequency heart rate variability is related to respiratory frequency in individuals with severe mental illness but not healthy controls. *Sci Rep.* 2016;6:37212.

    doi: 10.1038/srep37212

50. Rabellino D, D'Andrea W, Siegle G, *et al*. Neural correlates of heart rate variability in PTSD during sub- and supraliminal processing of trauma-related cues. *Hum Brain Mapp.* 2017;38(10):4898-4907.

    doi: 10.1002/hbm.23702

51. Rottenberg J. Cardiac vagal control in depression: A critical analysis. *Biol Psychol*. 2007;74(2):200-211.

    doi: 10.1016/j.biopsycho.2005.08.010

52. Kemp AH, Quintana DS, Gray MA, Felmingham KL, Brown K, Gatt JM. Impact of depression and antidepressant treatment on heart rate variability: A review and meta-analysis. *Biol Psychiatry*. 2010;67(11):1067-1074.

    doi: 10.1016/j.biopsych.2009.12.012

53. Moon E, Lee SH, Kim DH, Hwang B. Comparative study of heart rate variability in patients with schizophrenia, bipolar disorder, post-traumatic stress disorder, or major depressive disorder. *Clin Psychopharmacol Neurosci*. 2013;11(3):137-143.

    doi: 10.9758/cpn.2013.11.3.137

54. Bar KJ, Letzsch A, Jochum T, Wagner G, Greiner W, Sauer H. Loss of efferent vagal activity in acute schizophrenia. *J Psychiatr Res*. 2005;39(5):519-527.

    doi: 10.1016/j.jpsychires.2004.12.007

55. Rechlin T, Beck G, Weis M, Kaschka WP. Correlation between plasma clozapine concentration and heart rate variability in schizophrenic patients. *Psychopharmacology* (*Berl*). 1998;135(4):338-341.

    doi: 10.1007/s002130050520

56. Mujica-Parodi LR, Yeragani V, Malaspina D. Nonlinear complexity and spectral analyses of heart rate variability in medicated and unmedicated patients with schizophrenia. *Neuropsychobiology*. 2005;51(1):10-15.

    doi: 10.1159/000082850

57. Tessier A, Sibon I, Poli M, Audiffren M, Allard M, Pfeuty M. Resting heart rate predicts depression and cognition early after ischemic stroke: A pilot study. *J Stroke Cerebrovasc Dis*. 2017;26(10):2435-2441.

    doi: 10.1016/j.jstrokecerebrovasdis.2017.05.040

58. Chung MS, Yang AC, Lin YC, *et al*. Association of altered cardiac autonomic function with psychopathology and metabolic profiles in schizophrenia. *Psychiatry Res*. 2013;210(3):710-715.

    doi: 10.1016/j.psychres.2013.07.034

59. Chellappa SL, Vujovic N, Williams JS, Scheer FAJL. Impact of circadian disruption on cardiovascular function and disease. *Trends Endocrinol Metab*. 2019;30(10):767-779.

    doi: 10.1016/j.tem.2019.07.008

60. Walker WH 2nd, Walton JC, Courtney DeVries A, Nelson RJ. Circadian rhythm disruption and mental health. *Transl Psychiatry*. 2020;10(1):28.

    doi: 10.1038/s41398-020-0694-0

61. Jung W, Jang KI, Lee SH. Heart and brain interaction of psychiatric illness: A review focused on heart rate variability, cognitive function, and quantitative electroencephalography. *Clin Psychopharmacol Neurosci*. 2019;17(4):459-474.

    doi: 10.9758/cpn.2019.17.4.459

62. Coll MP, Hobson H, Bird G, Murphy J. Systematic review and meta-analysis of the relationship between the heartbeat-evoked potential and interoception. *Neurosci Biobehav Rev*. 2021;122:190-200.

    doi: 10.1016/j.neubiorev.2020.12.012

63. Critchley HD, Wiens S, Rotshtein P, Ohman A, Dolan RJ. Neural systems supporting interoceptive awareness. *Nat Neurosci*. 2004;7(2):189-195.

    doi: 10.1038/nn1176

64. Schandry R, Montoya P. Event-related brain potentials and the processing of cardiac activity. *Biol Psychol.* 1996;42(1-2):75-85.

    doi: 10.1016/0301-0511(95)05147-3

65. Yuan H, Yan HM, Xu XG, Han F, Yan Q. Effect of heartbeat perception on heartbeat evoked potential waves. *Neurosci Bull*. 2007;23(6):357-362.

    doi: 10.1007/s12264-007-0053-7

66. Banellis L, Cruse D. Skipping a beat: Heartbeat-evoked potentials reflect predictions during interoceptive-exteroceptive integration. *Cereb Cortex Commun*. 2020;1(1):tgaa060.

    doi: 10.1093/texcom/tgaa060

67. Candia-Rivera D, Machado C. Reduced heartbeat-evoked responses in a near-death case report. *J Clin Neurol*. 2023;19(6):581-588.

    doi: 10.3988/jcn.2022.0415

68. MacKinnon S, Gevirtz R, McCraty R, Brown M. Utilizing heartbeat evoked potentials to identify cardiac regulation of vagal afferents during emotion and resonant breathing. *Appl Psychophysiol Biofeedback*. 2013;38(4):241-255.

    doi: 10.1007/s10484-013-9226-5

69. Lehrer PM, Gevirtz R. Heart rate variability biofeedback: How and why does it work? *Front Psychol*. 2014;5:756.

    doi: 10.3389/fpsyg.2014.00756

70. Amaya Y, Abe T, Kanbara K, Shizuma H, Akiyama Y, Fukunaga M. The effect of aerobic exercise on interoception

and cognitive function in healthy university students: A non-randomized controlled trial. *BMC Sports Sci Med Rehabil*. 2021;13(1):99.

doi: 10.1186/s13102-021-00332-x

71. Byun HM, Colicino E, Trevisi L, Fan T, Christiani DC, Baccarelli AA. Effects of air pollution and blood mitochondrial DNA methylation on markers of heart rate variability. *J Am Heart Assoc*. 2016;5(4):e003218.

doi: 10.1161/JAHA.116.003218

72. Jarusevicius G, Rugelis T, McCraty R, Landauskas M, Berškienė K, Vainoras A. Correlation between changes in local earth's magnetic field and cases of acute myocardial infarction. *Int J Environ Res Public Health*. 2018;15(3):399.

doi: 10.3390/ijerph15030399

## Appendix

**Video A1.** The electrical transmission from the brain to the intrinsic cardiac nervous system (ICNS) occurs through vagus nerve. In response to this signal from the brain, ICNS release acetylcholine, which regulates the autonomic functions of the heart, resulting in beat-to-beat variation in heart rhythm, explained by heart rate variability (HRV). HRV is correlated with heartbeat-evoked potential (HEP) amplitudes. Environmental factors influence HRV and hence can indirectly affect HEP amplitudes, thereby affecting heart-brain communication.

ACCSCIENCE PUBLISHING

Brain & Heart

CASE REPORT

# Approaching an undetermined diagnosis in the aftermath of rhombencephalitis: A case report

**Debabrata Chakraborty***

Department of Neurology, Apollo Multispeciality Hospital, Kolkata, West Bengal, India

## Abstract

A 49-year-old male patient manifested acute onset increased imbalance, quadriparesis, and speech impairment 1 month after undergoing ventricular-peritoneal shunt for normal pressure hydrocephalus (although magnetic resonance imaging [MRI] of the brain with contrast was otherwise normal), which showed improvement afterward. He had hypercalcemia and elevated erythrocyte sedimentation rate. Repeat brain MRI revealed pachymeningitis coupled with rhombencephalitis, while cerebrospinal fluid study unveiled only increased protein level without evidence of active infection. Given these findings, neurosarcoidosis was preliminarily considered a plausible cause of the recent clinical manifestations, and the patient was prescribed methylprednisolone, which led to significant improvement. However, the steroid treatment was discontinued on the revelation that the patient grappled with severe sepsis. Despite an initial improvement following a post-management of sepsis, his condition deteriorated, and he became lost to follow-up after 4 months of initial presentation. An infective etiology was ruled out since his condition improved with steroid. Precluding vasculitis or demyelinating disorder left the physicians with primary central nervous system (CNS) lymphoma or sarcoidosis as a proper diagnosis based on the fact that the patient experienced deterioration when steroid was excluded from the treatment regimen. This case study portrays a need to conduct a more specific and elaborate investigation, driven by a strong perception to both primary CNS lymphoma and sarcoidosis, to optimize clinical diagnosis, which facilitates the formulation of an appropriate treatment regimen.

***Keywords:*** Neurosarcoidosis; Rhombencephalitis; Hydrocephalus; Primary central nervous system lymphoma

***Corresponding author:**
Debabrata Chakraborty
(drdchakraborty1980@gmail.com)

**Citation:** Chakraborty D. Approaching an undetermined diagnosis in the aftermath of rhombencephalitis: A case report. *Brain & Heart.* 2024;2(2):2133. doi: 10.36922/bh.2133

**Received:** October 27, 2023

**Accepted:** January 26, 2024

**Published Online:** April 23, 2024



## 1. Introduction

In some neurological diseases, it is difficult to reach a definite diagnosis within a short period of time when patient is experiencing rapid deterioration. Under many circumstances, physicians need to leverage information gleaned from clinical findings, ancillary tests, and treatment response to make the final diagnosis. Very often, physicians prioritize saving patient's life based on any signs and symptoms presented to them when a definite diagnosis has yet to be finalized; simultaneously, more diagnosis-oriented investigations are conducted.

It is a challenging endeavor to diagnose neurosarcoidosis due to the difficulty to conduct a tissue biopsy. Even so, biopsy specimens do not always provide conclusive findings to aid the diagnostic process. In this case study, the patient was given a steroid

treatment to rule out certain possible etiologies and to save him from plunging into worse deterioration. He was eventually diagnosed with "possible neurosarcoidosis."

## 2. Case presentation

A 49-year-old man, suffering from diabetes, hypertension, and moderate obstructive sleep apnea, was diagnosed with normal pressure hydrocephalus based on the presentation of the classic triad of cognitive decline, imbalance, and incontinence lasting for over 6 months. Fundus examination and routine cerebrospinal fluid (CSF) study revealed normal results. He showed improvement in the "Timed Up and Go Test" post-therapeutic drainage. Magnetic resonance imaging (MRI) of his brain revealed features of hydrocephalus with periventricular oozing. Hence, he was indicated a ventricular-peritoneal shunt, which led to improved balance to some extent and regaining of his ability to walk independently.

One month after the treatment, he presented to us with exacerbated acute-onset imbalance and speech impairment. He declared no history of fever or trauma from the treatment leading up to the most recent medical consultation. The patient had stable vitals but was grappling with confusion and dysarthria. He had quadriparesis (MRC grading was 3/5 of all four limbs) and ataxia (both axial and appendicular) but showed no signs of meningitis. Routine blood investigations include assessment of biochemical parameters, unveiled hypercalcemia (calcium level of 11.8 mg/dL), high creatinine level of 1.4 mg/dL, and high erythrocyte sedimentation rate of 68 mm/h. Brain MRI revealed T2 hyperintensities in the thalamus, midbrain, pons, and medulla, and diffusion-weighted imaging showed facilitated diffusion, with post-contrast enhancement of the lesion in FLAIR along with pachymeningitis (Figure 1). The MRI of the spine did not yield any significant, relevant findings. Based on these findings, a preliminary diagnosis of rhombencephalitis was made, and the exact etiology was investigated afterward.

A new session of CSF study revealed only increased protein level (122 mg/dL), providing no evidence of an active infection, based on a polymerase chain reaction analysis for *Listeria* and the comprehensive infective panel. There was no history or findings suggestive of vasculitis, Bechet's disease, or histiocytosis. Radiologic findings from repeat brain MRI did not consistently align with features of either neuromyelitis optica spectrum disorder or other demyelinating disorders. In addition, an armada of investigations performed did not seem contribute to the indicative findings that could lead to a definite diagnosis: negative vasculitis markers; normal serum level angiotensin-converting enzyme; negative anti-NMO (neuromyelitis optica) and anti-myelin oligodendrocyte glycoprotein antibodies; negative results from human immunodeficiency virus serology, venereal disease research laboratory test and TB GeneXpert; and non-contributory findings from CSF oligo clonal band, central nervous system (CNS) autoimmune, and paraneoplastic encephalitis panel tests.

Given that he acquired pachymeningitis and rhombencephalitis with recent detection of hydrocephalus while presented with hypercalcemia, the physicians considered neurosarcoidosis a plausible diagnosis, after ruling out active infection as the principal cause of his condition. To validate the diagnosis, a brain biopsy was recommended but declined by the patient and his family. As an alternative, a positron emission tomography-computed tomography scan of the whole body was performed, yielding negative findings that rule out the involvement of a systemic factor. Evidence of peripheral nodule was not available since biopsy was not conducted.

The patient also suffered from a recent proteinuria, which was unveiled as a part of the evaluation of raised creatinine level (very high 24-h urinary protein: 2106.5 mg/day). Hence, a renal biopsy was recommended but again declined by his family.

While experiencing gradual deterioration, the patient was given methylprednisolone (1 g for 5 days) followed by oral prednisolone (60 mg orally) and mycophenolate mofetil (500 mg orally) twice a day, after active infection was ruled out as the etiology. His response to the medications was remarkable, leading to a resolution of encephalopathy, evidenced by a radiological resolution after a 5-day course of methylprednisolone (Figure 2). However, he developed psychosis afterward, which was initially perceived to have been caused by steroid. A detailed psychiatric evaluation was conducted on the patient based on the information; we could glean from his wife, who recounted that the patient had been experiencing a delusion of persecution over the previous 1 year and used to have violent behavior. A follow-up examination 7 days after the clinical consultation revealed that his cognitive function, ataxia, and quadriparesis all improved (MRC power improved to 4+/5 in all four limbs) and he regained the ability to walk independently albeit with mild ataxia. His psychiatric symptoms also alleviated to a considerable extent over time.

After 4 months, the patient was readmitted with a lower respiratory tract infection and sepsis. Treatment comprising steroid and mycophenolate mofetil was discontinued by the attending physicians. His condition improved following the administration of anti-infection treatment but he became subjected to rapid deterioration afterward, marked by declining senses and unstable vital

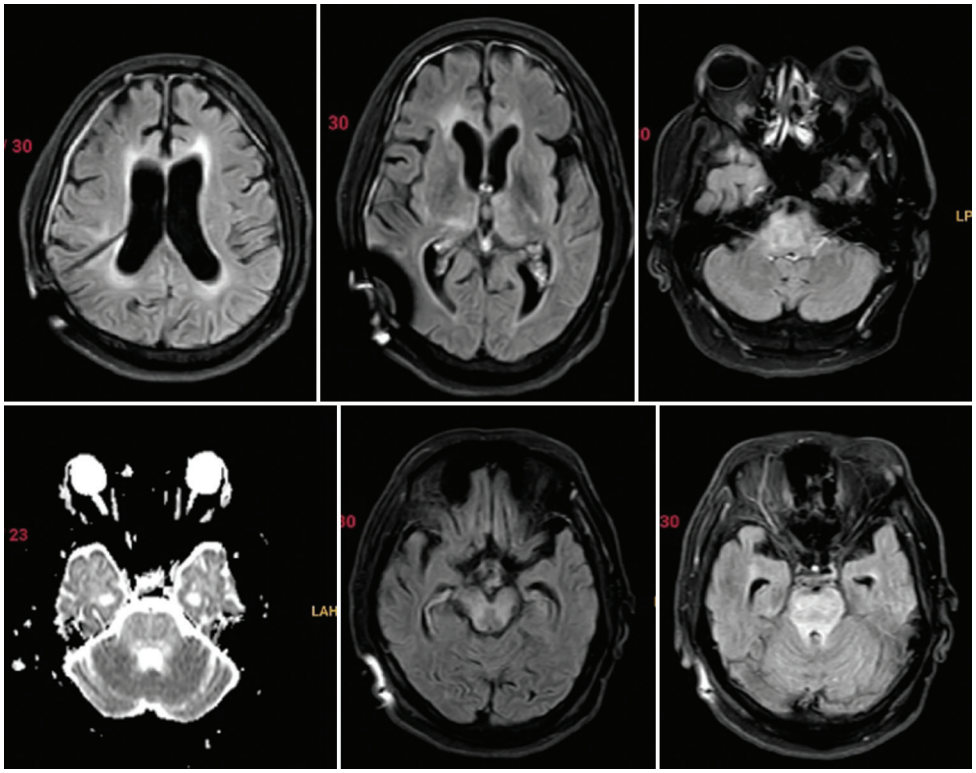

**Figure 1.** Brain magnetic resonance imaging revealing T2 hyperintensities in the thalamus, midbrain, pons, and medulla. Diffusion-weighted imaging showed facilitated diffusion based on increased apparent diffusion coefficient values, coupled post-contrast enhancement of the lesion in FLAIR and pachymeningitis

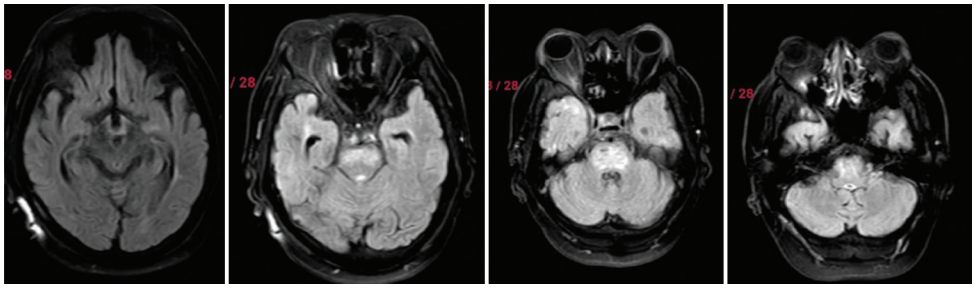

**Figure 2.** Repeat brain magnetic resonance imaging (MRI) demonstrating early resolution of the lesions. The repeat MRI was conducted after 12 days of initial MRI and following pulse methylprednisolone

parameters. Unfortunately, he was lost to follow-up for any of our further investigative efforts.

## 3. Discussion

Idiopathic normal pressure hydrocephalus is generally more common in individuals aged older than 40 years, featuring an insidious onset and progression of symptoms over a period of at least 3 months.[1] In this case report, the patient was 49 years old at the time of medical consultation, having suffered from insidious-onset symptoms for 6 months. Under most circumstances, the underlying pathology of normal pressure hydrocephalus is not well-understood during the initial evaluation, warranting a thorough evaluation of the etiology to guide therapeutic decision; however, a failure to determine the etiological factor usually necessitates a strict follow-up. Interestingly, the patient described in this report had the classic triad, coupled with normal brain MRI with contrast and negative CSF findings during the initial presentation. The opening pressure was high-normal (210 mm of water/210 mm $H_2O$) which, albeit high, was below the accepted cut-off threshold (250 mm of water/250 mm $H_2O$).[2]

Psychiatric manifestations were reported in 20% of patients with neurosarcoidosis and 1% of those affected

with sarcoidosis. These manifestations cause vivid psychosis, including auditory, visual hallucinations, and delusions.[3] Consistent with these standard presentations, our patient manifested delusion and aggressive behavior in the initial presentation, and subsequently delirium.

The diagnosis and treatment of neurosarcoidosis can be very challenging for several reasons. It affects clinically 5 – 10% of sarcoidosis patients, but according to autopsy examinations, up to 25% of deceased individuals are affected by sarcoidosis, representing a clear sign of under-diagnosis of this pathological condition.[4] Hence, physicians need to exercise caution while investigating cases featuring consistent characteristics with sarcoidosis to avoid mis-diagnosis and the ensuing catastrophic deterioration of the condition. To facilitate a definite diagnosis of neurosarcoidosis, nervous system biopsy is preferred for investigation, but it is not always practical due to on the site of disease. Thus, the general diagnostic process for a possible neurosarcoidosis involves confirming a neuroinflammatory basis of a pathological condition under investigation and evaluating the response to treatment after rigorous exclusion of implausible causes.[5]

Primary CNS lymphoma (PCNSL) stands as another possible diagnosis in this case. It is an uncommon type of extra-nodal non-Hodgkin lymphoma, which originates in a type of cell not normally present in the CNS. PCNSL is known to regress completely with corticosteroids but may recur later and cause fatal outcomes, as described in the current case. Brain parenchyma, spinal cord, leptomeninges, and eyes are affected in PCNSL, giving rise to highly variable presentations and even psychiatric symptoms (also described in the current case) in up to 43% of cases.[6] In fact, hydrocephalus may be the sole manifestation of PCNSL.[6] CSF cytology approach, which was employed in this case, is not very sensitive in detecting PCNSL (with a rate of 2–32%), and flow cytometry has been reported to have higher sensitivity.[7] To enhance sensitivity (up to 85%) in this respect, several CSF markers, such as CSF lactate dehydrogenase isozyme 5 and β2-microglobulin, can be assayed. Few other markers may be utilized to increase specificity (up to 95%) like proteomics and microRNA analysis.[7] However, brain/leptomeningeal/vitreous biopsy remains the current gold-standard diagnostic approach for PCNSL. On a separate note, CNS infections represent another etiological facet of PCNSL that should not be neglected, as evidenced by the increased uptake of thallium 201 in single-photon emission CT scan that is strongly indicative of the disorder.[7]

In this case, a definite diagnosis of the disease cannot be reached due to the suspended investigative works caused by patient's loss to follow-up. Autoimmune encephalitis or Bickerstaff brainstem encephalitis emerges as another possibility, but the pathogenesis of these conditions does not align with the disease process of hydrocephalus; therefore, these conditions were not considered. After close possibilities such as tuberculosis or CNS infections were ruled out, sarcoidosis was regarded as a plausible diagnosis, on the basis of the multisystemic involvement of the disease process, and the quick, progressive, and sustainable improvement with steroid. Sarcoidosis is a disease with an unknown origin, which provides the rationale for the lack of definite evidence in support of diagnosis. Hence, patients with undetermined pathological condition featuring attributes as described above should be indicated an aptly-designed treatment regimen, through which treatment response can be used to justify the exclusion of implausible conditions, leading up to a definite diagnosis.

## 4. Conclusion

Our study portrays the need for a detailed evaluation of the etiology of hydrocephalus in a young patient besides performing ventriculoperitoneal shunt for symptomatic improvement. We need to conduct a more specific and elaborate investigation, driven by a strong clinical suspicion, and rule out rare possibilities: primary CNS lymphoma and sarcoidosis are one of them. This approach will help us start proper treatment regimen as early as possible and save valuable time as "time is brain".

## Acknowledgments

None.

## Funding

None.

## Conflict of interest

The author declares no competing interest.

## Author contributions

This is single-authored article.

## Ethics approval and consent to participate

The patient gave consent to participate in the study.

## Consent for publication

Patient gave consent to release their data and images in this paper.

## Availability of data

Not applicable.

## References

1. Shprecher D, Schwalb J, Kurlan R. Normal pressure hydrocephalus: Diagnosis and treatment. *Curr Neurol Neurosci Rep.* 2008;8(5):371-376.

   doi: 10.1007/s11910-008- 0058-2

2. Lee SC, Lueck CJ. Cerebrospinal fluid pressure in adults. *J Neuroophthalmol*. 2014;34(3):278-283.

   doi: 10.1097/WNO.0000000000000155

3. Westhout FD, Linskey ME. Obstructive hydrocephalus and progressive psychosis: Rare presentations of neurosarcoidosis. *Surg Neurol*. 2008;69(3):288-292.

   doi: 10.1016/j.surneu.2007.01.068

4. Tana C, Wegener S, Borys E, *et al*. Challenges in the diagnosis and treatment of neurosarcoidosis. *Ann Med*. 2015;47(7):576-591.

   doi: 10.3109/07853890.2015.1093164

5. Stern BJ, Royal W 3rd, Gelfand JM, *et al*. Definition and consensus diagnostic criteria for neurosarcoidosis: From the neurosarcoidosis consortium consensus group. *JAMA Neurol*. 2018;75(12):1546-1553.

   doi: 10.1001/jamaneurol.2018.2295

6. Boshrabadi AP, Naiem A, Ghazi Mirsaeid SS, *et al*. Hydrocephalus as the sole presentation of primary diffuse large B-cell lymphoma of the brain: Report of a case and review of literature. *Surg Neurol Int*. 2017;8:165.

   doi: 10.4103/sni.sni_446_16

7. Scott BJ, Douglas VC, Tihan T, Rubenstein JL, Josephson SA. A systematic approach to the diagnosis of suspected central nervous system lymphoma. *JAMA Neurol*. 2013;70(3):311-319.

   doi: 10.1001/jamaneurol.2013.606

ACCSCIENCE PUBLISHING

Brain & Heart

CASE REPORT

# Surgical anastomosis of vertical vein to left atrial appendage: A case report of technical aspects

**Gananjay G. Salve*, Danish A. K. Memon, Veeresh Manvi, Parishwanath B. Patil, Nidhi G. Manvi, Mohan D. Gan, and Richard Saldanha**

Department of Cardiovascular and Thoracic Surgery, KLE's Dr. Prabhakar Kore Hospital and Medical Research Centre, Belgaum, Karnataka, India

## Abstract

Management of partial anomalous pulmonary venous connection (PAPVC) differs significantly between the defect on the left side, which is adjacent to left atrial appendage, and that on the right one adjacent to the interatrial septum. Here, we report two patients operated at our center. The first case is an adult diagnosed with the left-sided PAPVC draining to an innominate vein through a left-sided vertical vein, and with a large ostium secundum atrial septal defect. The second case is a neonate with mixed-type total anomalous pulmonary venous connection with all right pulmonary veins opening into the coronary sinus, and all the left pulmonary veins connecting to the innominate vein through a left-sided vertical vein. Both patients experienced severe pulmonary arterial hypertension, necessitating surgical treatment involving disconnection of the vertical vein from its junction, or, ligation of the vertical vein-innominate vein junction, coupled with its redirection to the left atrial appendage. We employed different surgical procedures on these patients, given the distinct age difference, intending to anastomose their respective vertical veins to the adjacent left atrial appendage. In this report, the technical aspects of anastomosing vertical vein to left atrial appendage, to avoid pulmonary venous obstruction in these two patients, are discussed.

***Keywords:*** Anomalous pulmonary venous connection; Vertical vein; Left atrial appendage; Secundum atrial septal defect; Technical aspects

***Corresponding author:**
Gananjay G. Salve
(gananjay.salve@gmail.com)

**Citation:** Salve GG, Memon DAK, Manvi V, *et al.* Surgical anastomosis of vertical vein to left atrial appendage: A case report of technical aspects. *Brain & Heart.* 2024;2(2):2376.
doi: 10.36922/bh.2376

**Received:** December 5, 2023

**Accepted:** February 27, 2024

**Published Online:** May 2, 2024



## 1. Background

Partial anomalous pulmonary venous connection (PAPVC) reportedly occurs at a rate of 0.4 – 0.7% on autopsy examination,[1] with only 10% of the cases affecting left-sided pulmonary veins.[2] The incidence of total anomalous pulmonary venous connection (TAPVC) accounts for approximately 2% of all congenital heart defects.[3] Constituting only 5% of all the TAPVC cases, its mixed-type form has the least incidence rate.[4]

In this report, we describe two patients, the first patient is an adult diagnosed with the left-sided PAPVC draining to the innominate vein through a vertical vein, coupled with a large ostium secundum atrial septal defect (ASD). The second patient is a neonate diagnosed with mixed-type TAPVC, characterized by the right-sided pulmonary veins opening into the coronary sinus directly, and the left-sided ones forming a vertical vein and draining into the innominate vein. Drawing on the treatment experiences for these patients, we compile the key technical aspects of administering the surgical treatment,

that is, anastomosis connecting vertical vein to left atrial appendage, and highlight the procedural nuances for patients with distinct age difference.

## 2. Case presentation

### 2.1. Case 1

The first case is a 32-year-old patient presented with symptoms of intermittent palpitations and breathlessness for a couple of years. According to an echocardiography study, the patient had a large secundum ASD with a left upper pulmonary vein and lingual vein draining through a vertical vein to an innominate vein. All right-sided pulmonary veins and the left lower vein were draining normally, confirmed by the catheterization study (Figure 1).

The patient was surgically treated with routine median sternotomy and cardiopulmonary bypass, which involved dissecting the vertical vein and looping it in the left paracardiac gutter (Figure 2A). All the pulmonary veins joining the vertical vein were dissected and their anatomical course was confirmed. The junction of the vertical vein to the innominate vein was then divided and transfixed (Figure 2B). Left atrial appendage was opened longitudinally on its dorsal surface after inducing cardioplegic cardiac arrest. The open end of the vertical vein was fashioned to facilitate its anastomosis to the left atrial appendage opening without any twist or tension, using a 5-0 polypropylene continuous suture (Figures 2C-E, and 3). The ASD was closed using autologous pericardium (Figure 2F).

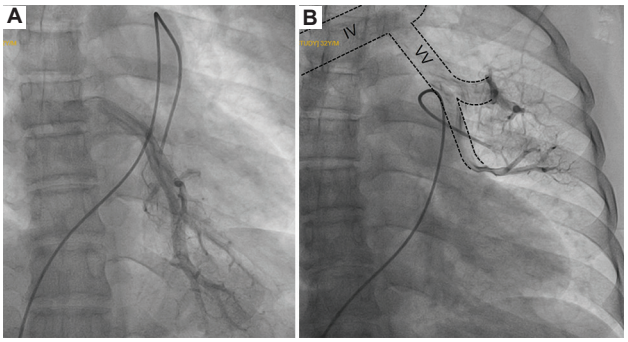


**Figure 1.** Catheterization study images. (A) Left inferior pulmonary vein draining normally to the left atrium. (B) Left superior pulmonary vein and lingual vein draining to innominate vein (IV) via vertical vein (VV).

Intraoperative transesophageal echocardiography studies conducted in different time sessions, that is, immediately after the surgery and following a 6-month follow-up, revealed no gradient in the left atrial appendage anastomosis (Figure 4).

### 2.2. Case 2

The second case is a 15-day-old neonate who developed respiratory distress and bluish discoloration of extremities since birth. An echocardiography study revealed that the neonatal patient was diagnosed with the mixed-type TAPVC with restrictive ASD, characterized by the right pulmonary veins directly draining into the coronary sinus, and the left pulmonary veins draining to the innominate vein through a left-sided vertical vein (Figure 5A).

Due to obstructed atrial communication, median sternotomy was implemented, and cardiopulmonary bypass was established with an aortobicaval cannulation. The vertical vein was dissected in the left paracardiac gutter after cardioplegic cardiac arrest was induced. All the pulmonary veins joining the vertical vein were dissected around the vertical vein. The vertical vein was then ligated and clipped at the innominate vein junction without dividing it and proximally controlled with silk suture loop (Figure 5B).

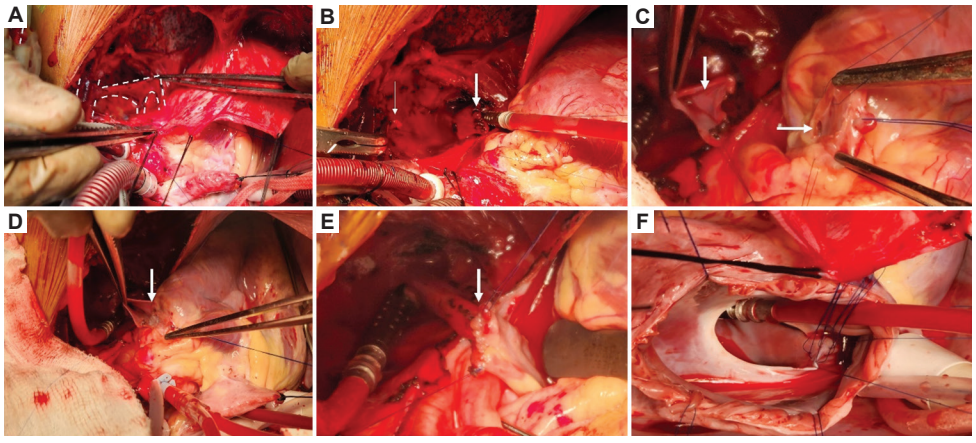


**Figure 2.** Intraoperative photos of Case 1. (A) Two pulmonary veins joining to form the vertical vein and draining to the innominate vein (dotted lines). (B) Vertical vein divided at the innominate vein junction. Thin arrow indicates ligated end, and thick arrow denotes open end. (C) Open end of vertical vein (vertical arrow) and opened left atrial appendage (transverse arrow). (D) Posterior anastomosis of vertical vein to left atrial appendage (arrow). (E) Completed anastomosis (arrow). (F) Closure of the atrial septal defect using autologous pericardium.

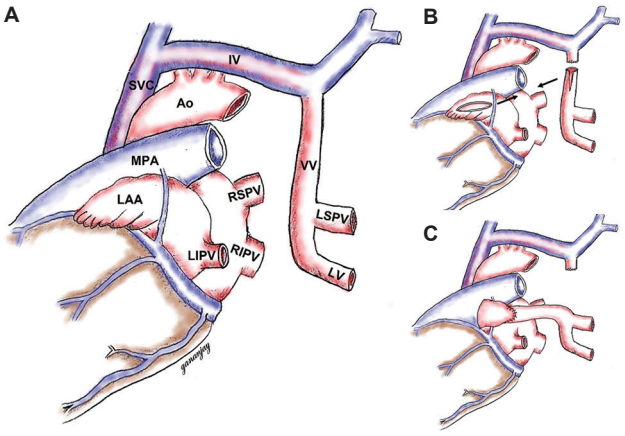


**Figure 3.** Illustrated cardiac anatomy and surgical procedure of Case 1. (A) Illustration depicting cardiac anatomy of Case 1, viewed from the left posterolateral angle. (B) Illustration depicting anastomosis of dissected vertical vein with an opening on the left atrial appendage incision. (C) Illustration depicting completed anastomosis.
Abbreviations: Ao: Aorta; IV: Innominate vein; LAA: Left atrial appendage; LIPV: Left inferior pulmonary vein; LSPV: Left superior pulmonary vein; LV: Lingual vein; MPA: Main pulmonary artery; RIPV: Right inferior pulmonary vein; RSPV: Right superior pulmonary vein; SVC: Superior vena cava; VV: Vertical vein.

The vertical vein was then opened along its length between the ligature distally and the silk loop proximally. The dorsal surface of the left atrial appendage was then opened for a length of >1 cm (Figure 5B) to correspond to the vertical vein opening. A wide anastomosis was created between these openings using 7-0 polypropylene continuous suture, in a side-to-side fashion (Figure 5C), without disconnecting the vertical vein from the innominate vein.

The roof of the coronary sinus is split/divided so that the coronary sinus along with the right pulmonary venous drainage now drains into the left atrium. Echocardiography revealed no blood flow turbulence in the vertical vein-left atrial appendage anastomosis.

## 3. Discussion

In this paper, we present two cases with distinct age difference, who were treated surgically to anastomose their vertical veins to left atrial appendage.

In both cases, due to the absence of a common venous chamber, the chances of compromising the pulmonary venous drainage during the surgical repair were high. In adults, due to the bigger size of all cardiac structures, the vertical vein can be safely disconnected from the innominate vein and anastomosed to the left atrial appendage in an end-to-side fashion. For precaution, the surgeons should avoid twisting the vertical vein after its disconnection by making use of stay sutures or marking the trimmed vessels with a sterile marker pen. It is recommended to anastomose

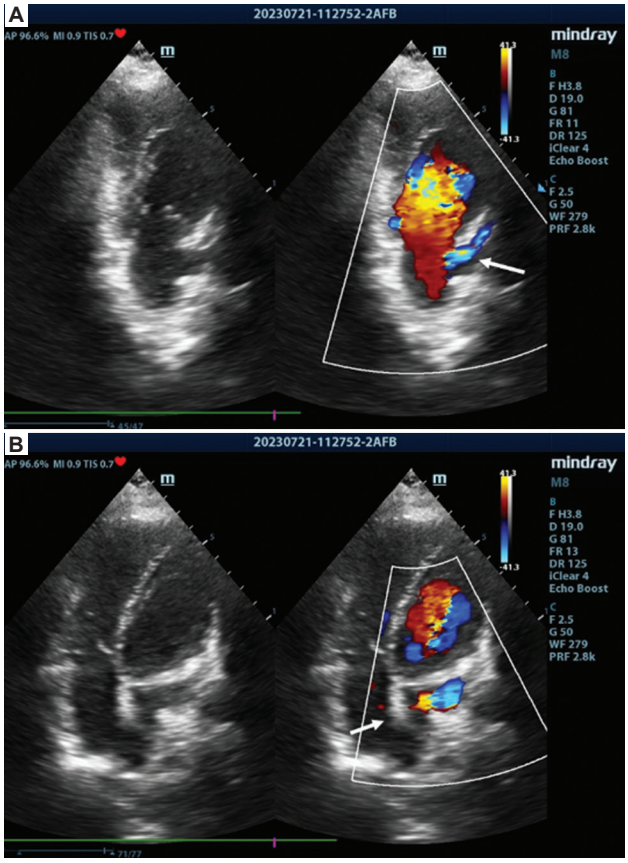


**Figure 4.** Two-dimensional and color Doppler echocardiography images of Case 1 patient at 6 months follow-up. (A) Unobstructed pulmonary venous flow into the left atrial appendage (arrow). (B) No flow across the interatrial septum (indicated by arrow).

vertical wall with a finer polypropylene suture since its wall can be relatively thin even in adults.

It is advisable to dissect the left-sided vertical vein after establishing cardiopulmonary bypass, particularly in adults, due to severe pulmonary artery hypertension and to prevent right ventricular dysfunction and arrhythmias as a result of pulmonary artery retraction during dissection. In addition, it is safer to open the left atrial appendage on the arrested heart, as clamping its base for anastomosis on the beating heart can distort it and is likely to injure important structures in the left atrioventricular groove such as the left circumflex artery and the coronary sinus.

The vertical vein wall is extremely thin in neonates and difficult to handle. Recommended approach to treating PAPVC in neonates involves dividing and then anastomosing the vertical vein,[5] but in our experience, this method renders the subsequent suturing extremely challenging, and formation of any kink or twist unavoidable. Therefore, we suggest ligating the vertical vein-innominate vein junction, without disconnecting it, to maintain the straight position

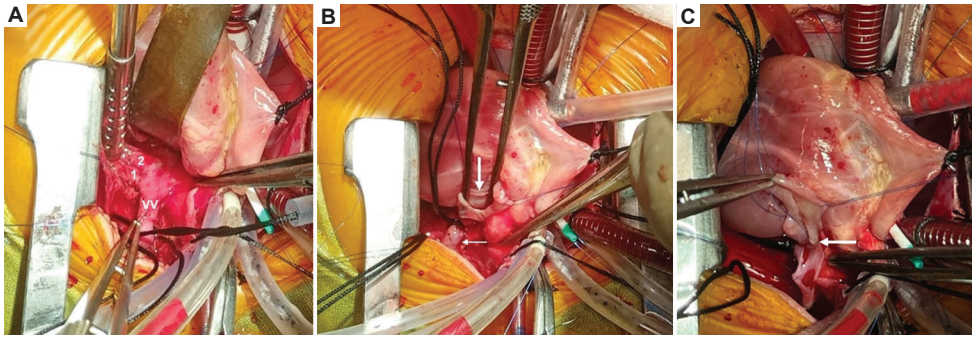


**Figure 5.** Intraoperative photos of Case 2. (A) Left-sided pulmonary veins (indicated by 1 and 2) draining to the vertical vein (VV). (B) Ligated VV (transverse arrow) and opened left atrial appendage (vertical arrow). (C) Anastomosis between VV and left atrial appendage (transverse arrow).

of vertical vein and to facilitate an uncluttered and wide anastomosis using a finer polypropylene suture.

To conduct the same surgical treatment for both adults and neonates, it is advisable to perform resection of left atrial appendage trabeculations and creation of a left pericardial slit to support the suture line. A slit in the left pericardial edge can prevent tension from building up on the vertical vein-left atrial appendage suture line. Caution should be exercised while creating the slit to avoid injuring the left phrenic nerve. This step is particularly critical if the left atrial appendage is short. Furthermore, a slit in the adjacent pericardium may ensure long-term patency of the anastomosis. In relation to this, it is advisable to start anticoagulation as soon as possible during the post-operative period, followed by antiplatelet therapy for 3 – 6 months, to avoid late pulmonary venous obstruction.

Atrial arrhythmias, particularly atrial fibrillation, remain one of the most common causes of arrhythmia-related morbidity and mortality. Current treatment options for atrial arrhythmias include medical management, catheter ablation, and surgical procedures.[6] Complex atrial tachycardias can be profiled using ultra high-density mapping, which is a is safe, feasible, and effective avenue for precisely identifying tachycardia sites to guide successful catheter ablation.[7] To ease such catheter procedures, if indicated in future, a wide anastomosis of the vertical vein to the left atrial appendage is necessary.

## 4. Conclusion

Vertical vein-left atrial appendage anastomosis for PAPVC is a patient-centric approach, requiring cautious attention of the attending surgeons. The prime objective while conducting the surgical repairs is to avoid pulmonary venous obstruction by following procedures featuring technical nuances targeting different age groups.

## Acknowledgments

None.

## Funding

None.

## Conflict of interest

The authors declare no conflicts of interest.

## Author contributions

*Conceptualization:* Gananjay G. Salve, Parishwanath B. Patil
*Investigation:* Danish A.K. Memon, Mohan D. Gan
*Writing – original draft:* Gananjay G. Salve, Danish A.K. Memon, Richard Saldanha
*Writing – review & editing:* All authors

## Ethics approval and consent to participate

Ethics committee of KLES Academy of Higher Education and Research, Belgaum granted permission to publish this article. Verbal consent was obtained from the patient prior to participation.

## Consent for publication

A verbal consent was obtained from the involved patients' before writing the manuscript. No patient identifiable data have been mentioned in the manuscript.

## Availability of data

Data are available from the corresponding author on reasonable request.

## References

1. Healey JE Jr. An anatomic survey of anomalous pulmonary veins: Their clinical significance. J Thorac Surg. 1952;23:433-444.
2. Javangula K, Cole J, Cross M, Kay PH. An unusual manifestation of left partial anomalous pulmonary venous connection. Interact Cardiovasc Thorac Surg. 2010;11:846-847.

doi: 10.1510/icvts.2009.231100

3. Bharati S, Lev M. Congenital anomalies of the pulmonary veins. Cardiovasc Clin. 1973;5:23-41.

4. Darling RC, Rothney WB, Craig JM. Total pulmonary venous drainage into the right side of the heart; report of 17 autopsied cases not associated with other major cardiovascular anomalies. Lab Invest. 1957;6:44-64.

5. Delius RE, De Leval MR, Elliot MJ, Stark J. Mixed total pulmonary venous drainage: Still a surgical challenge. J Thorac Cardiovasc Surg. 1996;112:1581-1588.

doi: 10.1016/S0022-5223(96)70017-X.6

6. MacGregor RM, Khiabani AJ, Damiano RJ Jr. The surgical treatment of atrial fibrillation via median sternotomy. Oper Tech Thorac Cardiovasc Surg. 2019;24:19-37.

doi: 10.1053/j.optechstcvs.2019.07.001

7. Schaeffer B, Hoffmann BA, Meyer C, *et al*. Characterization, mapping, and ablation of complex atrial tachycardia: Initial experience with a novel method of ultra high-density 3D mapping. J Cardiovasc Electrophysiol. 2016;27:1139-1150.

doi: 10.1111/jce.13035

ACCSCIENCE PUBLISHING

Brain & Heart

CASE REPORT

# Patent foramen ovale closure in a patient with extensive lipomatous hypertrophy of the septum secundum: A case report

**Sergey Terekhin[1], Dmitry Shchekochikhin[1], Alexandr G. Osiev[2], and Eustaquio Maria Onorato[3]***

[1]Department of Cardiology, Ilynskaya Hospital JSC, Moscow, Russia

[2]Department of Endovascular Cardiology, JSC Hospitals Medsi, Moscow, Russia

[3]Department of Cardiology University Hospital, I.R.C.C.S. Ospedale Galeazzi - Sant'Ambrogio, Milan, Italy

## Abstract

Lipomatous hypertrophy of the septum secundum (LHSS) is a benign disorder characterized by the accumulation of fat in the interatrial septum, presenting with an hourglass appearance that spares the fossa ovalis on echocardiography. Typically asymptomatic, LHSS is often incidentally detected through two-dimensional transthoracic echocardiography/transesophageal echocardiography, computed tomography, and cardiac magnetic resonance imaging. It primarily affects elderly and obese individuals, with a higher prevalence among females, and may cause atrial arrhythmias, syncope, and heart failure. Transcatheter closure of patent foramen ovale (PFO) associated with LHSS has traditionally posed challenges due to the lack of specifically designed devices and the risk of suboptimal results. Our case report details the off-label implantation of a flexible atrial septal defect closure device for a PFO closure in an elderly patient presenting with an embolic stroke of undetermined source, severe kyphosis, platypnea-orthodeoxia syndrome, and a large LHSS. In addition, strategies adopted to enhance the success of percutaneous closure are discussed.

***Keywords:*** Lipomatous hypertrophy of the septum secundum; Patent foramen ovale; Atrial septal defect; Platypnea-orthodeoxia syndrome; Thoracic kyphosis; Transcatheter closure

***Corresponding author:**
Eustaquio Maria Onorato
(eustaquio.onorato@gmail.com)

**Citation:** Terekhin S, Shchekochikhin D, Osiev AG, Onorato EM. Patent foramen ovale closure in a patient with extensive lipomatous hypertrophy of the septum secundum: A case report. *Brain & Heart.* 2024;2(2):2190.
doi: 10.36922/bh.2190

**Received:** November 6, 2023

**Accepted:** December 29, 2023

**Published Online:** May 2, 2024



## 1. Background

Patent foramen ovale (PFO) is associated with various medical conditions, including platypnea-orthodeoxia syndrome (POS), which is characterized by dyspnea and hypoxemia in the sitting or standing position, usually resolved by lying down.[1,2] With aging, spondylosis and severe kyphosis of the thoracic spine, as observed in our patient, alter intrathoracic relationships and may contribute to increased venous blood shunting into the left atrium, exacerbating hypoxemia, and requiring oxygen support. Notably, percutaneous PFO closure has been demonstrated to alleviate symptoms and may offer a potential cure. In PFO patients with lipomatous hypertrophy of the septum secundum (LHSS), catheter-based closure procedures are often considered technically demanding. Prominent LHSS hinders a proper coaptation of the leaflets with traditional occluders,

necessitating the use of devices designed for the occlusion of atrial septal defect. This case report details that the anatomical and functional aspects of LHSS are detailed, with a focus on the technical features of percutaneous interventions.

## 2. Case report

A 76-year-old male patient suffering from arterial hypertension, chronic obstructive pulmonary disease (COPD), and severe kyphosis of the thoracic spine was admitted for a sudden onset of dysarthria, dysphagia, and moderate left facial weakness occurring 12 h before admission. Brain magnetic resonance imaging confirmed a right parietal lobe infarction. Paroxysmal atrial fibrillation was observed during electrocardiogram (ECG) monitoring, leading to the initiation of apixaban 5 mg twice daily. Contrast-transcranial Doppler revealed a severe right-to-left shunt (RLS) through PFO under basal conditions. The patient demonstrated neurological improvement following treatment. On discharge, long-term anticoagulation therapy with warfarin was prescribed. However, he was readmitted weeks later for pneumonia associated with fever and exacerbation of COPD, manifesting severe shortness of breath and hypoxemia that necessitated oxygen support. ECG at admission indicated sinus rhythm, leftward QRS axis deviation, and poor R wave progression in the right precordial leads. Chest X-ray revealed signs of increased pulmonary flow and right heart chamber enlargement. One-week treatment with antibacterial drugs, short-acting beta-agonists (SABAs), and systemic glucocorticosteroids resulted in normalization of temperature, improvement of wheezing, and reduction of acute inflammatory markers. However, severe hypoxemia ($O_2$ saturation of 86–88% on room air) persisted in the upright position, improving with recumbency, confirming the diagnosis of POS. Poor acoustic echocardiographic window hindered the assessment of cardiac structures and function using two-dimensional (2D) transthoracic echocardiography (TTE). 2D transesophageal echocardiography (TEE) color Doppler provided better visualization and identified a giant LHSS with a fat tissue thickness of 25 mm, a floppy septum primum convex to the left, preserved left ventricle ejection fraction (60 %).

After heart team discussion, the decision to proceed with catheter-based treatment was confirmed based on the presence of POS exacerbated by kyphosis progression. Written informed consent was obtained from the patient. The procedure was performed under general anesthesia, with continuous 2D/three-dimensional (3D) TEE and fluoroscopic guidance. Pulmonary artery pressure was within the normal range (systolic/diastolic/mean: 30/10/20 mmHg), while the right atrial pressure was elevated (systolic/diastolic/mean: 20/10/15 mmHg). Intraprocedural 2D contrast-TEE color Doppler confirmed a significant RLS, a permanent leftward displacement of the hypermobile septum primum, and a prominent LHSS with a thickness of 25 mm (Figure 1). After an uncomplicated septal crossing, a 0.035" ×260 cm exchange stiff wire was positioned in the left upper pulmonary vein. A 25 × 45 mm balloon (Occlutech sizing balloon, OSB, Abbott, USA) revealed a 12 mm waist due to LHSS, which did not completely disappear with further balloon inflation above its nominal level (Figure 2). Test occlusion of the tunnel was carried out for 15 min, ensuring the patency of pulmonary veins or the mitral valve's orifice. Subsequent hemodynamic measurements revealed a remarkable increase in $O_2$ saturation up to 98%, with no changes in pulmonary and systemic arterial pressures. A third-generation 15 mm Figulla Flex II atrial septal defect device (FSO, Occlutech GmbH, Germany), with distal and proximal discs measuring 30 mm and 26 mm, respectively, featuring a very flexible double-disc design with adjustable waist length, hubless left disk, and unique ball-connection between pusher and occluder was selected (with adjustments in 3 mm increments of the waist size as per FSO Technology). It was successfully implanted, with the discs splayed appropriately, aligned correctly with the interatrial septum, and anchored appropriately to the LHSS rims, attributed to the unique discs and connecting waist flexibility, resulting in no residual shunt (Figure 3 and Video A1). Post-procedure hemodynamic parameters remained stable, with $O_2$ saturation at 99%. The patient, who demonstrated improved clinical condition the following day, was discharged home on a medication regimen including clopidogrel 75 mg daily, apixaban 5 mg twice daily, atorvastatin 20 mg daily, and bisoprolol 2.5 mg daily. At the 12-month follow-up, 2D TTE color Doppler confirmed correct device positioning with no residual shunt (Figure 4). In addition, there was a significant clinical improvement, with $O_2$ saturation ranging from 94–96% on room air. The patient became more active, and a course of physical rehabilitation was started. To date, no complications such as device embolism, endocarditis, or significant RLS have occurred.

## 3. Discussion

Lipomatous hypertrophy of the septum secundum, first described by Prior[3] in 1964 during a post-mortem examination, is defined as fatty infiltration exceeding 20 mm in thickness within the atrial septum.[4] This benign condition entails an accumulation of excessive mature adipose tissue and brown fetal adipose tissue deposition in the septum secundum, excluding the fossa ovalis (septum primum), giving it a pathognomonic dumbbell

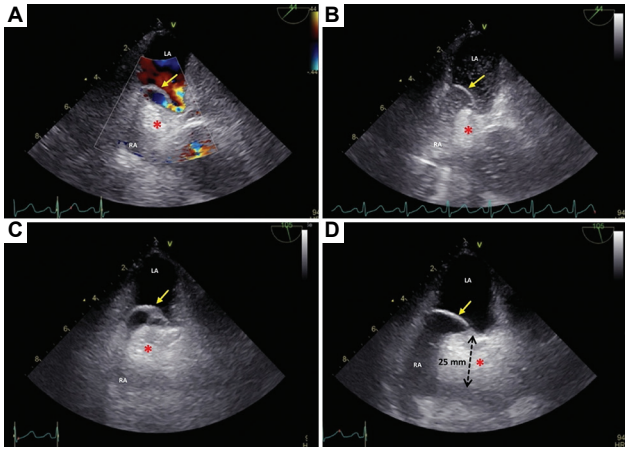


**Figure 1.** The right atrial angiogram by the pigtail catheter in the antero-posterior projection confirms the correct alignment of the 15mm FSO to the interatrial septum with no residual right-to-left shunt. (A and B) Intraprocedural two-dimensional (2D) transesophageal echocardiogram (TEE) color Doppler at 44° showing unusual lipomatous hypertrophy of the septum secundum (red asterisk), a permanent leftward displacement of the hypermobile septum primum (yellow arrow), and a significant right-to-left shunting after agitated saline contrast injection; intraprocedural 2D TEE at 105°, systolic (C) and diastolic (D) frames, showing a permanent leftward displacement of the hypermobile septum primum (yellow arrow) and the giant lipomatous hypertrophied septum secundum (red asterisk) measuring at a thickness of 25 mm. Abbreviations: LA: Left atrium; RA: Right atrium.

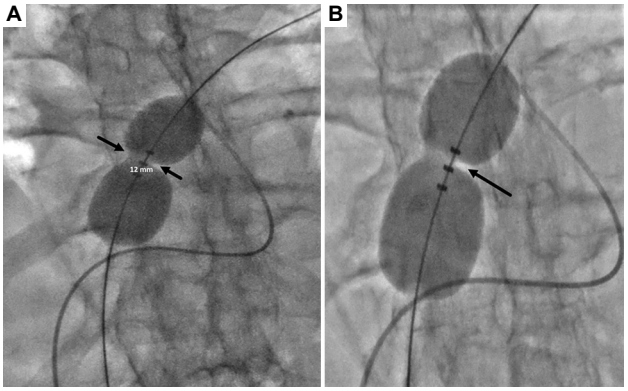


**Figure 2.** Intraprocedural fluoroangiographic images of the 25 × 45 mm sizing balloon engaged inside the tunnel showing a waist (black arrows) (A) that did not disappear completely with further balloon inflation above its nominal level (B). Three radiopaque markers, spaced at 10 mm as measured from leading edge to leading edge, are located at the balloon center and are used as a distance reference.

shape. Its prevalence varies, ranging from 2% (in patients undergoing cardiac tomography) to 8–10% when detected by TEE, which appears to be the most sensitive technique for identifying the mass.[5]

The incidence of LHSS increases with age, body mass, and chronic corticosteroid therapy, with a higher incidence among women.[6] In contrast to LHSS, cardiac lipoma is a genuine neoplasm typically found in a younger

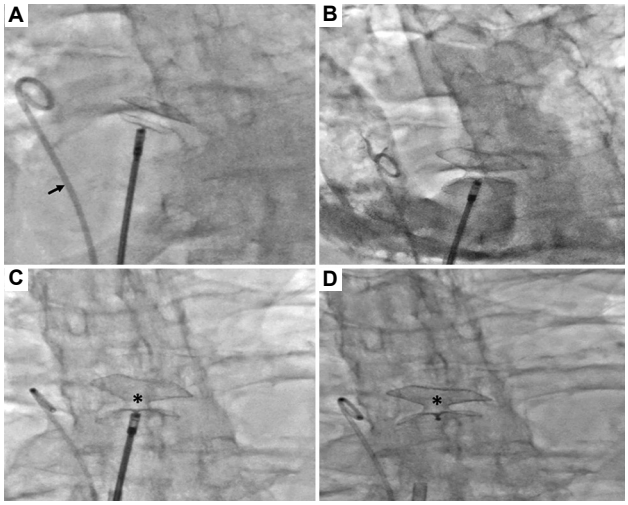


**Figure 3.** Fluoroangiographic procedural steps. A 6-Fr pigtail angiographic catheter (small black arrow) in the right atrium and the distal and proximal discs of the 15-mm FSO device well aligned to the interatrial septum (A); right atrial angiography with the 6-Fr pigtail catheter showing complete abolition of the right-to-left shunting (B); and the 15-mm FSO device (black asterisk) still anchored to the delivery system (C) and finally deployed (D).

age group. A milder form of atrial septal thickening can occur in conditions such as amyloidosis, tumors, and from a surgical patch covering repaired atrial septal defect.

Symptoms of heart failure may manifest when the large mass causes obstruction of the right atrial inflow or the superior vena cava.[7,8] LHSS may be discovered incidentally during autopsy or could be associated with atrial arrhythmias, obstructive symptoms, or sudden death.[9]

LHSS might be more prevalent than reported due to the lack of routine examination for it. The use of multimodal imaging, including 2D/3D TTE and TEE, computed tomography, and cardiac magnetic resonance imaging, is crucial for making an accurate diagnosis and excluding primary and secondary neoplasms.

While LHSS is often identified incidentally, it can also be associated with atrial arrhythmias, including atrial fibrillation, supraventricular tachycardia, and junctional rhythm. Furthermore, LHSS poses a technical challenge for transseptal puncture, alongside atrial septal aneurysm and previous atrial surgery.

Transcatheter PFO closure in patients with LHSS has been deemed technically demanding due to several factors. Conventional PFO closure devices often feature a central disk length that does not cover the entire thickness of the interatrial septum. In addition, the short connection between the two discs may result in inappropriate anchoring to the LHSS rims, leading to unstable apposition

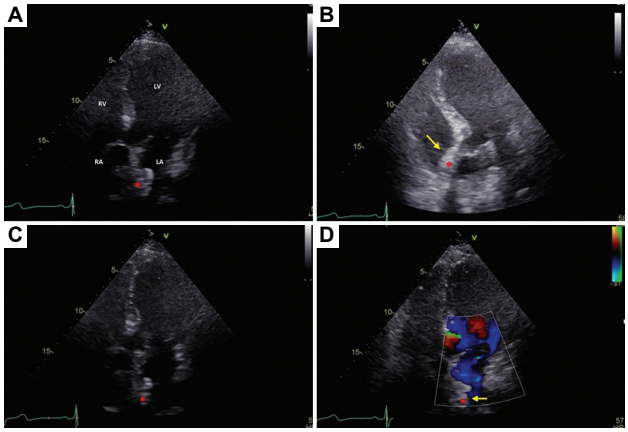


**Figure 4.** At the 6-month follow-up, 2D transthoracic echocardiography (A-C) color Doppler (D) in the apical four-chamber view showed a correctly aligned, well-seated, and apposed the septum secundum device with no residual shunt.

of the occluder, residual shunt, and an increased risk of device embolization. To address this anatomical challenge, utilizing a device with a wider waist that can encompass the entire length of the septum is crucial, similar to techniques employed in atrial septal defect closure procedures.[10,11]

Various devices, such as cribriform Amplatzer septal occluder (Abbott, USA)[12] and the Amplatzer post-infarct muscular VSD occluder (Abbott, USA),[13] have been considered for PFO closure in patients with LHSS. These options are based on the premise that longer or adjustable waist lengths may optimize the positioning of the two device disks over the hypertrophied rims of the septum secundum.

## 4. Conclusion

Our case nicely illustrates the effectiveness of a third-generation atrial septal defect device in achieving optimal apposition of the discs to the rims of LHSS. This success is attributed to the device's unique flexible nitinol braiding technology, which offers an ideal technical solution for RLS abolition.

## Acknowledgments

The authors would like to acknowledge Dr Alexey Knigin, Senior Clinical Specialist, Department of Clinical Support and Therapy Development, Cardiomedics, Moscow, Russia, for his assistance and logistic help with this case.

## Funding

None.

## Conflict of interest

Eustaquio Maria Onorato is a consultant for Occlutech. The remaining authors declare no conflicts of interest.

## Author contributions

*Conceptualization:* Alexandr G. Osiev, Eustaquio Maria Onorato
*Investigation:* Sergey Terekhin, Dmitry Shchekochikhin
*Methodology:* Alexandr G. Osiev
*Supervision:* Eustaquio Maria Onorato
*Writing – original draft:* Alexandr G. Osiev
*Writing – review & editing:* Eustaquio Maria Onorato

## Ethics approval and consent to participate

Permission was obtained from each of the subjects to participate in the study.

## Consent for publication

The patient consented to the publication of the data.

## Availability of data

Data are fully available under explicit request to the corresponding author.

## References

1. De Vecchis R, Baldi C, Ariano C. Platypnea-orthodeoxia syndrome: Multiple pathophysiological interpretations of a clinical picture primarily consisting of orthostatic dyspnea. *J Clin Med*. 2016;5:85.

   doi: 10.3390/jcm5100085

2. Agrawal A, Palkar A, Talwar A. The multiple dimensions of platypnea-orthodeoxia syndrome: A review. *Respir Med*. 2017;129:31-38.

   doi: 10.1016/j.rmed.2017.05.016

3. Prior JT. Lipomatous hypertrophy of cardiac interatrial septum. A lesion resembling hibernoma, lipoblastomatosis and infiltrating lipoma. *Arch Pathol*. 1964;78:11-15.

4. Laura DM, Donnino R, Kim EE, Benenstein R, Freedberg RS, Saric M. Lipomatous atrial septal hypertrophy: A review of its anatomy, pathophysiology, multimodality imaging, and relevance to percutaneous interventions. *J Am Soc Echocardiogr*. 2016;29:717-723.

   doi: 10.1016/j.echo.2016.04.014

5. Pochis WT, Saeian K, Sagar KB. Usefulness of transesophageal echocardiography in diagnosing lipomatous hypertrophy of the atrial septum with comparison to transthoracic echocardiography. *Am J Cardiol*. 1992;70:396-398.

   doi: 10.1016/0002-9149(92)90629-d

6. Patsia L, Lartsuliani K, Intskirveli N, Ratiani L. Lipomatous hypertrophy of the interatrial septum - a benign heart anomaly causing unexpected problem in electrophysiology (case report). *Georgian Med News*. 2021;318:72-74.

7. Xanthos T, Giannakopoulos N, Papadimitriou L. Lipomatous

hypertrophy of the interatrial septum: A pathological and clinical approach. *Int J Cardiol*. 2007;121:4-8.

doi: 10.1016/j.ijcard.2006.11.150

8. Cheezum MK, Jezior MR, Carbonaro S, Villines TC. Lipomatous hypertrophy presenting as superior vena cava syndrome. *J Cardiovasc Comput Tomogr*. 2014;8:250-251.

doi: 10.1016/j.jcct.2014.04.005

9. Arbarello P, Maiese A, Bolino G. Case study of sudden cardiac death caused by lypomatous hypertrophy of the interatrial septum. *Med Leg J*. 2012;80:102-104.

doi: 10.1258/mlj.2012.012012

10. Fernandes FH, do Amaral LV, Borges PA, de Almeida e França VE, Masson Silva JB, Gardenghi G. Patent foramen ovale closure with prosthesis for occlusion of atrial septal defect in lipomatous hypertrophy of atrial septum. Report of two cases. *J Transcat Intervent*. 2020;28:eA20200003.

doi: 10.31160/JOTCI202028A20200003

11. Takafuji H, Obunai K, Kato N, Honda M, Watanabe H. Lipomatous atrial septal hypertrophy and atrial septal defect with rim deficiency. *JACC Cardiovasc Interv.* 2022;15(3):e31-e33.

doi: 10.1016/j.jcin.2021.09.040

12. Seemann A, Dorman S, Juliard JM. Platypnoea-orthodeoxia syndrome due to a patent foramen oval with marked lipomatous hypertrophy. *Arch Cardiovasc Dis.* 2011;104:261-262.

doi: 10.1016/j.acvd.2010.10.010

13. Lin CH, Balzer DT, Lasala JM. Defect closure in the lipomatous hypertrophied atrial septum with the Amplatzer muscular ventricular septal defect closure device: A case series. *Catheter Cardiovasc Interv*. 2011;78:102-107.

doi: 10.1002/ccd.22858

## Appendix

**Video A1.** Right atrial angiography with the 6-Fr pigtail catheter showing the third-generation 15-mm Flex II ASD occluder (FSO) device well aligned to the interatrial septum, still anchored to the delivery system, with complete abolition of the right-to-left shunting.

ACCSCIENCE PUBLISHING

Brain & Heart

CASE REPORT

# Clinical course and treatment challenges in post-COVID-19 rhino-orbital-cerebral mucormycosis in an immunocompetent host: A case report

**Rajat Verma*, Awdhesh Yadav, and B. K. Ojha**

Department of Neurosurgery, Kings George Medical University, Lucknow, Uttar Pradesh, India

## Abstract

The aggressive and invasive nature of rhino-orbital-cerebral mucormycosis (ROCM) in immunocompromised patients is well documented. However, this case report aims to narrate its progression in an immunocompetent patient post-recovery from COVID-19. This case report provides a glimpse into the patient's journey through multiple complications and painful surgeries inflicted by the disease. It emphasizes the necessity of a multidisciplinary approach to overcome the challenges posed by ROCM. In our patient, ROCM initially manifested with orbital cellulitis and paranasal sinusitis, requiring exenteration and functional endoscopic sinus surgery. Within a brief period, it advanced to the brain, resulting in a fungal abscess requiring craniotomy, abscess excision, and excision of an infiltrated maxilla through hemimaxillectomy. In addition, the exenteration and maxillectomy cavities were infiltrated by maggots, requiring further debridement. At the time of writing, the patient was undergoing a series of reconstructive surgeries to improve his social acceptability. While medical management with surgical debridement remains the gold standard in the literature, the extent of surgical debridement is still debated. Our case report not only highlights the continuous need for radical surgical interventions, which often extend to the next invaded organ but also reflects the prolonged hospital stay resulting from serial reconstructive surgeries, which take a toll on the patient. In conclusion, good teamwork with clinical foresight is required to achieve favorable treatment outcomes.

***Keywords:*** Rhino-orbital-cerebral mucormycosis; Immunocompetent; COVID-19

***Corresponding author:**
Rajat Verma
(vermarajat107@gmail.com)

**Citation:** Verma R, Yadav A, Ojha BK. Clinical course and treatment challenges in post-COVID-19 rhino-orbital-cerebral mucormycosis in an immunocompetent host: A case report. *Brain & Heart.* 2024;2(2):2083.
doi: 10.36922/bh.2083

**Received:** October 22, 2023

**Accepted:** January 2, 2024

**Published Online:** May 6, 2024



## 1. Introduction

COVID-19 has emerged as one of the most formidable and challenging pandemics of this decade, causing considerable morbidity and mortality worldwide. One of the insidious side effects of the virus is immunosuppression, which heightens susceptibility to opportunistic infections. Zygomycetes, a group of fungi known for their invasive and aggressive nature, pose a significant threat to immunocompromised patients, resulting in a rise in cases of rhino-orbital-cerebral mucormycosis (ROCM).

Before the COVID-19 pandemic, Mucorales primarily affected immunocompromised individuals with conditions such as poorly controlled diabetes mellitus, hematological disorders, chronic renal failure, organ transplant recipients, trauma and burns, malnutrition, immunosuppressive therapy, and malignancies[1]. For example,

uncontrolled diabetes is commonly associated with ROCM, a condition that has become more prevalent due to the increasing incidence of diabetes in our society[2-4]. Diverse vulnerabilities in host immunity result in varying degrees of organ involvement and clinical presentations[5-7].

The manifestation of ROCM in COVID-19 patients without traditional risk factors is now evident. Early diagnosis and intervention are crucial to combat the aggressive and fulminant nature of this disease and the overlapping symptoms with bacterial facial or orbital cellulitis, which pose a diagnostic challenge[8]. A high index of clinical suspicion is vital, and a definitive diagnosis relies on the presence of non-septate broad hyphae with right-angle branching in potassium hydroxide mounts, lactophenol cotton blue mounts, and histopathological examinations[8].

The primary aim of reporting this case was to illustrate the significant burden experienced by the patient, including the challenges endured by the patient during multiple surgeries, serial complications, psychological distress resulting from living with a ghastly face, mental anguish due to social repulsion, the torment of separation from his spouse, and the financial and social strain on his caretaker. The secondary aims included reflecting the aggressive and challenging nature of the disease, which makes it typically troublesome to recognize and extremely challenging to treat, evaluating the radicality of surgical debridement, highlighting the role of staged reconstruction surgeries, and signifying the importance of multidisciplinary teamwork.

## 2. Case presentation

A 38-year-old patient presented with pain, redness, swelling, ptosis, and vision loss in his left eye over the past 20 days before seeking medical consultation (Figure 1A). He had a history of left upper molar tooth extraction 5 days before symptom onset and had experienced a past COVID-19 infection without corticosteroid treatment 2 months earlier. The patient reported no history of diabetes mellitus or other chronic medical conditions. Initial clinical suspicion pointed toward maxillary and sphenoethmoidal sinusitis with involvement of the medial orbital wall, leading to orbital cellulitis.

Broad-spectrum antibiotics were initiated, but 4-day post-admission, a necrotic black ulcerative patch appeared along the left nasolabial fold (Figure 1B), indicating zygomycete-related periarteritis, vascular thrombosis, infarction, and angioinvasion. Intravenous amphotericin therapy was promptly initiated. Before presentation at our facility, the patient had undergone functional endoscopic sinus surgery (FESS) elsewhere, although the relevant documentation was unavailable. On examination, the patient exhibited a dilated and fixed left pupil, conjunctival chemosis, and periorbital edema.

Imaging tests revealed a left temporal hypodensity on contrast computed tomography (CT) (Figure 1C), while contrast magnetic resonance imaging (MRI) demonstrated smooth, regular wall rim enhancement (Figure 1D) with diffusion restriction (Figure 1E), indicating abscess formation. The abscess extended into the sphenoethmoidal air sinuses, gangliocapsular area, and retroorbital region (Figure 1F), leading to the final diagnosis of stage IV ROCM). An ear swab smear confirmed the presence of aseptate hyphae with right-angle branching, identifying the pathogen as mucor. Subsequently, the patient underwent left orbital modified lid-sparing exenteration, resulting in the formation of a fistula (Figure 1G). Despite this intervention, the patient's condition continued to deteriorate, leading to agitation and altered mental status. Consequently, a left temporo-parietal craniotomy with abscess excision and augmentation duroplasty was performed. Post-operative contrast CT revealed satisfactory results (Figure 1H). The biopsy result was suggestive of mucormycosis. Following surgery, the patient underwent hemimaxillectomy of the left maxilla due to disease progression. Despite medical interventions, the patient was discharged with a disfigured face (Figure 2A), significantly affecting his personal and social life. In addition, he experienced a single episode of generalized tonic-clonic seizures, prompting the escalation of antiepileptic medication.

6 months later, the patient experienced another seizure episode, necessitating the addition of a second antiepileptic drug. However, he subsequently presented with a bogie swelling over the left temporal region, along with intermittent pus discharge from the previous surgical site (Figure 2B). Imaging revealed bone flap osteomyelitis and an epidural pus collection, necessitating neurosurgical intervention and a tracheostomy due to microaspirations from palatal perforation (Figure 2C). Sutures were removed 10-day post-surgery, and the patient was discharged (Figure 2D).

Subsequently, the reconstruction phase began to improve the cosmetic appearance of the patient's face. The left orbitonasolabial fistula repair and debridement were performed by the plastic surgery team a couple of months after the previous surgery. While planning for reconstructive flap cover surgery during the same admission, the patient developed a maggot infection at the apex of the orbit (Figure 2E). Contrast MRI of the brain, orbit, and paranasal sinuses revealed mucosal thickening of the left sphenoethmoid and frontal air sinus with cavernous sinus infiltration and carotid artery encasement

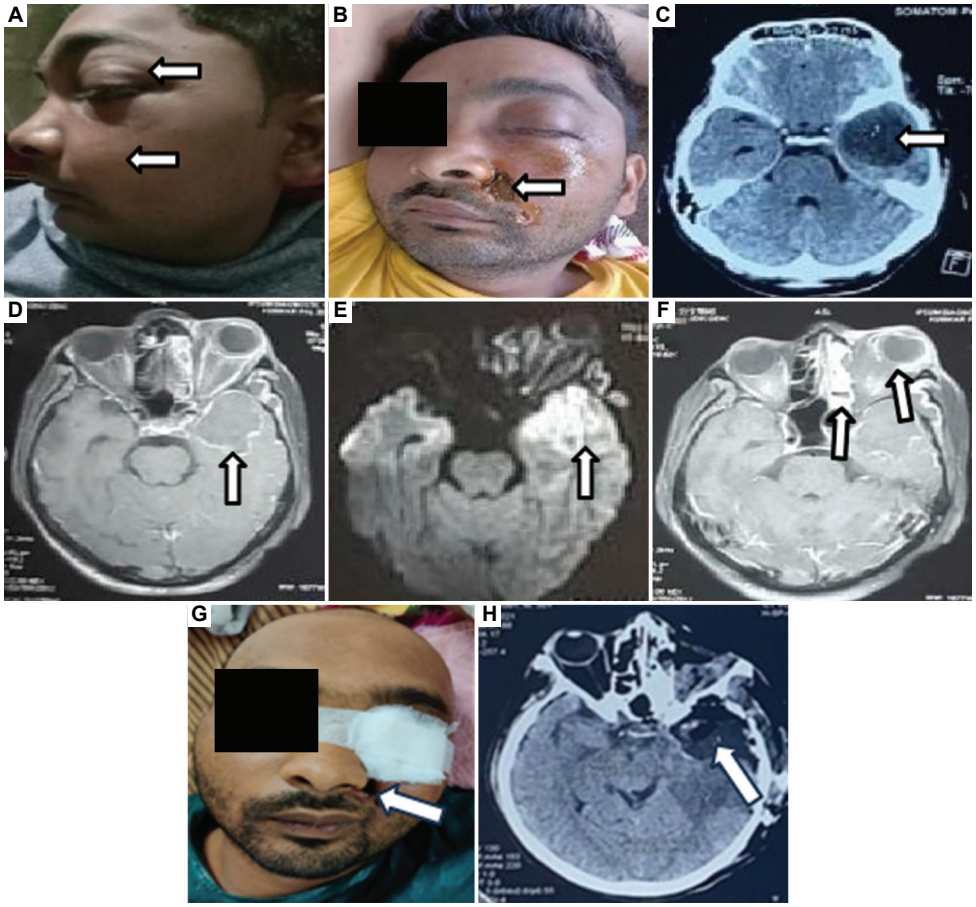


**Figure 1.** Clinical manifestations and surgical outcomes in the case of rhino-orbital-cerebral mucormycosis. (A) Gross periorbital edema, ptosis, and maxillary fullness on the left side of the face. (B) A black necrotic ulcerative eschar along the left nasolabial fold by the side of the ala of the nose, indicating fungal etiology (a hallmark of Mucorales infection). (C) Contrast computed tomography (CT) head revealing left temporal hypodensity with well-defined margins and surrounding edema. (D and E) Axial magnetic resonance imaging (MRI) cuts revealing abscess wall enhancement and diffusion restriction. (F) Axial contrast MRI cuts revealing extension into left spenoethmoid and retroorbital regions. (G) Post-exenteration figure of the patient with dressing *in situ* and formation of fistula due to shredding off of necrotic eschar. (H) Post-operative contrast CT showing complete excision of the abscess cavity with no residual contrast enhancement.

by necrotic tissue. This complication not only delayed the reconstruction surgery but also necessitated debridement of necrotic tissue and maggot removal (Figure 2F) over the left orbital region, along with redo tracheostomy. After surgery, the patient was left with a large cavity, which was visually displeasing (Figure 2G). He was discharged 4 days later with instructions for a high-protein diet via Ryle's tube feeding, tracheostomy care, aseptic dressing, and regular follow-up.

The patient needed an additional 9 months to strengthen his immunity, improve his nutritional status, and clear all necrotic tissue and residual infestations. However, this progress came with a cost. The patient was left with an asymmetric face, an exenterated left socket, a sagging and sunken scalp flap, and a disagreeable, unsightly, and gruesome colossal tissue defect over the maxillary area adjacent to the ala of the nose (Figure 2H). Finally, after 9 months, the day of reconstruction arrived. Debridement of the left orbital necrotic tissue, along with free anterolateral thigh flap cover and split skin graft cover (taken from the left thigh), was performed (Figures 3A and B).

Over the course of approximately 26 months, the patient underwent nine major surgical procedures, including extensive reconstructive surgeries. His journey was marked with physical and psychological challenges, complications, and significant cosmetic deformities. His older brother played a pivotal role in his care and support, accompanying him through multiple medical departments. In addition to surgical treatments, he received liposomal amphotericin and posaconazole to combat mucormycosis. However, his struggles persist as he continues to undergo regular follow-ups in the plastic


**Figure 2.** Complications encountered during the treatment course and their management. (A) A cosmetically unacceptable face with palatal perforation with a black patch, loss of lower eyelid, exposed exenteration cavity, exposed orbital floor and maxilla, fistula opening at the nasolabial fold, facial asymmetry, and a black patch over the exposed orbital floor. (B) Pus discharge coming from the surgical site. (C) Patient with a tracheostomy and wound dressing *in situ*. (D) Post-decompression craniectomy photo of the patient with loss of scalp contour due to sagging of flap and tracheostomy scar mark, adding the burden of cosmetic deformity to his facial appearance. (E) Pus mixed with blood along with maggots (arrow) coming out of the exenteration cavity. (F) Maggots removed from the exenteration cavity and collected in a bag. (G) Radical debridement and maggot removal resulted in the formation of a large hideous cavity, so substantial that the orbital exenteration cavity appears as a trivial fusiform gap. (H) Photo of the patient at the time of discharge with Ryle's Tube and tracheostomy *in situ,* along with a humongous maxillary cavity, sunken scalp flap, and orbital exenteration cavity, resulting in a ghastly repugnant facial appearance.

surgery department. Unfortunately, another complication had arisen: split skin graft necrosis with only partial uptake (Figure 3C). At the time of writing this report, he was still awaiting another reconstructive surgery for refinement and further correction of his cosmetic deformity, while being instructed to remain under close observation in the plastic surgery department.

## 3. Discussion

This case report offers a unique insight into the clinical progression of ROCM in an immunocompetent patient who had recovered from mild COVID-19 without steroid treatment.

The existing literature primarily focuses on immunocompromised patients with diabetes as the primary predisposing factor for mucormycosis. Our case highlights the importance of recognizing ROCM in non-immunocompromised individuals and underscores the importance of follow-up care after COVID-19 recovery.

After extensive research, we found a retrospective, observational study involving 2826 patients with COVID-19-associated ROCM in India from January 1, 2020, to May 26, 2021[9]. Only 2% of these patients had no history of glucose intolerance and steroid intake (similar to our patient), and merely 0.4% underwent all


**Figure 3.** Status of patient post-reconstruction surgery. (A) Raw area of thigh (split skin graft site) covered by occlusive dressing. (B) Flap (anterolateral thigh) filling the large tissue defect with a split skin graft cover. (C) Split skin graft necrosis with only partial uptake of the graft.

forms of treatment, as our patient did (amphotericin B + posaconazole + FESS + exenteration)[9]. The main inferences of this study were that corticosteroids and diabetes mellitus are the most important predisposing factors for COVID-19-associated ROCM, and it emphasized the necessity of post-recovery follow-up for COVID-19 patients[9]. In our case, the patient developed symptoms approximately 2 months after recovering from COVID-19. At the time of writing, he had been under observation for the past 2 years and remained in our follow-up. His case signifies that COVID-19 can act as an independent risk factor for ROCM.

To date, only a literature review summarizing 11 cases of ROCM in immunocompetent individuals has been published[10] (Table 1).

Out of eleven cases reviewed, eight patients survived only after undergoing extensive radical debridement and orbital exenteration, a similar scenario to our patient (Figure 4). This indicates that even if the disease is localized, surgeons should not try to preserve vision first but should aim to preserve life, keeping the invasive and arduous nature of the disease course in mind. Our report is noteworthy for highlighting the challenge of determining the appropriate extent of surgical intervention. This case raises questions about considering the disease trajectory when planning surgical interventions. Surgeons must consider the course of the disease and potential complications arising from residual infected tissue before deciding on surgical debridement margins. Increasing the radicality of debridement and decreasing the time between clinical presentation and surgery can help prevent further invasion of adjacent organs, serial debridement surgeries,

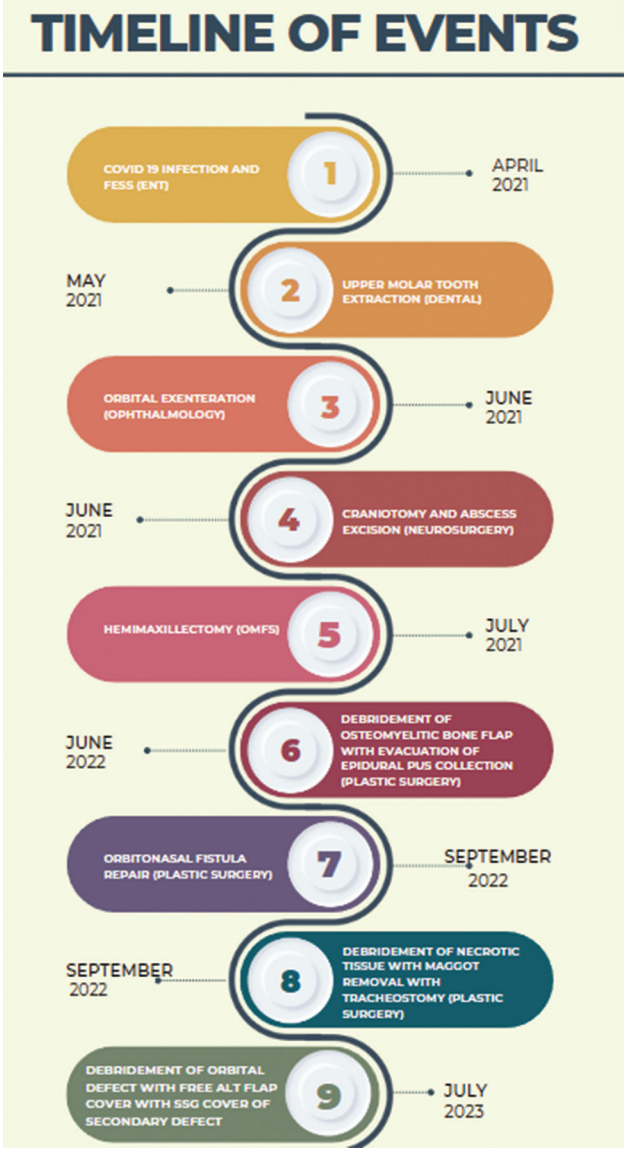


**Figure 4.** A timeline chart detailing the patient's journey through multiple surgeries across various specialties, highlighting the invasive course of the disease and the requirement of a multidisciplinary approach with a long follow-up.
Abbreviations: ENT: Ear nose throat; FESS: Functional endoscopic sinus surgery; SSG: Split skin graft.

loss of facial cosmesis, and long hospital stays. The invasive nature of ROCM is evident in the patient's journey through multiple surgeries.

Before the COVID-19 pandemic, Mucor was a rare entity in India, with only two large retrospective series reported from PGIMER Chandigarh. These studies, covering 129 cases over 10 years (1990 – 1999)[4] and 178 cases over the subsequent 5 years (2000 – 2004)[6], raised awareness about the threat of invasive zygomycosis. They prompted the development of an institutional zygomycosis

**Table 1. Summary of literature on rhino-orbito-cerebral mucormycosis in immunocompetent patients published in PubMed**

| Literature | Number of cases | Survival outcomes |
|---|---|---|
| Fairley *et al.*[11] | 1 | Survived |
| Garcia-Covarrubias *et al.*[12] | 1 | Survived |
| Chakrabarti *et al.*[13] | 1 | Survived |
| Rao *et al.* (2006)[14] | 5 | Four survived, and one died |
| Schütz *et al.*[15] | 1 | Died |
| Bhadani *et al.*[16] | 1 | Survived |
| Baradkar *et al.*[17] | 1 | Died |

registry. It is imperative for every apex institute in our country to establish similar measures.

## 4. Conclusion

This case report serves as a valuable addition to the understanding of ROCM in immunocompetent individuals. The meticulous documentation of the patient's journey through this disease highlights the challenges in diagnosis and treatment and the importance of considering the extent of surgical intervention. In addition, it reinforces the importance of post-COVID-19 recovery follow-up care among patients.

## Acknowledgments

None.

## Funding

None.

## Conflict of interest

The authors declare no conflicts of interest.

## Author contributions

*Conceptualization:* Bal Krishna Ojha
*Investigation:* Rajat Verma
*Methodology:* Awdhesh Yadav
*Writing-original draft:* Rajat Verma
*Writing-review & editing:* Rajat Verma

## Ethics approval and consent to participate

A written informed consent was taken from the patient before writing the case report.

## Consent for publication

An informed consent was taken for publishing the patient data.

## Availability of data

The data that support the study is available in the medical record section of the department of neurosurgery, King George's Medical University. Data are available with the permission of department of neurosurgery, King George's Medical University. Medical University (URL: https://kgns.in/).

## References

1. Bodenstein NP, McIntosh WA, Vlantis AC, Urquhart AC. Clinical signs of orbital ischemia in rhino-orbitocerebral mucormycosis. *Laryngoscope*. 1993;103:1357-1361.

   doi: 10.1288/00005537-199312000-00007

2. Chakrabarti A, Das A, Mandal J, *et al*. The rising trend of invasive zygomycosis in patients with uncontrolled diabetes mellitus. *Med Mycol*. 2006;44:335-342.

   doi: 10.1080/13693780500464930

3. Kauffman CA. Zygomycosis: Reemergence of an old pathogen. *Clin Infect Dis*. 2004;39:588-590.

   doi: 10.1086/422729

4. Chakrabarti A, Das A, Sharma A, *et al*. Ten years' experience in zygomycosis at a tertiary care centre in India. *J Infect*. 2001;42:261-266.

   doi: 10.1053/jinf.2001.0831

5. Ribes JA, Vanover-Sams CL, Baker DJ. Zygomycetes in human disease. *Clin Microbiol Rev*. 2000;13:236-301.

   doi: 10.1128/CMR.13.2.236

6. Roden MM, Zaoutis TE, Buchanan WL, *et al*. Epidemiology and outcome of zygomycosis: A review of 929 reported cases. *Clin Infect Dis*. 2005;41:634-653.

   doi: 10.1086/432579

7. Spellberg B, Edwards J Jr., Ibrahim A. Novel perspectives on mucormycosis: Pathophysiology, presentation, and management. *Clin Microbiol Rev*. 2005;18:556-569.

   doi: 10.1128/CMR.18.3.556-569.2005

8. Singh V, Singh M, Joshi C, Sangwan J. Rhinocerebral mucormycosis in a patient with type 1 diabetes presenting as toothache: A case report from Himalayan region of India. *BMJ Case Rep*. 2013;2013:bcr2013200811.

   doi: 10.1136/bcr-2013-200811

9. Sen M, Honavar SG, Bansal R, *et al*. Epidemiology, clinical profile, management, and outcome of COVID-19-associated rhino-orbital-cerebral mucormycosis in 2826 patients in India - Collaborative OPAI-IJO study on Mucormycosis in COVID-19 (COSMIC), report 1. *Indian J Ophthalmol*. 2021;69(7):1670-1692.

   doi: 10.4103/ijo.IJO_1565_21

10. Shatriah I, Mohd-Amin N, Tuan-Jaafar TN, Khanna RK, Yunus R, Madhavan M. Rhino-orbito-cerebral mucormycosis in an immunocompetent patient: Case report and review of literature. *Middle East Afr J Ophthalmol*. 2012;19:258-261.

doi: 10.4103/0974-9233.95269

11. Fairley C, Sullivan TJ, Bartley P, Allworth T, Lewandoski R. Survival after rhino-orbital-cerebral mucormycosis in an immunocompetent patient. *Ophthalmology*. 2000;107:555-558.

doi: 10.1016/s0161-6420(99)00142-6

12. Garcia-Covarrubias L, Bartlett R, Barratt DM, Wassermann RJ. Rhino-orbitocerebral mucormycosis attributable to *Apophysomyces elegans* in an immunocompetent individual: Case report and review of the literature. *J Trauma*. 2001;50:353-357.

doi: 10.1097/00005373-200102000-00027

13. Chakrabarti A, Ghosh A, Prasad GS, *et al*. *Apophysomyces elegans*: An emerging zygomycete in India. *J Clin Microbiol*. 2003;41:783-788.

doi: 10.1128/JCM.41.2.783-788.2003

14. Rao SS, Naresh KP, Pragache G, Chakrabarti A, Saravanan K. Sinoorbital mucormycosis due to *Apophysomyces elegans* in immunocompetent individuals--an increasing trend. *Am J Otolaryngol*. 2006;27:366-369.

doi: 10.1016/j.amjoto.2006.01.002

15. Schütz P, Behbehani JH, Khan ZU, *et al*. Fatal rhino-orbito-cerebral zygomycosis caused by *Apophysomyces elegans* in a healthy patient. *J Oral Maxillofac Surg*. 2006;64:1795-1802.

doi: 10.1016/j.joms.2006.05.010

16. Bhadani PP, Bhadani UK, Thapliyal N, Sen R. A rare presentation of invasive rhino-orbital mucormycosis in an immunocompetent young girl: A case report. *Indian J Pathol Microbiol*. 2007;50:785-786.

17. Baradkar VP, Mathur M, Taklikar S, Rathi M, Kumar S. Fatal rhino-orbito-cerebral infection caused by *Saksenaea vasiformis* in an immunocompetent individual: First case report from India. *Indian J Med Microbiol*. 2008;26:385-387.

doi: 10.4103/0255-0857.43572

# Our Journals

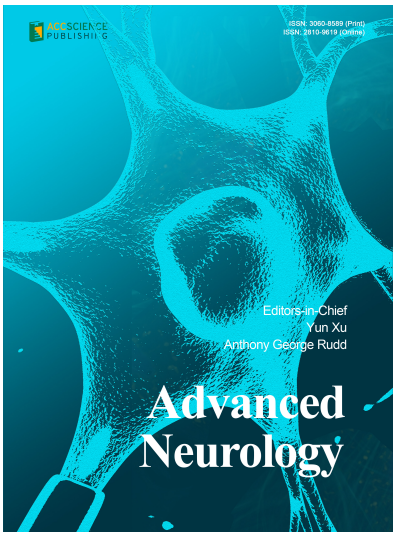


*Advanced Neurology* is a peer-reviewed and open-access journal that aims to publish and disseminate novel research in the breadth of neurology and neuroscience. The journal aims to advance our understanding in the nervous system and provide a platform to neuroscientists and physicians to showcase their findings in original fundamental and clinical research as well as to present new ideas that highlight the changes in the neurological clinical practice.

*Advanced Neurology* covers subject areas, including but not limited to the following:

- Neurological disorders
- Neurodegenerative disease
- Cerebrovascular disease
- Epilepsy and movement disorders
- Neuroimmune disease
- Neurological infections
- Muscle disease
- Molecular and cellular neuroscience
- Systems neuroscience
- Cognitive neuroscience
- Computational modeling of nervous system

*Global Translational Medicine* is a quarterly journal that focuses on medicine, biological sciences, and biomaterials engineering. The goal of *Global Translational Medicine* is to provide a platform to researchers for showcasing their latest research works in translational medicine so as to advance the field towards the betterment of human health. Despite the advancement of omics and new technologies, the process of transforming these technologies and scientific research results into effective therapies and putting them into clinical use still has a long way to go. *Global Translational Medicine* provides a platform to fill the gaps in preclinical and inter-disciplinary research, to promote clinical translation of scientific research results, and to contribute to the conception of new and improved preventive measures as well as diagnostic and therapeutic techniques of diseases.

*Global Translational Medicine* covers the following themes: cardiovascular disease, metabolism/diabetes/obesity, neuroscience/neurology, cancer, biomaterials and their applications in medicine, proteomics/metabolomics, pharmacogenomics, biomarkers, bioinformatics and data mining, animal and clinical research, and medical methods arising from interdisciplinary crossover.


## Start a new journal

Write to us via email if you are interested to start a new journal with AccScience Publishing. Please attach your CV, professional profile page and a brief pitch proposal in your email. We shall inform you of our decision whether we are interested to collaborate in starting a new journal.

**Contact:** info@accscience.com

https://accscience.com/journal/BH

Contact

www.accscience.com

8 Burn Road, #15-03 Trivex, Singapore 369977

E-mail: editorial@accscience.com

Phone: +65 8182 1586